POLITECNICO DI MILANO

Master of Science in Nuclear Engineering

Department of Energy

COMBINING MAGNETIC HYPERTHERMIA WITH HADRONTHERAPY: AN IN-VITRO STUDY ON PANCREATIC TUMOR CELLS

Relator: Prof. Stefano Luigi Maria GIULINI CASTIGLIONI AGOSTEO
Correlator: Prof. Daniela BETTEGA (INFN)

Master Thesis of:
Maria Claudia MANSI

Academic Year: 2016-2017

ad Adriana e Chiara,
donne eroiche

Contents

List of Figures

List of Tables

List of Graphs

Abstract

The aim of this project is to implement the survival curves of a population of pancreatic tumor cells subjected to hadrontherapeutic treatment in combination with magnetic hyperthermia. This combined procedure involves the insertion into the in vitro cell samples of magnetite nanoparticles that, once the uptake is performed, can release heat through the external action of an alternating magnetic field. The increase in temperature would represent a radiosensitizing factor which, in addition to irradiation by hadronic particles (carbon ions), would enhance the action of such radiotherapy, bringing damage difficult to repair to the tumor area. The experiments included a preliminary phase of characterization of the BxPC3 cells line, the study of cytotoxicity as a function of different concentrations of nanoparticles and in the presence of hyperthermic treatment, so as to choose the most suitable protocol for the final experiment: irradiation with bundles of carbon ions on cell samples already sensitized by the presence of nanoparticles, and consequent heating by the hyperthermia system. The results allowed to obtain survival curves with the same decreasing exponential trend, but gradually increasing slope in relation to the addition of radiosensitizers: this shows that the combination of nanoparticles, hyperthermia and irradiation with such densely ionizing particles brings an improvement in efficiency of the hadrontherapy, even if in percentages not too high. In fact, at the same dose, there is an increase in mortality (and therefore a decrease in survival) of about ten percent, a good result that can be improved with further research. The next step will be to use the same protocol for photonic radiation, applicable to conventional radiotherapies.

Estratto

Lo scopo di questo progetto è implementare le curve di sopravvivenza di una popolazione di cellule tumorali pancreatiche sottoposta a trattamento adroterapico in combinazione con l'ipertermia magnetica. Questa procedura combinata prevede l'inserimento nei campioni cellulari in vitro di nanoparticelle di magnetite che, una volta effettuato l'uptake, sono in grado di rilasciare calore tramite l'azione esterna di un campo magnetico alternato. L'innalzamento della temperatura rappresenterebbe un fattore radiosensibilizzante che, in aggiunta all'irraggiamento da parte di particelle adroniche (ioni carbonio), potenzierebbe l'azione di tale radioterapia, portando danni difficilmente riparabili alla zona tumorale. Gli esperimenti hanno previsto una fase preliminare di caratterizzazione della linea cellulare BxPC3, lo studio della citotossicità in funzione di diverse concentrazioni di nanoparticelle ed in presenza di trattamento ipertermico, di modo da poter scegliere il protocollo più idoneo per l'esperimento finale: irraggiamento con fasci di ioni carbonio su campioni cellulari già sensibilizzati dalla presenza di nanoparticelle, e conseguente riscaldamento tramite il sistema di ipertermia. I risultati hanno consentito di ottenere curve di sopravvivenza con stesso andamento esponenziale decrescente, ma pendenza via via crescente in relazione all'aggiunta di radiosensibilizzanti: ciò dimostra che la combinazione di nanoparticelle, ipertermia e irradiazione con particelle così densamente ionizzanti porta un miglioramento dell'efficienza del trattamento adroterapico, anche se in percentuali non troppo elevate. A parità di dose si ha infatti un incremento della mortalità (e quindi un decremento della sopravvivenza) di circa il dieci per cento, risultato buono e potenziabile con ulteriori ricerche. Infatti, il prossimo passo sarà utilizzare lo stesso protocollo per la radiazione fotonica, applicabile alle radioterapie convenzionali.

Riassunto

L'*adroterapia* è una tecnica radioterapica che sfrutta le proprietà fisiche delle particelle adroniche (principalmente i protoni e gli ioni carbonio) per ridurre la presenza di un'area tumorale ed impedirne la crescita cellulare. Infatti, gli *adroni* sono in grado di rilasciare gran parte della propria energia alla fine del percorso in un mezzo, in corrispondenza del *picco di Bragg*, consentendo di effettuare un piano di trattamento in modo tale da trasferire tutta (gran parte) dell'energia nella regione in cui è presente il tumore. Inoltre, trattandosi di radiazione di alto LET (Linear Energy Transfert, i.e. trasferimento di energia per unità di percorso) il danno causato sulla popolazione cellulare è maggiore rispetto alle tecniche radioterapiche convenzionali (in cui si utilizzano raggi gamma e x – radiazioni di basso LET), poiché non permette il riparo delle strutture biologiche danneggiate dalla ionizzazione della radiazione incidente. Questa ultima caratteristica può dunque essere impiegata nella cura dei tumori radioresistenti, come il *tumore del pancreas*.

Lo scopo di questo lavoro di tesi è la valutazione della citotossicità indotta in una popolazione di cellule tumorali pancreatiche (BxPC3), dovuta all'irraggiamento da parte di particelle adroniche, e nello specifico di fasci di ioni Carbonio. Poiché le curve di sopravvivenza di popolazioni bombardate da radiazione ad *alto LET* evidenziano la diminuzione esponenziale della proliferazione cellulare, vi sono importanti vantaggi riguardo la probabilità di controllo del tumore durante i trattamenti radioterapici. Infatti, si è pensato di introdurre due agenti radiosensibilizzanti con l'intento di apportare maggiore mortalità alla popolazione sotto indagine: è il caso delle *nanoparticelle* di magnetite e dell'*ipertermia magnetica* (i.e. innalzamento della temperatura fino ad un valore di circa 42°C). Va da se che per ottenere l'andamento della *sopravvivenza* della popolazione in vitro (e quindi la mortalità promossa dagli agenti) è stato necessario effettuare diversi test sperimentali, di modo da identificare:

- l'andamento di crescita della popolazione in esame in condizioni simili a quelle dell'organismo biologico (temperatura di 37 °C, no agenti esterni introdotti),

- la sopravvivenza della popolazione all'irraggiamento da parte di una radiazione di basso LET (fotoni di 6 MV, con valori di dose 0, 0.5, 1, 2, 3, 5, 7 Gy),

- la sopravvivenza della popolazione all'inserimento di nano particelle di magnetite Fe_3O_4 (con concentrazioni di 0, 10, 25, 50, 100 μg/ml e un tempo di assorbimento (o *uptake*) di 24 o 48 ore),

- la funzionalità del sistema di ipertermia magnetica, e quindi la valutazione del corretto innalzamento della temperatura all'interno della popolazione (opportunamente propagata e tenuta in provette da 1 o 0.2 ml), sia senza sia con l'uptake delle nano particelle,

- la sopravvivenza della popolazione al bombardamento da parte di fasci di Ioni Carbonio (esperimento effettuato al Centro Nazionale di Adroterapia Oncologica (CNAO) di Pavia con accelerazione delle particelle adroniche tramite il Sincrotrone),

- la sopravvivenza della popolazione al bombardamento da parte di fasci di Ioni Carbonio, con precedente uptake (48 ore) della concentrazione di nano particelle più ottimale (50 μg/ml, ovvero la concentrazione che dà una bassa percentuale di sopravvivenza della popolazione, circa 30 %, valore molto simile a 100 μg/ml, quantità che avrebbe richiesto dell'utile spreco a parità di risultato),

- la sopravvivenza della popolazione al bombardamento da parte di fasci di Ioni Carbonio, con precedente uptake di 48 ore di 50 μg/ml di nano particelle di magnetite e conseguente trattamento di ipertermia.

È chiaro che il progetto in questione ha visto una lunga fase preliminare, durante la quale si sono ricercati i risultati più confacenti, così da creare un protocollo per l'esperimento complessivo che coinvolgesse i due fattori radiosensibilizzanti e l'irraggiamento con radiazione di alto LET. Inoltre, ogni test ha richiesto i tempi biologici necessari affinché la popolazione in esame potesse propagare per avere un campione contenente sufficiente numero di cellule, soprattutto nel caso di trattamento ipertermico; infatti, per la popolazione BxPC3 ed un numero dell'ordine del milione di cellule il tempo stimato per la propagazione e la crescita è di circa dieci giorni.

L’utilizzo delle nano particelle con proprietà magnetiche, combinato al trattamento ipertermico, è stato pensato per via dei meccanismi di rilascio termico conseguenti all’applicazione di un campo magnetico alternato (AMF). Infatti, nella magneto-fluido ipertermia (MFH), l’inibizione della crescita della popolazione tumorale è ottenuta attraverso l'inserimento delle nano particelle (ferro-fluido) nella zona da scaldare (nel nostro caso nella provetta o nelle flasks). L'energia necessaria a provocare il surriscaldamento del campione è dunque generata dall'esposizione delle nanoparticelle al AMF, la cui intensità deve essere sufficiente a raggiungere gli scopi del trattamento (campo di 16,2 kA/m alla frequenza di 110 kHz), ma non è troppo elevata per evitare danni ai tessuti sani se sperimentata durante un ipotetico trattamento in vivo.

L’esperimento al CNAO (Centro Nazionale di Adroterapia Oncologica) ha permesso di ottenere i dati per la realizzazione di tre curve di sopravvivenza:

- *Curva di Sopravvivenza* in funzione della dose dei soli Ioni Carbonio
- *Curva di Sopravvivenza* in funzione della dose degli Ioni Carbonio e uptake delle Nanoparticelle
- *Curva di Sopravvivenza* in funzione della dose degli Ioni Carbonio, uptake delle Nanoparticelle e conseguente Ipertermia.

La pendenza della curva di sopravvivenza relativa al trattamento combinato ioni carbonio e nanoparticelle e quella relativa al trattamento combinato ioni carbonio, nanoparticelle e ipertermia è rispettivamente maggiore del 13 e 18 % di quella relativa al trattamento con i soli ioni carbonio. I risultati dimostrano che l’ultima delle curve citate mostra un andamento più ripido e induce maggior citotossicità alla popolazione in esame, così da confermare l’ipotesi del potenziamento apportato dall’ipertermia magnetica.

Introduction

Among the most serious and obscure questions of the individual nowadays are those concerning the onset of cancers. In Italy, about 280,000 patients undergo radiation treatment every year in the 187 radiotherapy centers operating in the national territory [1] and in the last fifteen years, the increase in cases of pancreatic cancer has reached almost 60 percent.

How can we prevent and combat the occurrence of this disease? They are manifested in various forms and have different cure depending on the organ and the stage reached at the time of diagnosis. One of the most difficult forms to treat is cancer of the pancreas; in fact, it does not give any sign at an early stage, but in an advanced state, when survival possibilities are low, and dimensions have reached considerable levels. These conditions do not allow successful surgical removal, which would cause serious damage to the organ and the surrounding tissues, but as a viable alternative, radiotherapy treatment is proposed.

Hadrocombi is a project financed by the INFN (Istituto Nazionale di Fisica Nucleare) to make a significant contribution to refining the parameters involved in such techniques so that they can successfully cure those pathologies, involving several groups at national level, which have carried out tests and experiments to pursue their goal for the overall project. The main goal is to investigate the co-operative action of Hadrontherapy (radiotherapy using hadronic radiation) and Magnetic Fluid Hyperthermia, considering both interesting alternative techniques in those cases where conventional techniques fail. As a valid comparison with this proposed technique we have used an X-ray radiotherapy control combined with Magnetic Fluid Hyperthermia. The group I took part in developing this master thesis project was responsible for the response of cultures of BxPC3 pancreatic tumour cells in vitro in relation to introduction of nanoparticles, the magnetic hyperthermia and the irradiation, and the

resulting cytotoxicity due to these factors, single or combined. Along with other groups involved in the project, we carried out several tests to find out what the best choice of convoluted parameters was to achieve the best result of cellular mortality. Specifically, we had changed the uptake time and the concentration of nanoparticles, the radiation dose, the size of the test tubes used, and we evaluated the cytotoxicity induced by a clonogenic assay.

We finally found the standard of values that gives more mortality to the specific cell population, hoping that this result could be used in vivo as a valid support in vivo for Hadrontherapy.

Chapter 1

The Importance of Radiotherapic Techniques in Cases of Pancreatic Cancer

1.1

Introduction to Carcinogenesis

It is well known that our body is made up of so many compartments capable of performing specific tasks to maintain a regular functioning of our vital functions. In general, such compartments are the organs, which in turn are made up of tissues composed of eukaryotic cells. These cells have different composition depending on their function, and we can classify them into four categories, depending on tissue that they constitute: epithelial, connective, muscular and nervous.

For example, the connective tissue is composed by macrophage blood cells such as lymphocytes (which are part of the immune system), as well as all blood cells, but also adipocytes, cells that collect and preserve lipids (fat), or bone cells like osteoblasts.

To study biological systems from the most elementary physical entities (molecules and atoms inside cells), we need to look at the phenomena that underlie the structure and functions of living organisms: these include atomic and molecular motions, molecular aggregations and chemical reactions. The interactions among atoms, molecules and supramolecular structures are the basis of the main functions that determine the natural processes that give rise to inorganic, organic and biological matter. Current knowledge of the nature of such interactions is constantly developing and provide descriptions useful to understand the functionality of cellular and tissue substrates.

It is therefore normal to think that mistakes in the homeostasis, that is the balance between proliferation and programmed cell death maintained by strictly regulating both processes to ensure the integrity of organs and tissues, could lead to abnormalities in small scales (DNA mutations), which can then be transposed into a series of tissue or systemic complications.

The process of neoplastic transformation finds its birth: normal cells become cancerous due to the subsequent accumulation of genetic mutations that govern cell proliferation and it could lead tissues to apoptosis or necrosis.

The alterations leading to this malignant transformation can be grouped according to some essential features:

- the ability to proliferate independently of the presence of growth factors (oncogene activation);
- the ability to escape apoptotic signals, which favor cell death;
- the insensitivity to antiproliferative signals (inactivation of antithorogens);
- the capacity of unlimited cell divisions;
- the potential to colonize sites away from the onset (metastasis);
- the ability to stimulate the production of new blood vessels (neoangiogenesis).

The acquisition of these characteristics, each one capable of conferring the cell on a selective growth advantage, proceeds both through staged phases and by alternative chronological sequences, not only in the different types of tumors, but within the same tumor type.

This phenomenon is called Carcinogenesis, term that derived from greek "*καρκίνος*" or from latin "c*ancer*", which means "crab" and with the suffix "-genesis", from greek "*Γένεσις*", with means "genesis"; the entire word actually means "that raises cancer".

The growth of tumor mass is different depending on the type of tissue, and hence the organ involved in the neoplastic transformation; in fact, we know that there are low and high cellular turn-over organs, defined as life cycle of the cells, then the speed of tissue regeneration.

The choice to treat pancreatic cancer cells lies in this fundamental difference: it is a high activity proliferating organ, which is therefore able to regenerate its cells quickly, unlike systems like the nervous system that have the same cells, neurons, throughout the life cycle.

This feature of rapid regeneration leads to the fast development and expansion of the cancerous area, up to the formation of metastasis and secondary tumors, preventing from noticing any signs at an early stage but in an advanced state, when survival possibilities are now low, and dimensions have reached considerable values.

These conditions do not allow for successful surgical removal, which would cause serious damage to the organ and surrounding tissues, but as a valid alternative radiotherapy treatment is proposed. For a good understanding of how radiation therapy sensitizes the affected tumor area and promotes mass reduction, it is important to understand first what are the basal characteristics of a cell, its normal functioning, and possible neoplastic transformations; then we will discuss the basis of the interaction between ionizing agents and those biological components.

1.1.1 Cell-division Cycle

"The dream of every cell is to become two cells"

François Jacob

The cell is the fundamental unit of every living organisms, which can be distinguished in unicellular (such as bacteria or protozoa) and pluricellular ones, a category which, without a doubt, humans belong to.

Unicellular organisms are composed of cells with morphologic characteristics usually uniform; by increasing the number of cells in an organism, however, they differ in form, size and specialized functions, up to the constitution of tissues, organs and apparatus.

It is therefore important that within each cell there is a regular exchange of nutrients and waste materials, to ensure homeostasis and so proper cell survival.

Obviously after a while, each cell will run out of its own life cycle depending on its characteristics and functions; for example, pancreatic cells have a life cycle of about two days, but it is different for other cells, as neurons that are the same for the entire human life.

We can therefore give a general definition of a cell cycle: sequence of events between two successive cell divisions; such events, better defined as cellular phases, place the cell under varying conditions. In fact, for example, during the Synthesis phase, the cell is organized to perform a synthesis of its genetic heritage, to ensure the division into two daughter cells with the same genetic information.

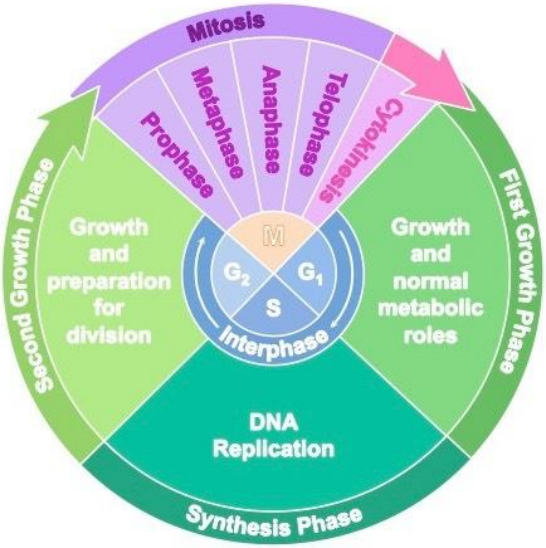

Fig 1.1 Main phases of the cell cycle. [3]

Interphase: G0, G1 (Pre-Synthesis), S (DNA Synthesis), G2 (Pre-Mitosis). Mitosis: M.

Each component involved in the cell cycle will have a different evolution depending on its role within the cellular environment. For example, microtubules are composed of proteins and they play an essential role in cell division because of their responsibility for producing mitotic spindle; without them the cell would not be able to make the cell fit for the division of its membrane.

In radiobiology it is important to understand at which time the cell's life cycle is present, since it is in a condition of greater or less radiosensitivity.

In general, some factors influence this propensity: for example, high-rate division tissue has more probability to be radiosensitive. Moreover, the radiosensitivity of a tissue depends on the percentage of mitotic activity and the inverse of the degree of cell differentiation; cells are more sensitive in G2-phase (pre-mitosis) and M-phase (mitosis).

In an actively proliferating population each cell progresses in its cycle independently of the others and hence the fraction of cells occupying the different phases is proportional to the duration of the phases.

The loss of proliferative activity could be attributed to two factors: chemical agent and radiation; the first one has a dose threshold, but the second one has an unfavorable behavior and an asymptotic behavior.

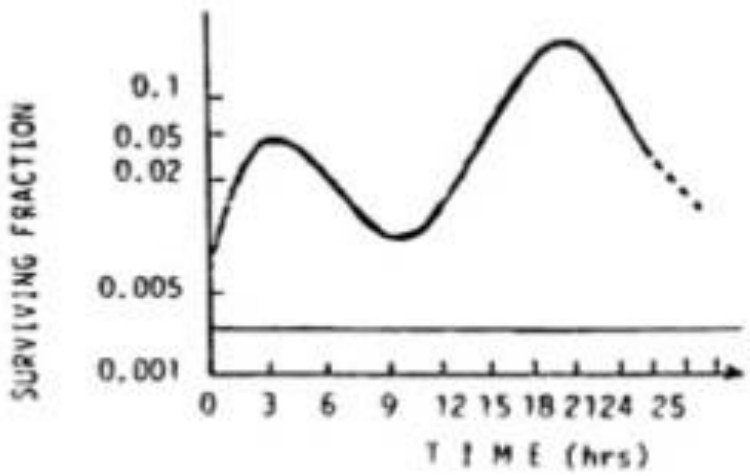

Fig. 1.2 Radiosensitivity variation in time. [4]

1.1.2 Neoplastic Transformation

As mentioned above, a normal cell can become carcinogenic due to spontaneous genetic mutations or induced by chemical agents or ionizing radiation.

In our case, it is interesting to understand the general concept of neoplasia, as the project involves studies on an already tumoural population, for which it is desired to have a high mortality rate because of high LET radiation incidence; it will break DNA bonds, giving apoptosis and/or necrosis of the affected area and thus reducing tumor mass.

The problem of radiation-induced neoplastic transformation is only related to the chance that irradiation will strike healthy tissue around the tumoural area that you want to reduce.

Now let us make a general definition of neoplasia: it is an "abnormal mass of tissue that grows excessively and in an uncoordinated manner with respect to normal tissues, and which persists in this state after cessation of the stimuli that have induced the process" [1] as clarifies the internationally accepted definition coined by Rupert Allan Willis.

Mutations in the genetic heritage of some cells alter tissue homeostasis, and continued proliferation promotes the formation of a significant tumor mass.

Moreover, it is important to say that cancer cells grow in multilayer, so we could distinguish them to the normal ones.

The rate of growth of a neoplasia is influenced by three fundamental factors:

- Growth Fraction: the percentage of cells in a neoplastic population that is included in the proliferative compartment.
- Growth rate of the tumor, and hence with which neoplastic cells complete the cell cycle;
- The ability of the mass to ensure sufficient trophic contribution through neoangiogenesis, and therefore the position within the tissue.

The growth of the tumor mass may have an exponential trend, for which the volume increases with a constant fraction in equal intervals of time. The formula describing this situation is as follows:

$$V(t) = V_0 \, e^{\frac{0{,}693}{Td} t} \qquad (1.1)$$

where T_d is the time of tumor duplication, for which the tumor grows slower when it has reached a significant size. Instead, non-exponential growth may be due to cellular loss, to passage to a non-proliferating layer, and to increased duplication time. We can also consider a relationship between the number of cell divisions and the tumor mass achievable, assuming that:

- Cells grow exponentially according to the law : $N(t) = 2^{t/Td}$ (1.2),
- The mass of the single cell is in the order of 10^{-9} g,
- There is no cell loss.

For example, for forty divisions it will have 10^{12} cells and then 10^3 g of tumor mass; therefore, above the thirtieth divisions the tumor is detectable (m=1 g).

Neoplastic cells divide into p - cells, q - cells, differentiated cells, and dying cells. This distinction is due to the alternation between highly proliferating cells and those that are part of the necrotic tumor tissue. Specifically, dying cells are found in the tumoural area with insufficient vascularization, so they go against necrosis (cell death) due to lack of oxygen supply. In contrast, "p" cells are part of the growth fraction of the cancerous

population, and are highly proliferating. Among proliferating cells are also those defined as "q", quiescent cells that activate if necessary to give tumor repopulation. The category that does not cause problems because it is not able to divide is that of differentiated cells.

The loss of some cells, due to the entry of differentiated ones or the lack of oxygen-free division, is regulated by growth, if there is no excess of proliferation.

1.1.3 Pancreatic Adenocarcinoma

The final goal of this project is to improve hadrontherapy in case of pancreatic cancer. This choice comes from the seriousness of this kind of pathology: in fact, pancreas is a high-rate of proliferation organ, so the increasing of tumoural mass is rapid and it is often no possible to identify it until the most critical states.

The incidence of pancreatic cancer varies greatly across regions and populations: incidence rates for pancreatic cancer in 2012 were highest in Northern America (7.4 per 100000 people) and Western Europe (7.3 per 100000 people), followed by other regions in Europe and Australia/New Zealand (equally about 6.5 per 100000 people). [5]

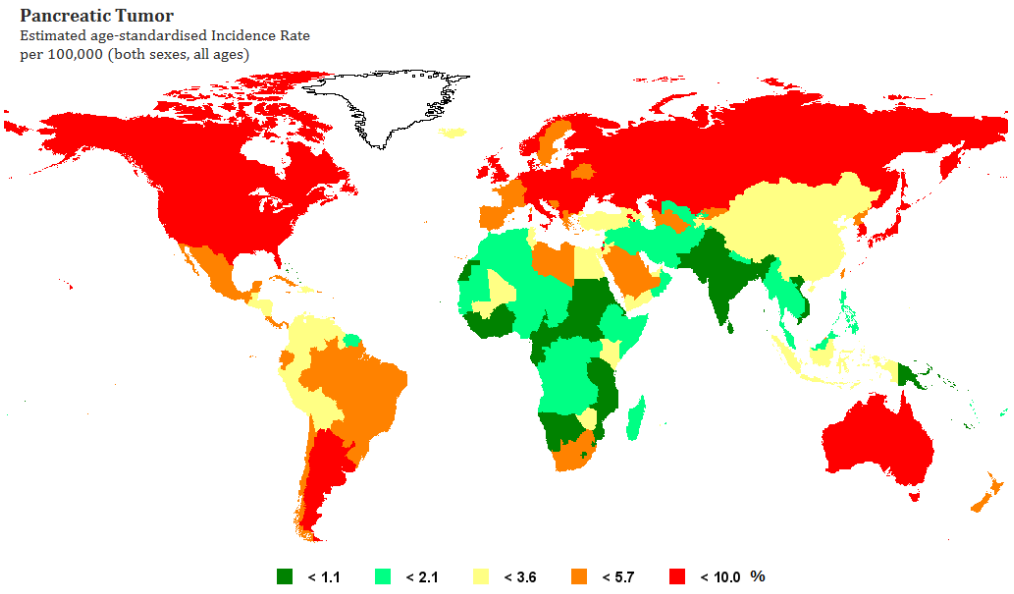

Fig.1.3 Incidence of pancreatic cancer all over the world. [6]

he lowest rates (about 1.0 per 100000 people) were observed in Middle Africa and South-Central Asia. For now, during the 2017 about 54000 cases were estimated, of

which about 3% of new diagnosis. The estimated deaths during the 2017 were about 43000 and survival percentage is almost 8%. [7]

Clearly, this type of cancer brings several problems and significant mortality, so this project focuses on the choice of experimenting about one of the most common stabilized cellular line: BxPC3 (cell dimension about nine μm). This line is capable to produce important colonies of cells in not so long time, so it is easy to implement experiments.

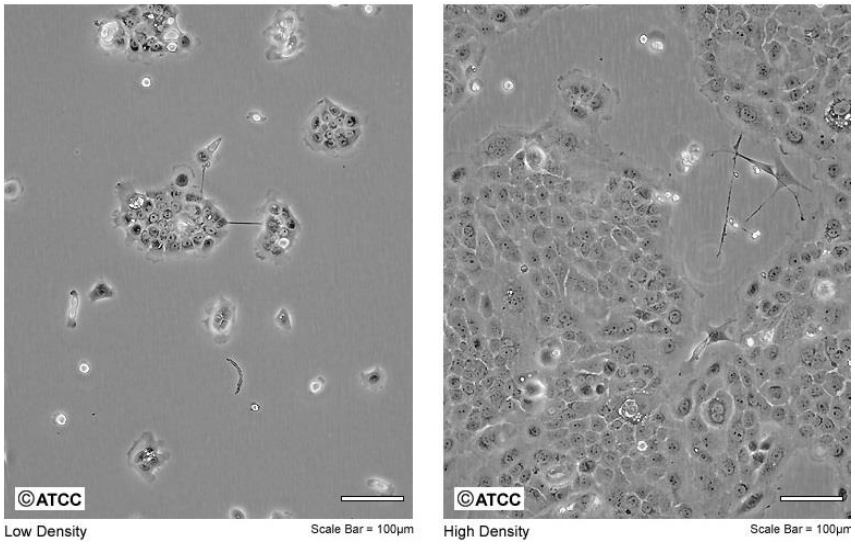

Fig. 1.4 Imaging from electronic microscope of density of BxPC3. [8]

1.2

Fundamentals of Ionizing Radiation and Human Body Interaction

1.2.1 History

Nowadays it is common knowledge to consider radiation as an energy source that, if incident on the human body, causes alterations in genetic heritage and therefore significant immediate or tardive damages.

Thus, this destructive capability can be exploited to eliminate tumoural masses from the body, which is the role of oncology radiotherapy; in the next paragraphs we will see the properties and the consequences induced by different types of radiation, and hence the different results obtained by conventional radiotherapy (taking advantage of the physical characteristics of photonic radiation) and by Hadrontherapy (where the radiation involved is the hadronic one).

Before that it is best to remember what the first discoveries were about the interaction between the body and the radioactivity.

In the Autumn of 1895 the German physicist and mechanical engineer Wilhelm Conrad Röntgen observed a strange and penetrating radiation (called X-Rays) came from his vacuum tube, without immediately knowing the great potential of his discovery. That evening, concluded daily experiments on cathode ray, he had left the Crookes tube covered with black paper sheets on the table, a few meters away from a sheet of fluorescent material. Exiting the laboratory lights, as he came out, he observed an intense fluorescence of green colour emitted by the barium platinum cyanide crystals, of which the plate was made.

Thus, began the study of the radiation that Röntgen called "X" to indicate that it was still of unknown type. The name remained, although many of his colleagues suggested calling it "Röntgen Rays" in his honour.

The characterization of these rays led to the knowledge of high frequency electromagnetic waves, that is, highly energy and low wavelengths, capable of penetrating the bodies and to "see inside".

After that, in the Spring of 1896 the French physicist Antoine Henri Becquerel discovered the natural radioactivity and, two years later, the Polonium and Radio were

discovered by the French physicist and spouses Pierre Curie and Maria Sklodowska Curie.

Fig. 1.5 Portrait of Wilhelm Conrad Röntgen and his discovery. [9]

Although the biological effects of ionizing radiation were not yet well-known at the time, it was understood that exposure to it would cause cutaneous burns, so the idea of treating the tumours using these mysterious radiations was soon accomplished and some surface tumours were successfully treated by applying a radioactive source directly in contact with the skin.

These pioneering treatments marked the birth radiotherapy (RT). Unfortunately, however, a problem arisen immediately which is still today one of the biggest challenges in the radiotherapy field: to really have effectiveness must be achieved so that radiation reaches only the tumour mass, saving as much as possible the surrounding healthy tissues.

The idea of using accelerators in the medical field to focus the beam radiation came to American physicists Ernest Lawrence and Stan Livingston, who in 1931 built the first cyclotron.

At first, patients with salivary gland tumours were irradiated, and neutron beams were used for accelerated deuton collisions up to 5 MeV with a Beryllium target. Considering that such neutrons produce nuclear fragments, these treatments can be considered the first use of ions for cancer treatment.

Subsequently, he was the American physicist Robert Rathbun Wilson who in 1946 had the idea of curing the tumours using charged particles and published his famous article "Radiological Use of Fast Protons". He was called by Harvard University in the same

year to lead the team that would have to design and build the new 160-MeV cyclotron, thus commencing collaboration with Ernest Lawrence at Berkley.

From this work the idea of ion-beam therapy (IBT) was born: during cyclotron shielding studies, Wilson realized that the protons in the matter released energy in a totally different way from a beam of X-rays.

We can now justify this fact with the knowledge of the Bragg peak, high energy release at the end of the typical pathway of the defined hadronic particles.

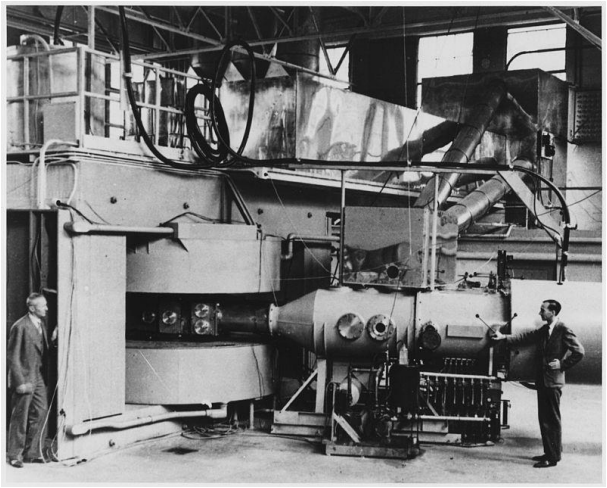

Fig. 1.6 Cyclotron at Lawrence Radiation Laboratory, Berkley (California). [10]

In the next paragraph, there will be an array of radiobiology basics to understand what is the mechanism that causes cancer cell deterioration due to radiotherapy techniques and what are the different modes for more efficient treatments.

1.2.2 Fundamentals of Radiobiology

Radiobiology is the branch of Physics that deals with the interaction of ionizing radiation with biological matter; its study contributes to the development of new methods of radiotherapy and of the prediction of the most suitable treatment for the individual patient, and provides knowledge of the processes underlying the tumour and normal tissue responses.

The interaction between radiation and human body is manifested by the transfer of energy through processes of excitation and ionization of the atoms and molecules involved in the tissue crossed by radiation.

The excitation process, typical of the interaction between optical radiation and matter, consists in the absorption of an amount of energy such as to bring an atomic electron to a higher energy level, usually followed by de-excitation: the electron returns to its fundamental state which results in the emission of photons (quantum of electromagnetic energy) with energy equal to the difference between the energy states involved.

We speak of ionization when the energy absorbed by the material is higher than the typical binding energy of the electrons in the material (ex. the binding energy for the water molecule is about 0.8 eV).

The kinetic energy that characterizes the released electron is given by the difference between the energy transferred by radiation to matter and its binding energy; thus, this could be released, breaking bonds and damaging the matter.

Types of Radiation		
Electromagnetic	Quantum of Energy	X-Rays
		γ-Rays
Corpuscolar	Charged or Neutral Particles	Protons
		Electrons
		Neutrons
		α particles
		Ions

Tab.1.1 Electromagnetic and corpuscular types of radiation.

The incident radiation can ionize directly or indirectly due to energy absorption mode in matter; in fact, the following tables show types of ionizing radiation and how the ionization process takes place.

Modalities of Ionization		
Directly	Radiation can produce directly chemical and biological alterations in matter.	Protons Ions Electrons
Indirectly	Interacting with matter, give up energy to release charged particles, such as electrons and ions. These are secondary products are responsible for biological damage.	Neutrons X-rays γ-rays

Tab.1.2 Modalities of ionization and correspondent type of radiation.

Absorbed Dose

The biological, chemical or physical effects induced in the biological matter by ionizing radiations are therefore related to the physical characteristics of the radiation field and are manifested only because of a transfer of energy to matter.

So, in order to solve the problem intuitively, it is appropriate to introduce a magnitude, the absorbed dose, which represents the ratio between the imparted energy dEa actually absorbed in the mass volume dm, and the infinitesimal mass dm. Ea represents the sold energy average to a certain volume; it is a stochastic quantity and may also have large fluctuations if small volumes or modest fluxes of particles are considered, but if we consider the mean value no longer considered stochastic.

$$D = \frac{dEa}{dm} \tag{1.3}$$

with

$$E_a = R_{in} + R_{out} + \sum Q(J) \tag{1.4}$$

which means that the energy absorbed into a volume V of interaction in matter is the difference between the amount of energy delivered by the directly and indirectly ionizing radiation, which “enters” into the volume considered and the one that exits,

plus the sum of the energies liberated minus the sum of those consumed in each transformation of nuclei and elementary particles in that volume.

The term ΣQ expresses the mass conversion processes in energy and vice versa: it considers, for example, the fact that within the volume considered can occur phenomena such as the production of pairs. In the first case this term gives a positive contribution to the absorbed energy, on the contrary, the contribution is negative.

The unit of measurement in the International System is J / kg, defined as Gray (Gy).

Can we understand if 1 Gy is a significant value and what is the absorbable limit of a human before going to a catastrophe?

If we take the example of raising 1 ° C of a litre of water, we know that it is possible if we supply 1000 cal of energy, which corresponds to 4160 Gy; so, Gray is a small unit of measurement, but this is true only if the energy is absorbed as the heat of the mass. In fact, damage mechanisms are triggered by ionization and not by heat, so a dose of 1 Gy is a high dose.

If we consider that the lethal dose for an average man is 4 Gy, and we make a calculation to find the corresponding energy in cal, we find a ridiculous value comparable to a cup of coffee.

The big difference is that the energy is deposited locally and breaks the bonds into the most important molecule of our organism, causing local or systemic damage.

Thus, if an average person weighs 70 kg and the absorbed dose is 4 Gy, we find an energy value of about 67 cal, much higher than the chemical bond energies between biologically important atoms.

To be able to characterize biological effects, it is important to consider the absorbed dose but also the time frame at which it is administered: The Dose Rate $\frac{dD}{dt}$ is then introduced.

The absorbed dose is an important magnitude when dealing with ionizing radiation, such as it describes the energy transfer (power supply) at the macroscopic level; however, to describe more completely the effects of ionizing radiation on biological matter, it is important to introduce other quantities, such as the Linear Energy Transfer

(LET), Relative Biological Effectiveness (RBE), and the Oxygen Enhancement Ratio (OER). These quantities will be better defined in the following paragraphs.

Densely and Sparsely Ionizing Radiation & Linear Energy Transfer

To understand how radiation interacts with the human body and bring about considerable damage such as carcinogenesis, it is necessary to ask immediately what area is affected by the interaction. Specifically, the incident radiation on an organism interferes with and deposits energy with the fundamental part of the genetic cell: DNA (Deoxyribonucleic Acid).

It is a biological macromolecule made up of nucleic acids (biopolymers composed by monomers, which are nucleotides made of three components: a 5-carbon sugar, a phosphate group and a nitrogenous base) and consisted in turn by nitrogenous bases (adenine, guanine, cytosine, thymine). This molecule has a double helix structure: the nitrogenous bases of a DNA helix combine to the other of the complementarity rule: Adenine joins Thymine and Guanine joins Cytosine.

The sequence of these components gives the DNA the gene information that gives the corresponding cell its function and allows it to transfer that information to the two daughter cells. The ionizing radiation incident breaks the bonds of such molecules, altering the gene information of DNA and thus leading to the mutation of the cells themselves.

For a better understanding of how important this interaction and its consequences are, we must distinguish radiations that deposit locally small energy from those that instead deposit them several, causing hence damages.

So, it is important to define the Linear Energy Transfer (LET) and make a distinction between densely and sparsely ionizing radiation.

Together with time, radiosensitizing substances and phases of the cell cycle, LET represents one of the modulating factors for cellular response to ionizing radiation; it is a term used in dosimetry and describes how much energy an ionizing radiation transfers to the material traversed per unit distance.

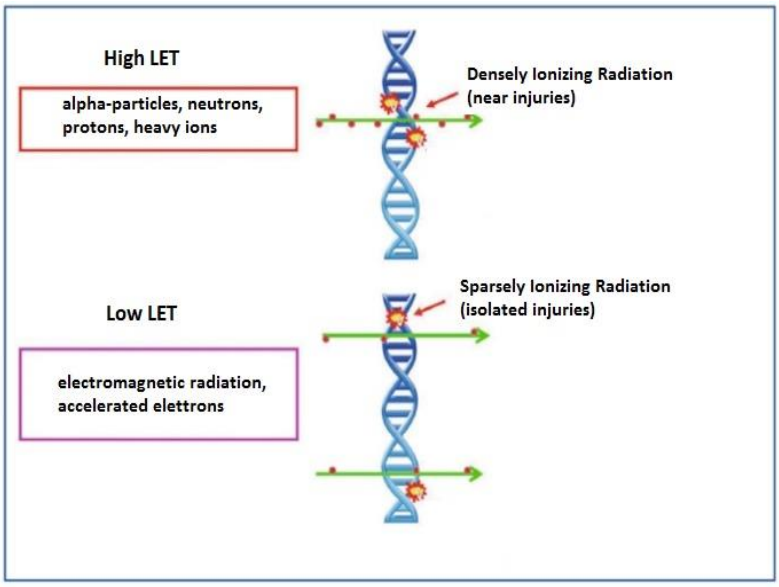

Fig. 1.7 Injuries to DNA due to high and low LET. [11]

By definition, LET is a positive quantity and depends on the nature of the radiation as well as on the material traversed:

$$LET = \frac{dE}{dx} \tag{1.5}$$

where dE represents the average energy transferred locally to matter and dx the infinitesimal displacement of the particle inside the tissue crossed.

For a LET estimate, local energy deposition events must be calculated within a generic dm mass element due to both the primary particle (in the case of directly ionizing radiation) and any secondary particle produced.

The LET calculation is complicated for several reasons: first, radiation is never monochromatic, i.e. characterized by particles or photons all with the same energy. Since LET depends on energy, if radiation has an energy spectrum, it will also be characterized by a spectrum of LET.

Second, the energy sold during the transfer events made by the various particles or photons that constitute the radiation is never the same; secondary particles are then generated at different speeds, expanding the spectrum of the LET.

An average value of LET can be calculated from empirical bases, measuring the energy transferred along the path and mediating the results. So, typically the unit of measurement used is the keV/μm.

For energy release to be considered local, secondary particles must possess kinetic energy such that their path is within the mass element dm chosen; by convention it is considered that the release is local for electrons produced with energies of up to 100 eV, which can move away from the production site up to a maximum of 5 nm.

Thus, LET defined is indicated by LET_{Δ}, where Δ is an energy limit of 100 keV, that is therefore a maximum range for secondary electrons, above which the power supply is no longer considered local; if an energy limit is set so high that all energy losses are considered local, the LET would coincide with the loss of energy for collisions (Stopping Power).

In the case of the LET∞, the total transfer events will be included in the calculation of the energy released, so that the LET∞ will actually be identical to the $-\frac{dE}{dx}$ described by the Bethe-Bloch formula (shown in Chapter 2 and typical of hadronic particles).

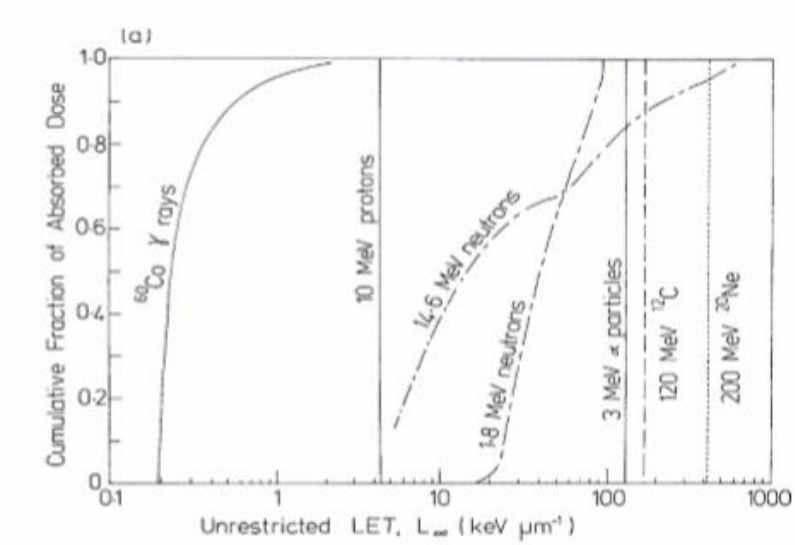

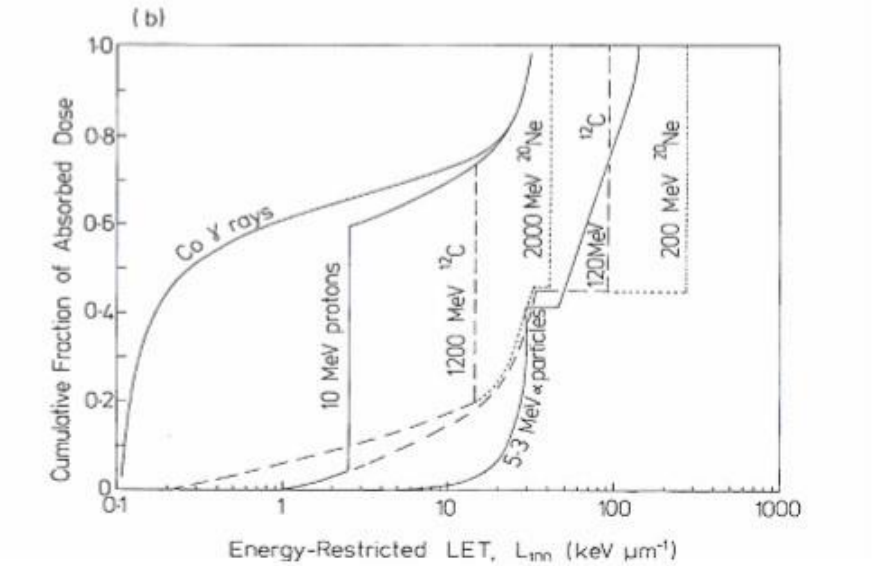

Fig. 1.8 Collective Distributions for several radiations of Absorbed Dose in function of LET in water. (a) Unrestricted LET distribution for spectrum of charged particles from γ-rays of Co^{60}, monoenergetic neutrons of 14.6 and 1.8 MeV for short paths of monoenergetic heavy ions tracks. (b) Energy-Restricted LET distributions with threshold energy for δ-rays of Δ=100 eV, for slowdown spectrum of charged particles from γ-rays of Co^{60}, for α-particles tracks of 5.3 MeV, and for short paths of tracks of some heavy ions with energy of 10 or 100 MeV/u. [12]

Since secondary particles have different speeds and different charges they are characterized by different LET values, so an average value of the LET is calculated, though it does not fully describe the properties of energy deposition events at the microscopic level, it is widely used to characterize the quality of radiation.

Secondary loads in motion may have sufficient energy to construct traces separate from those of the primary charge particle (δ-rays) and thus produce ionization at a distance from it, or they can form only a few ion groups near the primary track itself, if their energy is modest.

The value of this path is different between primary radiation and secondary tracks due to charging and different velocities; for example, if we consider secondary electrons (secondary particles released from indirectly ionizing radiation) and we get a power limit of 100 eV, we find that it is ionized every 5 nm. Considering that the double helix of the DNA has a width of about 2 nm, depending on the value of the distance between

ionization events it is possible to distinguish two types of radiation: low and high LET radiation.

In the first case, we have a Sparsely Ionizing Radiation, so the average ionization distance is about 100 nm. In fact, for electromagnetic radiation, LET is calculated from the kinetic energy of secondary produced electrons, which for X and γ is in the order of 0.1-1 MeV, bringing to LET values between 0.3 and 2.5 keV/μm. For example, LET of secondary electrons from γ-rays of Co^{60} is about 0,23 keV/μm, so the average distance between two ionization events is almost 200 nm.

In the second case, however, the track of primary radiation will be denser of ionization events, and this inevitably leads to greater damage inflicted on the crossed material (and thus on DNA); such radiation is also called Densely Ionizing and includes charged particles, ions and alpha particles, for which the transferred energy values are greater than 50-100 keV/μm. For example, LET of α-particles with energy is 43 keV/μm, so the distance between two ionization events is almost 1,4 nm, with the production of "track core". For carbon ions the LET varies in the range between 15 and 170 keV/μm, which is 100 times greater than in the case of conventional photon beams. [12]

When energy deposition events overlap along the path of the particle they create a "continuum" of ionizations on the track core. The track will also be characterized by a region called "track penumbra", which corresponds to region crossed by δ-rays that move away from the primary trace; the radius of the penumbra € will equal the maximum range of delta electrons. The energy released in the center of the track or in the penumbra is noticeably different. By leaving the core, the deposited energy decreases approximately as r^{-2}. The sparsely ionizing radiations on the contrary have a trace structure characterized by distinct and separate events in space.

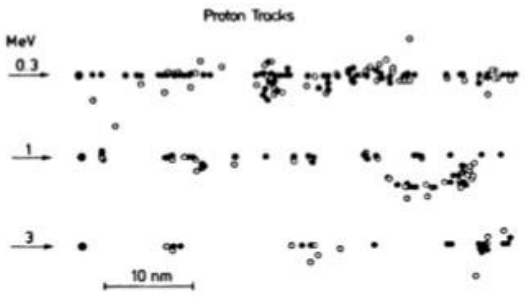

Fig. 1.9 Tracks produced by protons at different energies in water vapor, in case of Ionizations (black dots) and Excitation (white dots). [ICRU36 ref] [13]

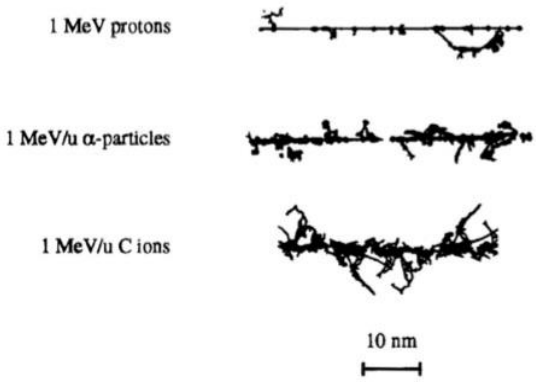

Fig. 1.10 Schematic view of different particle tracks against different biological targets. [14]

So, LET value doesn't completely describe properties of energy deposit at microscopic level, but because of it is a simple quantity it is used to characterize radiation quality.

DNA Damages

As mentioned earlier, the underlying problems arising from the interaction of ionizing radiation with biological matter are the consequent damages to DNA. The fact that the genome is unique within the cell makes it essential that the base sequence be preserved unaltered and that the DNA molecule is not damaged in order to guarantee the proper maintenance of cellular functions.

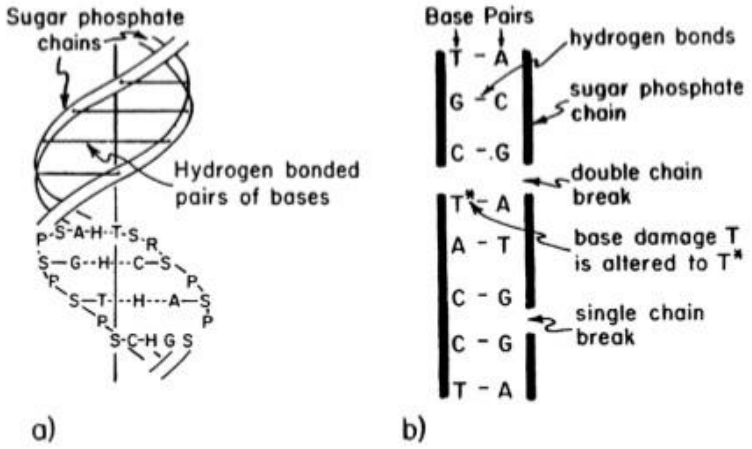

Fig 1.11 (a) Schematic view of DNA, with focus of components of nitrogenous bases; (b) Damages induced by ionizing radiation to DNA. [4]

Interactive radiation can ionize the atoms of the medium in direct or indirect modality.

For indirect ionization refers to the phenomenon whereby a generally low LET and sparsely ionizing moves secondary electrons (delta ray radiation) that will be the protagonists of the ionization of the medium atoms.

In the case of direct ionization, however, this is a radiation (generally) of high LET or densely ionizing that can directly break the bonds established in biologically important molecules such as DNA and water (of which it is composed of 80% (control) our body).

The phenomenon of water radiolysis involves the release of hydrates electrons and highly reactive radicals, such as ROS (Reactive Oxygen Species), capable of producing poisonous molecules to the cellular environment; this topic will be discussed in the next section.

As for DNA damages, if we assume that a deposition event of energy leads to split atomic bonds, the action of a secondary electron energy thus brings the ionization and/or excitation of atoms of the nucleic acids DNA, causing injuries of various degree of danger.

Damage with the most drastic consequences, that could lead the cell to death or mutations which are likely to lead to carcinogenesis, is the Double Strand Break, a phenomenon that breaks both helix chains. If the breaks are close, the repair of the damage is not enough to prevent such disastrous evolution; if such injuries are far enough away, damage can be repaired, as in the case of the Single Strand Break.

This last one can easily be repaired based on the complementary rule: the intact helix acts as a “mold” to rebuild the damaged helix part.

Clearly, densely ionizing radiation, for which ionizations are close, is more likely to lead to DSB lesions, and therefore carcinogenesis or cell deaths.

Other DNA damage can be related to the loss of nitrogenous bases or to the breaking of the existing bond between sugar and phosphoric acid, quickly fixed and no chain breaks; finally, incorrect nitrogenous bases match can lead to denaturation of certain areas resulting in chain broadening, while intramolecular or protein cross linkings alternating cellular vital functions could be created.

Also, considering that during Mitosis, the chromatin, made up of thickened DNA, tends to form chromosomes, so ionizing radiation can also cause damage to them, such as chromosomal aberrations.

From the above, magnitude and type of damage caused by ionizing radiation on DNA depends on the type of radiation, the modality of ionization action, the distinction between DNA in solution and cell DNA and, as we shall now deepen, on the production of hydroxyl radicals due to the radiolysis of water.

Radiolysis of Water

The human body, and therefore the cellular environment, consists mostly of water (> 70% in the body). The incidence of radiation causes ionization and/or excitation of the constituent atoms of this vital molecule, resulting in free radical liberation.

The problem arises when such radicals recombine with each other to give serious chemical damages to the body, such as hydrogen peroxide.

For a good understanding of the mechanism we see what happens to a single molecule of water when it is affected by radiation.

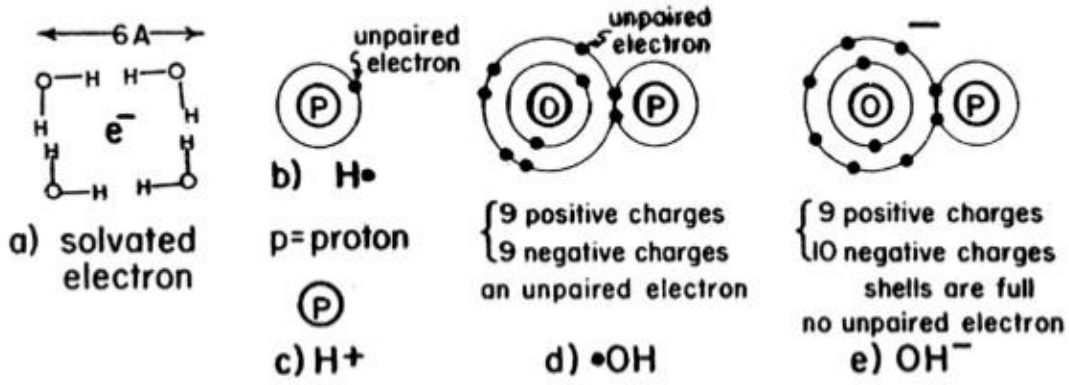

Fig. 1.12 Nature of Reactive Species produced in water by ionizing radiations. (a) Aqueous electron of solvated electron; (b) Hydrogen radical; (c) Hydrogen ion; (d) Hydroxyl radical; € Hydroxyl ion. [4]

The resulting processes can be:

- Ionization: $H_2O + rad \rightarrow H_2O^+ + e^- \rightarrow H_2O^+ + e^-_{hydrate}$
- Excitation: $H_2O + rad \rightarrow H^+ + OH^-$

and lead to the formation of the four primary radiolysis products, each of which will have a different path and a different mean life time. Specifically, $e^-_{hydrate}$ is defined as the “hydrate” electron, because electron in water is never free, but is surrounded by a

complex of water molecules; this is possible because the electron interacts electrostatically with the positive pole of the polar molecule of water and creates the typical structure (Fig.1.11).

The average life of hydrated electron is 2 * 10^{-4} s, much higher than that of the free electron which is of the order of a few picoseconds, because the molecules of water surrounding the electron shield it from the outside, not reacting immediately with the atoms of the surrounding environment. In contrast, for H^+ and OH^- radicals the average life value is about 1 μs. In the specific case of • OH is such that it can move within a range of 12 to 15 nm, so this radical must be created close to the target in the DNA molecule to be able to spread and interact, considering that the chains are 2 nm and bases 3.4 nm between them. Subsequently, the further interaction of these products between them yields secondary products, as can be seen in the reactions below:

$$H_2O^+ \rightarrow H \bullet + \bullet OH$$

$$e^- + H_2O \rightarrow e^-_{hydrate}$$

$$e^- + H_2O \rightarrow H_2O^- \rightarrow H \bullet + OH^-$$

$$e^- + H^+ \rightarrow H \bullet$$

It is also possible to have recombination, which leads to the formation of innocuous or devastating molecules, such as the above-mentioned hydrogen peroxide:

$$e^-_{hydrate} + e^-_{hydrate} + 2H_2O \rightarrow H_2 + 2OH^-$$

$$H \bullet + H \bullet \rightarrow H_2$$

$$\bullet OH + \bullet OH \rightarrow H_2O_2$$

$$\bullet OH + H \bullet \rightarrow H_2O$$

Effects due to Ionizing Radiation	Low LET	High LET
Production of H_2O_2	Low probability of recombination between hydroxide radicals •OH because of a major distance between following ionizations (ionic clusters).	High probability of recombination for smaller distance between ionizations.
Production of Chromosome Abnormalities	Low probability because of a requirement of almost two clusters close enough to involve breaking.	High probability of production for smaller distance between ionizations.
Inactivation of Enzymes	One single ionization is enough to inactivate enzymes.	Waste of energy, so minor inactivation events.

Tab.1.3 Effects due to phenomenon of ionization.

Hydrogen peroxide H_2O_2 is an oxidizing agent capable of penetrating into cell membranes by catalyzing metal ions to form • OH radicals.

Alternatively, it can react with Cl- ions to form hydrochloric acid ClOH. Such species can interact with DNA, causing the typical breaks mentioned above, and therefore critical consequences at cellular level.

The presence of O_2 favors further reactions with radiolysis radicals. In solutions containing Oxygen there is formation of a greater amount of H_2O_2, while the Oxygen is partially regenerated.

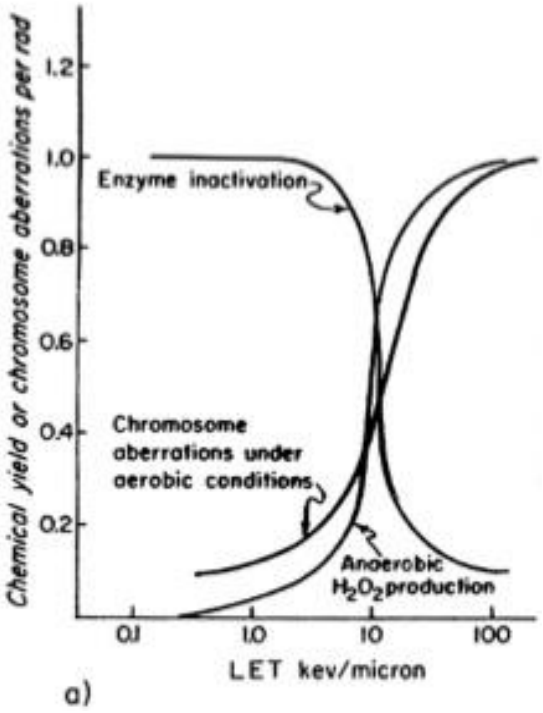

Fig. 1.13 The influences of LET on the following radiation effects on biological tissues: oxygenated water production, enzyme inactivation and chromosome aberrations. [4]

Loss of Reproductive Capacity & Surviving Curves

At the base of our project lies the concept of the mortality, and therefore the loss of proliferative capacity, caused by the incident radiation on the cellular population in question.

The term "cell survival" expresses an unlimited proliferation capability and the survival curves show a percentage of the population surviving at a given radiation dose value; knowing this trend you can choose the most appropriate dose for optimal hadrontherapy treatment.

Numerous studies have shown that for high-LET radiations the cell-survival curve is an exponential decrease, whereas low-LET radiation, the curve has a shoulder at low doses.

Normally, the curve is represented in semi-logarithmic scale, i.e. the x-axis indicates the dose and axis of the ordinates the logarithm of base 10 of survival.

Below is an example of the two trends:

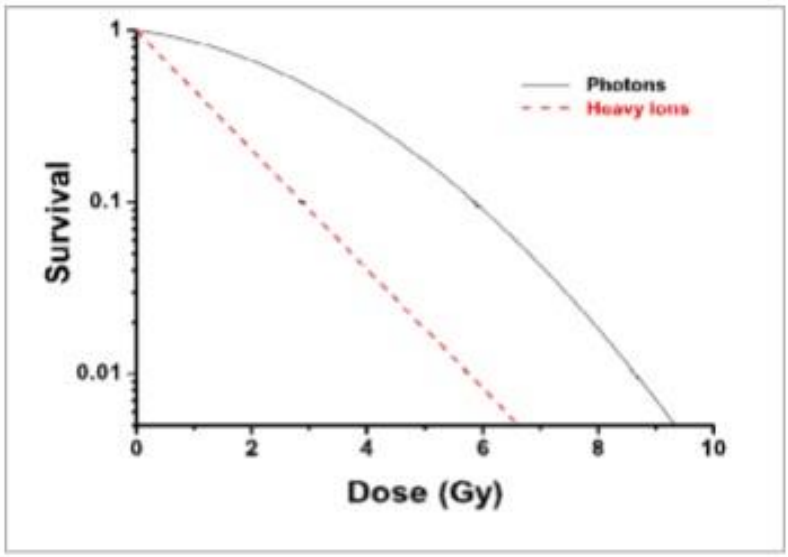

Fig 1.14 Survival curves in case of high and low LET. [15]

This effect is the key to the discussion, the endpoint of radiotherapy; in fact, following the irradiation of a cell population, it is possible to appreciate its survival and so the mortality induced by the treatment.

Irradiated cells do not immediately lose their proliferative capacity, and even in the case of high doses of radiation incident, many cell divisions may occur.

A cell is termed "survived" if it gave rise to at least fifty daughter cells, and then to a significant colony, visible macroscopically; it is possible to reach this size of the colony considering the generation time (the time it takes for a cell to divide into two daughters) of the cell line and the corresponding number of incubation days after irradiation.

We can thus evaluate the Planting Efficiency (or E.P.) and Survival (S) of the population at a certain dose.

Let N be the number of colonies formed, N_0 the number of cells in the initial inoculum, and EP (0) the Plating Efficiency of the Control Samples, then we define:

$$EP(D) = \frac{N}{N_0} \tag{1.6}$$

$$S(D) = \frac{EP(D)}{EP(0)} \tag{1.7}$$

considering that the control samples undergo the same treatment, except irradiation. The EP will, however, always be less than 100%.

In addition to the characteristics of the cellular line, the survival curve depends on the radiation characteristics.

Looking at Fig.1.14, the shoulder at low dose, typical of low LET radiation, is due to the ability of the irradiated cells to operate mechanisms, phenomena that cannot exist in the case of high LET radiation due to the proximity of ionization events, and therefore more general damage.

As already explained, these curves depend on the LET and the intensity of the radiation and the type of cell line under examination, and put in relation to the dose administered to the population in vitro and the number of surviving cells. Starting from the difference between high and low LET we find the equations of the exponential curves.

For low LET radiation, the shoulder at low doses represents a chance to repair the damage due to the low probability of DSB, in which repairable damage is equally distributed on the cell population with a high probability of survival. Higher the shoulder width is, greater the probability of recovering the damage.

Then, increasing the dose is less likely to repair the damage, so the curve becomes an inverse exponential.

Considering these two trends we find:

$$S = 1 - \left(1 - e^{-\frac{D}{D_0}}\right)^N \tag{1.8.a}$$

with S representing the fraction of surviving cells, D the dose given and D0 the dose corresponding to 37% of the survival or reciprocity of the slope.

This last value is the average lethal dose, and is therefore a constant indicating a dose increase able to reduce cell survival by a factor of 1 / e of 0.37.

As for high LET radiation, the curve is a pure exponential and the equation is as follows:

$$S = e^{-\frac{D}{D_0}} \tag{1.8.b}$$

considering that the D / D0 ratio is constant because the damage is no longer repairable for high LET radiation; this means that every dose increase kills a steady cell population.

From the union of high and low LET relationships we find the "Linear-Quadratic Model", which is the expression of different models of radiation-cell interaction:

$$S(D) = e^{-(\alpha D + \beta D^2)} \tag{1.9}$$

In the hypothesis that DSB takes cellular inactivation, consider α as probability that DSB occurs after each single event in the cell (hence define it as a linear coefficient) and β as a quadratic coefficient for generating one DSBs with 2 individual events.

Obviously, for high LET radiations consider the case of inactivation in a single event, ignoring the term β and thus obtaining a purely linear curve.

In general, these parameters depend on irradiation mode and cell line type, and have the size of Gy^{-1} and Gy^{-2}.

Relative Biological Effectiveness

As mentioned earlier, to know whether a radiation is directly or indirectly ionizing, sparsely or densely ionizing and its absorbed dose is not enough to assess the severity of the damage inflicted on the cell population.

Another factor to consider is Relative Biological Effectiveness (RBE), introduced to express the difference in damage caused by high and low LET radiation. It is a ratio between the photon radiation dose (X and γ rays) that produces the same effect and the absorbed dose of the incident radiation necessary to produce the effect studied in the system.

$$RBE = \frac{D_x}{D} \tag{1.10.a}$$

This means that higher the RBE value is, higher is the dose of photon radiation standard that will compensate for the most destructive action of hadronic radiation.

The figure below shows the survival curves referred to X-rays and a generic ionic species and an example of calculating the value of RBE based on the relation (1.10.a) for a level of 10% survival.

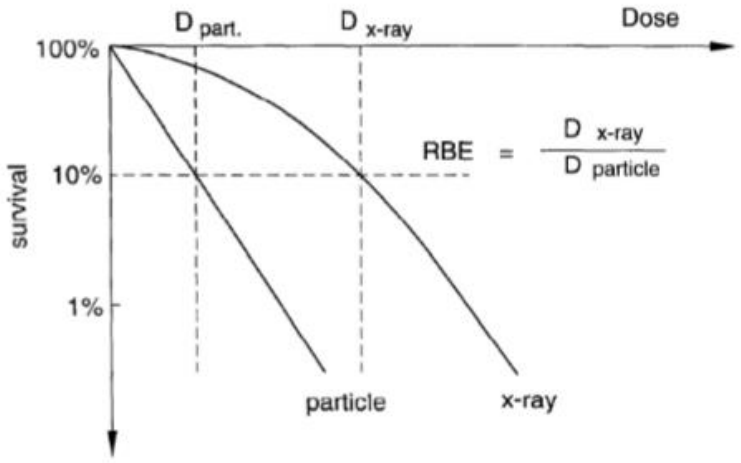

Fig. 1.15 Cell survival curves and RBE definition for a 10% survival level. [16]

Since the definition of RBE is based on the comparison with the X-ray *dose-effect curve*, the RBE strongly depends on the probability that the considered effect is present and, in general, assumes values close to the unit for high levels of dose, where the curves tend to approach becoming almost parallel, and increases significantly as the dose decreases, reaching the maximum value RBE_{α}, given by the ratio:

$$RBE_{\alpha} = \frac{\alpha_{Ion}}{\alpha_{XR}} \qquad (1.10.b)$$

where α_{Ion} and α_{XR} are respectively the coefficients of the linear terms of the effect dose curves that determine, therefore, the initial slope. The values of RBE for Carbon ions of energy equal to 11 MeV/u for different levels of survival are illustrated in Fig. 1.16. For a given ionic species, biological efficacy depends not only on the released dose to tissues, also from initial energy and LET.

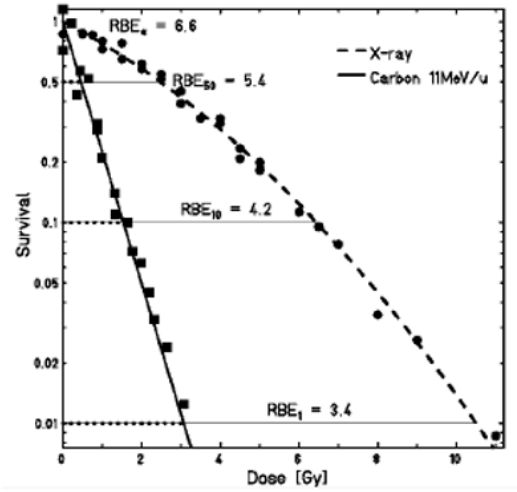

Fig. 1.16 Survival of CHO-K1 cells as a function of X-ray and 11 MeV/u Carbon ions and RBE values corresponding to different dose-effect levels. [17]

The connection between RBE and LET of radiation is inevitable: for low LET radiation, the RBE value is approximately equal to 1, just because the required standard dose that produces the same effect as that incident is about the same.

In contrast, for high LET radiation this value will be greater than 1, and more precisely around 3 for neutrons, and about 8 for alpha particles; thus, to achieve the same biological effect of low LET radiation, a high LET dose of 3 or 8 times lower is sufficient.

The following figure illustrates the different values of RBE between hadronic particles, highlighting an increase in RBE for heavier ions.

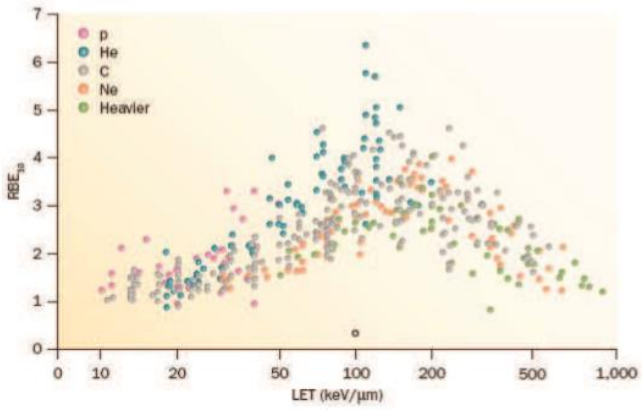

Fig. 1.17 RBE trend from experimental data collected for different types of ions from the Heidelberg Ion Beam Therapy center. A clear maximum is distinguished for LET of about 100 keV/µm, because the density of ionizing events reaches, for that value of the LET, at least one event every nanometer, a typical dimension of the DNA molecule. [18]

For a good explanation of this graph we must refer to the different types of radiation, which will differ with each other for LET value.

Specifically, for very low LET radiation, the rising trend begins with an RBE value equal to the unit, typical of photon or proton radiation (considering that protons are considered "non-invasive" hadrons).

Instead, the maximum values of RBE are for C ion or alpha particles and then have a very high LET decrease. It would be thought that increasing the LET would correspond to a higher RBE, but from the graph we notice it is not so: in fact, the action of the highest LET radiation does not cause high damage due to the low fluence of the radiation which does not allow some cells to be attacked.

At high energies the ionic track has a rather large diameter, the density of the events of ionization is rather low, so that the particles, in that case, behave as "low LET" radiation, producing a repairable biological damage (low RBE). As the energy decreases the track size decreases and the loss of specific energy grows considerably, so that the lesions produced are strongly located and, in most cases, non-repairable (high RBE). At the end of the track, the diameter is further reduced resulting in an increase in the LET such involve overproduction of lesions at the microscopic level, resulting dose dispersion, according to the process known as *overkill effect*. In this last case, the RBE decreases very rapidly over the Bragg peak, assuming very small values, around 0.1 or even lower, especially for very heavy ions, such as Uranium, or for cellular systems with reduced self-repair capacity.

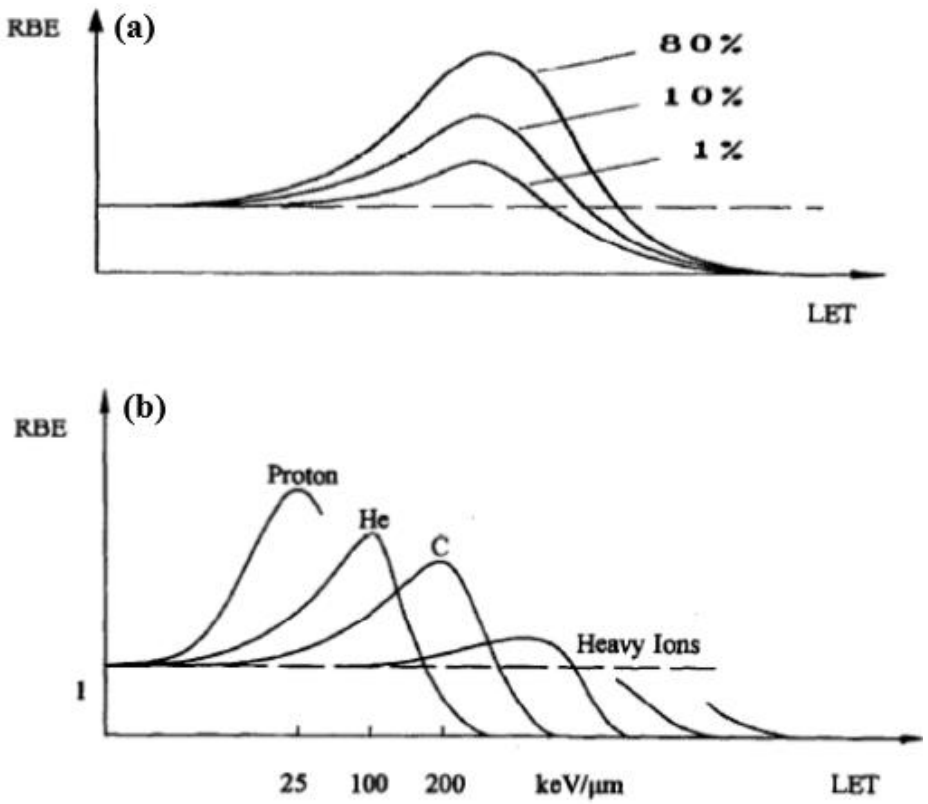

Fig. 1.18 (a) RBE as a function of the LET for a fixed atomic number Z value.

The dose dependence determines different RBE values depending on the survival level;

(b) Schematic comparison of RBE values for different types of hadron particles. For heavy ions, the maximum of the curves moves towards increasing values of the LET while its height decreases gradually. [19]

We will see further which other problems could arise with the use of heavy ions other than the two mentioned in the Hadrontherapy technique.

Finally, it can be stated that RBE depends on the LET of the incident radiation (and hence its ionization density), on the given dose, on the square of atomic number of corpuscular radiation (considering that the LET growth is directly proportional to the mass number), its energy and its ability to protect the damage of the tissue and obviously on radiosensibility due to different cellular phases. The RBE is experimentally affected by the ability to repair the damage, and by this we deduced that if the cells are unable to repair such damage, there will be no maximum outflow, and the survival curve at the reference photon radiation will be purely exponential.

In this regard, it is often preferred to administer a certain dose in multiple sessions rather than in a single irradiation, which would give an initial shoulder of possible damage recovery and then an exponential trend.

This possibility increases the chance of damage to the tumor area, but also creates problems to the surrounding tissues; if, however, the dose is fractionated, the shoulder moves more and more to the right and more and more to the down, so as to guarantee a repair mechanism and a change in survival curves.

The first dose fraction damages cells that are most sensitive to the cell cycle, leaving the more radiosensitive ones to survive. After 12-24 hours, the cells that were previously more radioresistant were in the most sensitive phase, so the administered dose gives mortality to them, and so on for the next fractions.

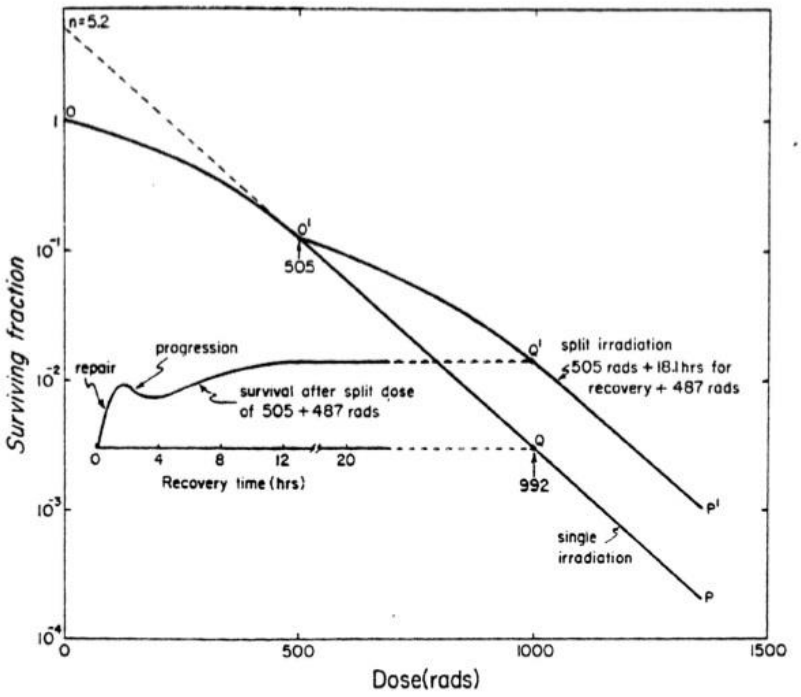

Fig. 1.19 Survival curves for a single irradiation and two subsequent irradiations. [4]

Oxygen Enhancement Ratio

In radiotherapy treatment it has been observed that a higher concentration of O_2 changes the biological results that would be expected on the irradiated medium under normal conditions, facilitating the recombination of radicals that lead to the production of toxic substances, such as hydrogen peroxide.

According to this phenomenon, the OER (Oxygen Enhancement Ratio) factor is defined as the ratio of dose $D_{hypoxic}$ required to produce a certain effect on the tissue under hypoxic conditions and the D_{oxygen} dose it would serve to produce the same effect if the fabric was completely oxygenated in air and under standard conditions.

$$OER = \frac{D_{hypoxic}}{D_{oxygen}} \tag{1.11}$$

A greater amount of O_2 reduces the dose required to produce a certain radiobiological effect; on the other hand, hypoxic tissue, whose low oxygen content is often attributed to poor vascularization of the tumor mass, is less sensitive to radiation, requiring a higher dose to balance the effect.

Clearly, during a radiotherapy treatment it is preferred that the irradiated tissues be as small as possible hypoxic, situation thus very recurrent and about which are also sought to overcome by choosing high LET radiation, that often give a value of OER close to the optimal unit, and therefore prevails as a direct action that involves the breakdown of target cell DNA molecules. (e.g. OERγ = 2.6; $OERn_0$ = 1.1).

We can therefore say that at high LET this effect is almost irrelevant because of the significant density of ionization.

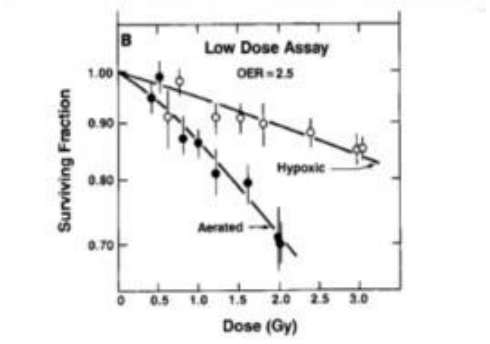

Fig. 1.20 Distributions represented cells under aerated and hypoxia conditions, i.e. cells that are much sensitive to x-rays in the presence of molecular oxygen than in its absence. [20]

Thus, more radiation is sensitive to the presence of oxygen, higher is the OER (therapies are not known on tissues with low oxygen content than they are on normal tissues).

The study of this parameter is a strong indication in favor of the hadrontherapic treatments, as it has been observed that high LET ions have a much lower OER than X-rays. In general, higher the LET and more OER tends to 1, as many experimental observations have confirmed.

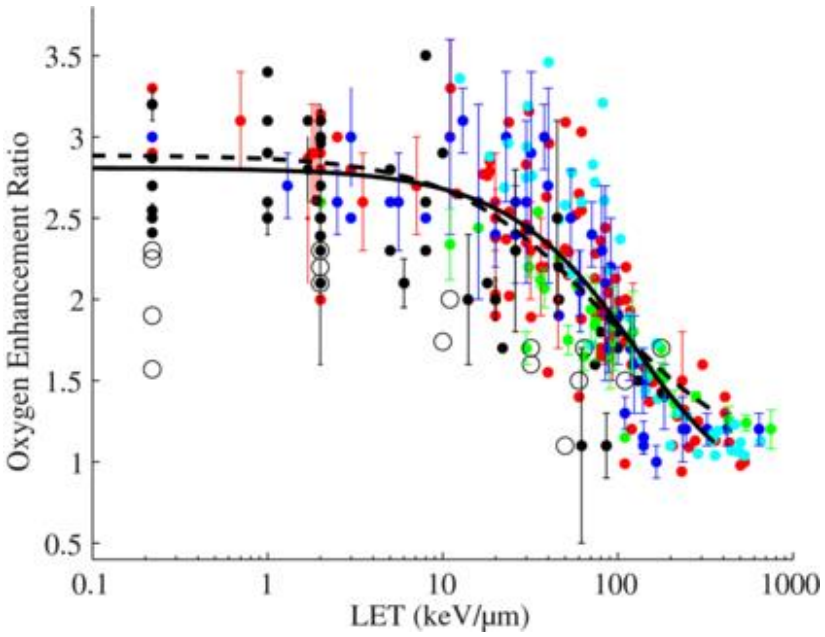

Fig. 1.21 OER trend, decreasing with the increase of LET. [21]

Chapter 2

Conventional Radiotherapy and Hadrontherapy

In oncology medicine is often not enough or possible to resort to the surgical removal of the tumor area to eliminate the problem: techniques such as chemotherapy and radiotherapy go systematically or appropriately to act causing neoplastic cell destruction mechanisms.

Specifically, chemotherapy is based on intravenous injection of substances that alter the reproductive cycle of the cells. Neoplasms are characterized by a high rate of proliferation and are therefore most affected by healthy tissue cells. However, other types of cells of the same high reproductive capacity, such as those of blood, hair bulbs, and digestive mucosa, are attacked by such drugs, leading to patient weakening and hair loss.

In addition, this treatment is very affected by the type of tumor to be cured, as the same drugs that lead to excellent results on a particular tumor may be totally ineffective on others. Finally, the single patient may react to the drug, for example, making it unusable for excessive or fatal collateral effects, or simply responding to treatment in a way that is superior to expectations.

On the other side, the goal of radiotherapy is to use ionizing radiation to prevent cells of a tumor mass from proliferating and therefore reach critical dimension. Clearly, the choice of the radiation depends on type of cancer and its state of growth.

In the cases of pancreatic tumor, it was already shown from the previous paragraph that they have a rapid cellular duplication time and high radioresistance, so for oncological clinical treatment it would preferred a type of radiation that could lead to a greater release of energy locally, such as not to allow the protection of DNA damage.

In fact, for high LET radiations, the survival rate of the cell survival is an exponential decreasing, so there is no shoulder at low doses, which guarantees a time to repair the damage. On the other hand, fractional treatments with low LET radiation are sometimes preferred which allow a time of repair between one irradiation and another, so as not to cause significant damage to the organism and to the surrounding areas.

Hence the need for a radiotherapy technique that exploits the properties of high LET particles: it is introduced the Hadrontherapy, a technique that utilizes the high RBE of hadronic radiation for better radiotherapy treatment.

In many cases the use of Conventional Radiotherapy is used which, with lower costs and thanks to a good dose conformation, is able to reduce the damage, but, in the cases of the most radioresistant diseases, Hadrontherapy offers a better radiotherapy result because of greater local control of tumor growth. The disadvantage of this therapy is in the costs of particle accelerators, much higher than conventional therapies: three times more in the case of protons, ten times more in the case of carbon ions.

In the specific case of this research, pancreatic neoplasms are often inoperable due to their tenacious adhesion to nearby vascular structures. The treatment in this case consists of chemotherapeutic and radiotherapy treatments aimed at increasing local control of the disease, but the pancreas is located in a critical region, that is, in the middle of organs very sensitive to radiation and which may limit the possibility of reaching the tumor enough doses to make it regress; in addition, pancreatic cancer has an inherent radioresistance that reduces the probability of response.

The use of Carbon Ion by Hadrontherapy has shown the possibility of reaching high doses on the tumor with the saving of the neighboring organs and, thanks to its greater biological efficacy, to overcome the radioresistance presented by the tumor.

This can allow control of the growth of the disease and the disappearance of symptoms; other advantages of the therapy in comparison to conventional radiotherapy are the better shape of the dose on the tumor, the saving of nearby organs such as kidneys, intestines, minimization of adverse effects and the possibility of returning to everyday life immediately after treatment. [1]

The two-year disease-free survival in case of pancreatic tumor treated with hadrontherapy is of 45%, in contrast to 20% of conventional radiotherapy. [1]

In the first chapter we focus at the beginning of radiation action observation on human body and the fundamental of radiobiology, now we see what the path has been to arrive to techniques of hadrontherapy.

2.1

Principles of Radiation Treatment

Radiotherapy treatment involves the use of high and low LET radiation beams (the second more used), depending on the specific clinical case, the affected area and the volume of the tumor mass.

Considering the purpose of our project, that is to investigate the correct aid of magnetic hyperthermia in the case of hadrontherapy on tumoural pancreatic population, we will see therefore the principles and the applications of conventional radiotherapy and of the hadrontherapy.

The factors affecting of the tumor response to radiotherapy treatment are discussed in the following, by recalling what was outlined in the first chapter on the principles of radiobiology.

Tumor Control and Normal Tissue Complication Probabilities

The goal of curative radiotherapy is to have good control of mortality in the tumor area; in fact, a tumor is controlled locally when all the present clonogenic cells have been inactivated.

In this regard, it is considered the Tumor Control Probability, a parameter that expresses the probability of having such local control of cancer, and therefore any improvement leads to prolong the survival of the patient undergoing radiation therapy. This probability depends on the dose and is determined by the number of clonogenic cells that survive.

The figure Fig.2.1 shows the trend of local control probability for cancerous tissues and healthy tissues.

The ratio of the dose D_2, relating to the 50% probability of inducing complications to healthy tissues, to the dose D_1 for the same probability of controlling the tumor is called *Therapeutic Ratio*. Radiation therapy aims at increasing this ratio, i.e., at increasing the gap between the curves.

If this relationship is unitary, it ensures a good treatment, since the two curves are not always separated by such a wide gap. It should be noted that the dose-effect curves show a threshold behavior, which is typical for deterministic effects of radiation.

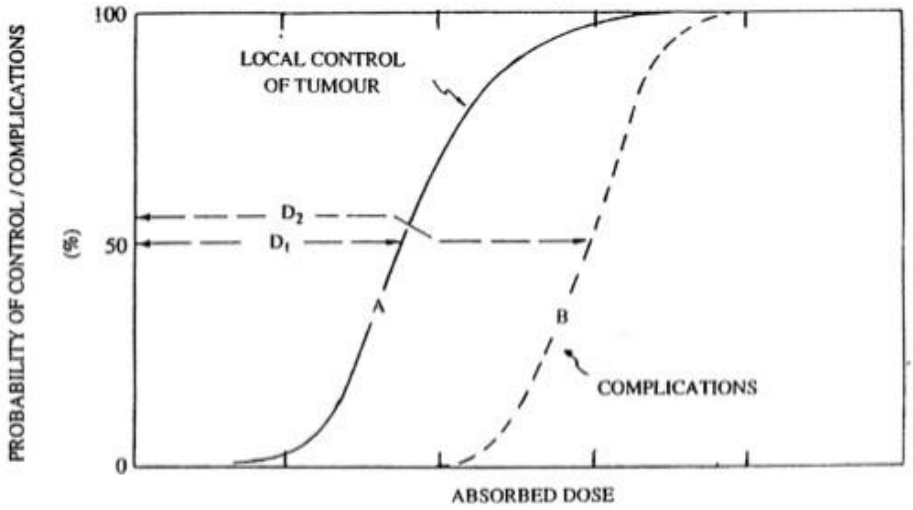

Fig 2.1 Dose – Effect curve for A) Tumor Control; B) Healthy Tissues Complications. [2]

Based on these considerations, the chances of success associated with treatment radiotherapy increase with the ballistic selectivity or irradiation conformity, defined as the difference between the dose delivered to the target and the dose absorbed by the healthy tissues involved.

In particular, the best ballistic selectivity of the beams of hadrons, with respect to the beams of photons and electrons, allows obtaining the same TCP at a lower probability of complications or greater TCP for a given NTCP value.

The cumulative effect for beams of hadrons results in a shift of the curve that describes the progress of the NTCP towards increasing dose values, with consequent increase in the therapeutic ratio.

The optimization of the absorbed dose is only a part of the treatment plan a neoplasm, as we must consider the involvement of other factors, such as the cellular radiosensitivity, which depends not only on the absorbed dose, related to the local cession energy at the macroscopic level, but at least by LET and OER, discussed in the first chapter.

Experiments in radiation biology have found that as the absorbed dose of radiation increases, the number of cells which survive decreases; moreover, if the radiation is fractionated into smaller doses, with one or more rest periods in between, fewer cells die.

This is because of self-repair mechanisms which repair the damage to DNA and other biomolecules such as proteins. [3]

Radiotherapy most often uses dose fractionation to limit damage to healthy tissues and promote mortality in cancer areas.

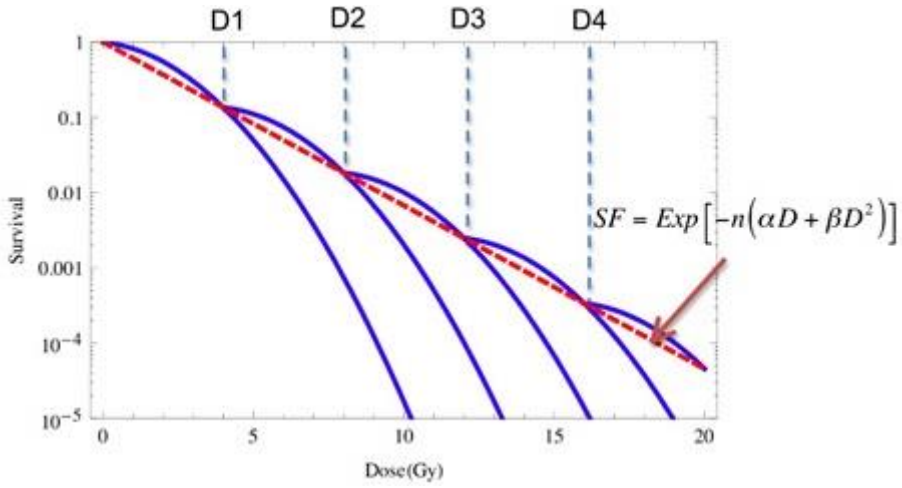

Fig. 2.2 Expected Survival Rate after Fractionation of dose during the radiation treatment. [4]

In fact, generally the tumors show a capability of repairing the damage which is lower than that of healthy tissues, so the method of administering small and frequent doses is used especially when healthy cells and tissues are allowed to repair the damage induced by radiation, without alter the efficacy on the tumor.

The splitting of the dose in radiation therapy involves a "therapeutic gain" because of the increase of the tolerance of normal tissues (for the phenomena of repair and repopulation) and at the same time allows to eliminate the radioprotective effects of hypoxia on the tumor (due to the phenomenon of re-oxygenation).

In the figure it is shown the formula of dose fractionation,

$$SF = e^{-[n(\alpha D + \beta D^2)]} \tag{2.1}$$

where n is the number of dose fractions.

So, below we see the biological factors that influence the response of healthy and tumor cells to fractional radiotherapy, defined the five “Rs” of radiation biology:

- *Repair*: occurs following sub lethal cellular injury which represents damage to the strands of the DNA and which can be repaired by enzymatic processes.

- *Redistribution*: is defined by cells that survive a dose of radiation due to synchronization in resistant phases of the division cycle and redistributing into more sensitive phases of the cell cycle during subsequent doses of radiation. (sensitivity is maximum in G2 and M, intermediate in G1 and minimum in S).

- *Repopulation*: describes cells responding to lethal injury by repopulating or regenerating themselves.

- *Reoxygenation*: occurs when radiation is delivered in multiple fractions to cells that may be relatively resistant due to hypoxia; cells may become re-oxygenated and therefore more radiosensitive.

- *Radiosensitivity*: is typical of the irradiated organ and it is measured by evaluating the 2Gy cell survival fraction, for each considered tissue. A cell is even more radiosensitive the more intense its mitotic activity and the lesser its differentiation. Fast-renewal tissues (marrow, lining epithelia) will be more radiosensitive than slow-renewal tissues (connective tissue, nerve tissue). [29] [30]

Therefore, the Repair and Repopulation processes make the tissues more radioresistant to a second dose of radiation; Redistribution and Reoxygenation make them more radiosensitive.

Target Volume

The target volume in radiotherapy is calculated considering the volume where the tumor mass is present together with the bordering zone of respect in which there may be oncogenic cells; moreover, the identification of the tumor volume depends on the spatial resolution and the diagnostic technique.

Gross Tumor Volume	Extension and position grossly palpable or visible and demonstrable of malignant growth. It is the primary tumor or other tumor mass shown by clinical examination.
Clinical Target Volume	It contains the GTV when present and/or subclinical microscopic disease that must be eradicated to cure the tumor.
Planning Target Volume	Geometric concept defined to select the beam size and the appropriate irradiation techniques, considering the effect of all possible geometric variations and uncertainties to ensure that the prescribed dose is effectively absorbed into the clinical volume.
Treated Volume	Volume planned to receive a specified dose and enclosed by an isodose surface selected and specified appropriately for therapy.
Irradiated Volume	Volume irradiated to a dose considered significant in terms of normal tissue tolerance and is dependent on the treatment technique used. [8]

Tab.2.1 Definitions of volumes involved in a radiotherapy treatment.

In the figure below the design of the different volumes just defined:

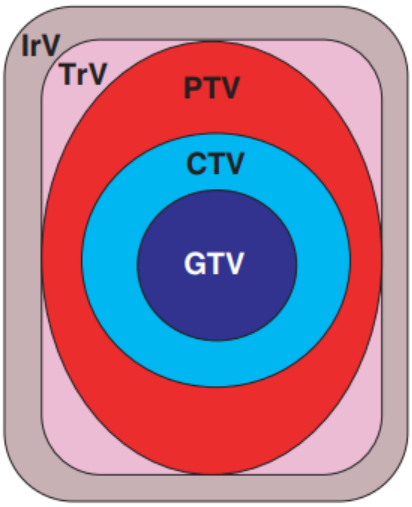

Fig. 2.3 Schematic showing the different volumes used in three-dimensional treatment planning a defined by International Commission on Radiation Units and Measurements Reports 50 and 62. [5]

Before planning treatment, a physical examination and medical history review will be conducted. Next, there is a treatment simulation session, which includes CT scanning, from which the radiation oncologist specifies the three-dimensional shape of the tumor and normal tissues.

Types of Radiation used to Treat Cancer

In the collision with matter, a radiation transfers all or part of energy to the molecules and atoms of the biological volume that absorb it, with consequences that depend on the amount of energy they yield and absorbed by the target atoms.

On the basis of these observations, the radiations are divided into exciters (with energy below 10 eV and the transferred energy is lower than that required to expel the atom one of its valence electrons) and ionizing (with energy higher than 10 eV, where the transferred energy exceeds that of binding and the valence electron is expelled from the atom which becomes a positive ion); radiation with energy less than 1 eV have only a thermal effect on the tissues.

The more common sources of radiation used for cancer treatment are:

- *High-energy photons* that come from radioactive sources such as Cobalt, Cesium, or a linear accelerator (or Linac). Photon beams of energy affect the cells along their path as they pass through the body to get to the cancer. This is by far the most common type of radiation treatment in use today.

- *Electron beams* are also produced by a linear accelerator. These are used for tumors close to a body surface since they do not go deeply into tissues.

- *Proton beams* and Ion beams are the newest form of particle beam radiation. They are charged parts of atoms that cause little damage to tissue they pass through but are very good at killing cells at the end of their path. This means that these beams may deliver more radiation to the cancer while causing fewer side effects to normal tissues. In this case radiation therapy requires highly specialized equipment and is currently only offered in certain medical centers.

- *Neutron beams* are used for some cancers of the head, neck, and prostate and for inoperable tumors. They can sometimes be helpful when other forms of radiation therapy don't work. Very few facilities in the United States offer this type of treatment. Its use has declined over the years partly because of problems with getting the beams on target. Because neutrons can cause more DNA damage than photons, the effects on normal tissue may be more severe. Beams must be aimed carefully, and normal tissue protected. Neutron beams are showing great promise in research with salivary gland cancers that can't be cured with surgery. [6]

It is possible to assemble radiations in two categories:

Photons (x-rays and gamma rays), which are most widely used;

Particle radiation (electrons, protons, neutrons, alpha particles, and beta particles).

Some types of ionizing radiation have more energy than others: the higher the energy is, the more deeply the radiation can penetrate the tissues. Energy is usually used in the range keV – MeV.

The way a certain type of radiation behaves is important in planning radiation treatments; the radiation oncologist (a doctor specially trained to treat cancer patients with radiation) selects the type and energy of radiation that is most suitable for each patient's cancer. [6]

Moreover, radiation beams are administered from outside or inside the organism concerned, according to the size and the type of tumoural volume:

- *External Beam Radiation* is the most widely used type of radiation therapy. The radiation comes from a machine outside the body and is focused on the cancer. This type of radiation is most often given by LINAC (see the Appendix). The radiation is aimed at the tumor, but it also affects the normal tissue it passes through on its way into and out of the body. External beam radiation can be used to treat large areas of the body. Moreover, it is usually given daily over several weeks in an outpatient clinic or treatment center, so it is not necessary to stay in the hospital.

Examples of External Beam Radiation Treatment: Intraoperative radiation therapy (IORT), Stereotactic radiosurgery (SRS), Intensity modulated radiation therapy (IMRT).

- *Internal Beam Radiation* is also known as Brachytherapy, which means short-distance therapy. With this method, radioactive containers are placed into the tumor or into a body cavity close to the tumor. The advantage of brachytherapy is the ability to deliver a high dose of radiation to a small area. It is useful for tumors that need a high dose of radiation or a dose that would be more than the normal tissues could stand if it had to come in from the outside.

Examples of Internal Beam Radiation Treatment: permanent or temporary Brachytherapy, Radiopharmaceuticals.

2.2

Conventional Radiotherapy

Radiotherapy in general is one of the ways in which cancer is clinically fought today, in addition to chemotherapy and surgery.

So far, conventional radiation therapy is understood to mean that radiation therapy carried out through external beams, the X-rays, which have a way of interacting with the living matter, made to release part of their energy at the beginning of the path to then instead have a decreasing exponential trend as the radiation penetrates inside the body.

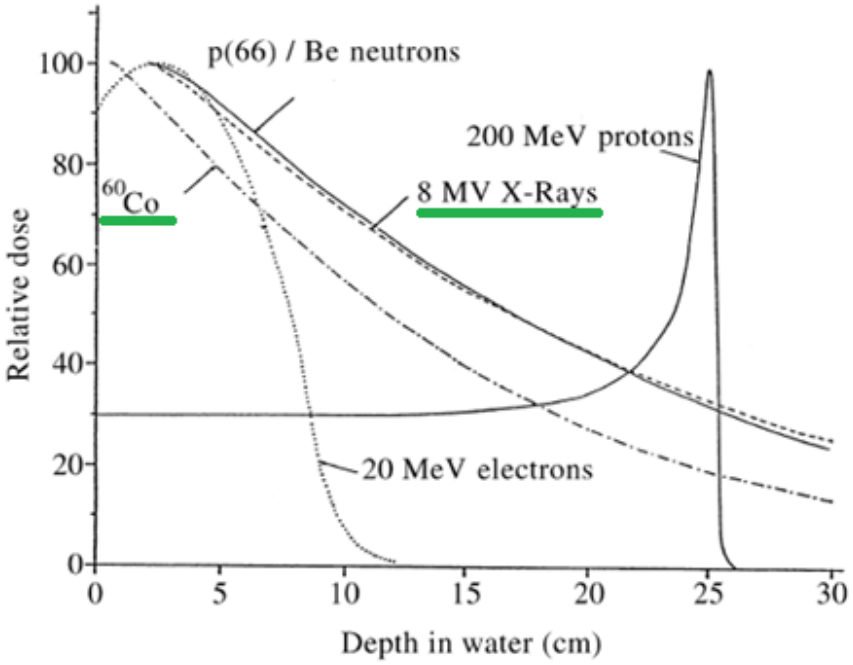

Fig. 2.4 Dose deposition of electrons, photons (X-rays produced by Bremsstrahlung from electrons accelerated to 8 MV, or gamma rays produced as a result of the decay of ^{60}Co) and beams of hadrons, depending on the depth of penetration in water. [7]

The results are therefore good, but it is still a technique that must necessarily be applied in an extremely accurate way to try to have a conformation of the dose to the target and to save the organs or tissues surrounding the tumor itself.

Radiation technology that uses advanced technologies, such as stereotactic radiotherapy (RTD), radiosurgery (RS) and modulated intensity radiotherapy (IMRT),

allows the delivery of high radiation doses to increase the degree of killing of malignant stem cells. [8]

In general, Conventional Radiotherapy is associated with chemo or hormone therapy or with modern biological therapies (monoclonal antibodies, tyrosine-kinase inhibitors) with the aim of having an antitumor effect or additivity for many medium-radiosensitive neoplasms.

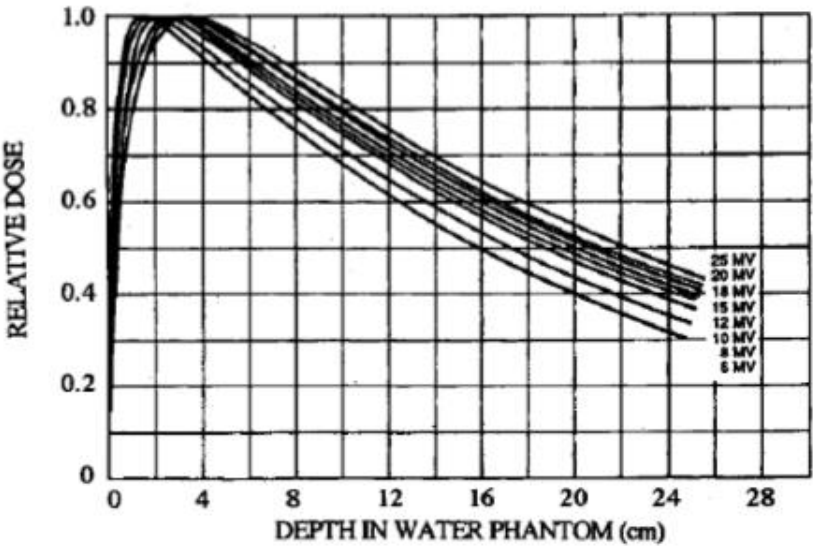

Fig.2.5 Dose-depth curves in water for photon beams having maximum energies in the range of 6 to 25 MeV. [2]

However, in many radioresistant tumors, as pancreas cases, these therapeutic associations seem to have reached a plateau of results that cannot be improved with the current strategies applied in clinical oncology. [9]

So, in cases of pancreatic cancers this type of therapy couldn't give good results in relation of high proliferation ratio of cellular population and proximity to healthy tissues, so we prefer the study of hadrontherapy because of the necessity to deliver radiation energy as close as possible within the volume area.

2.2.1 Mechanisms of Photons Interaction with Matter

The ionizing electromagnetic radiations are classified as X and γ rays, characterized by a wavelength of less than 1 Å.

The distinction between these two types of radiation is made based on their origin: with the term X-rays the electromagnetic radiations emitted during atomic de-excitation or

by accelerated electrons (Bremsstrahlung emission) are indicated, instead the γ rays have nuclear origin.

X and γ-Rays interact with matter mainly according to three processes:

- Photoelectric Effect,
- Compton Scattering,
- Production of Pairs,

each characterized by a specific cross section.

Penetrating the material, a photon beam is exponentially attenuated. This attenuation is due to the number of photons that interacted and to the characteristics of the vehicle crossed. [10]

The intensity of the beam after crossing a thickness x is given by:

$$I = I_0 e^{-\mu x} \tag{2.2}$$

where I_0 is the initial intensity of the beam and μ the absorption coefficient.

$$\mu = n\sigma_{tot} \tag{2.3}$$

where n is the density of atoms that make up the absorbing material and σ_{tot} is the total cross section per atom, due to the contribution of the three interaction mechanisms.

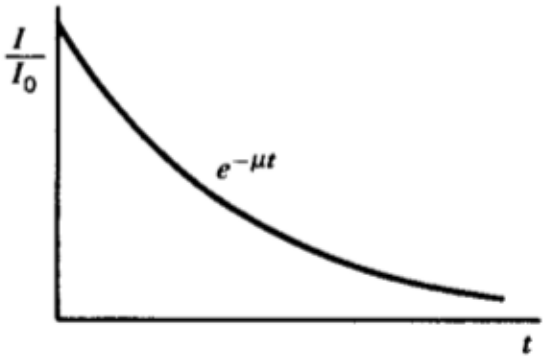

Fig. 2.6 The exponential transmission curve of γ-Rays measured under "good geometry" condition. [10]

Photoelectric Effect

A photon interacts with an atom and ejects one of the orbital electron form the atom.

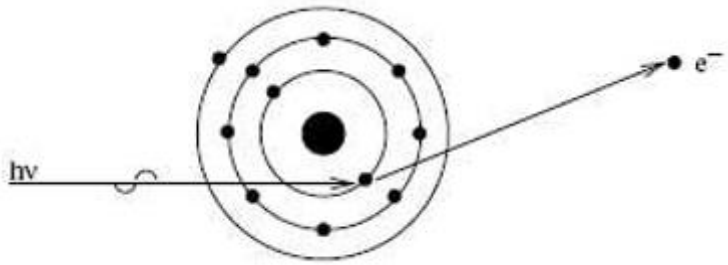

Fig. 2.7 Phenomenon of Photoelectric Effect. [11]

In this process, the entire photon energy is transferred to that of the atomic electron, becoming the kinetic energy of the ejected electron.

$$E_k = h\nu - E_B \tag{2.4}$$

where E_k is the kinetic energy of the electron during the process, $h\nu$ is the energy of the incident photon and E_B is the binding energy of the electron.

Interaction of this type can take place with electrons in the K, L, M or N shells. After the electron has been ejected from the atom, a vacancy is created in the shell, thus leaving the atom in an excited state. The vacancy can be filled by an outer orbital electron with the emission of characteristic X-rays.

There is also the possibility of emission of Auger electrons, which are monoenergetic electrons produced alternatively to a of characteristic X-Ray, internally by the atom.

Since the K shell binding energy of soft tissue is only about 0.5 keV, the energy of the characteristic photons produced in biologic absorbers is very low and can be locally absorbed. [12]

For higher energy photons and higher atomic number materials, characteristic photons are of higher energy and may deposit energy at large distances compared with the range of photo-electron. In such cases, the local energy absorption is reduced by the energy emitted as characteristic radiation.

The photoelectric cross section has a strong dependence on the atomic number Z of the material: materials with high Z are indicated to maximize the probability of

photoelectric effect. Furthermore, the probability of interaction by photoelectric effect decreases with increasing energy, as shown in figure 2.8.

A qualitative development of this cross section can be described in the relation:

$$\sigma_{ph} \propto \frac{Z^4}{(h\nu)^3} \tag{2.5}$$

This trend gives reason for the fact that the photoelectric effect is the predominant low-energy process in materials characterized by a high atomic number; in particular, among the biological tissues the bone allows a high attenuation of the beam, so this phenomenon finds useful application in radiographs.

Compton Effect

The photon interacts with an atomic electron as though it were a free electron. The terms free here means that the binding energy of the electron is much less than the energy of the bombarding photon.

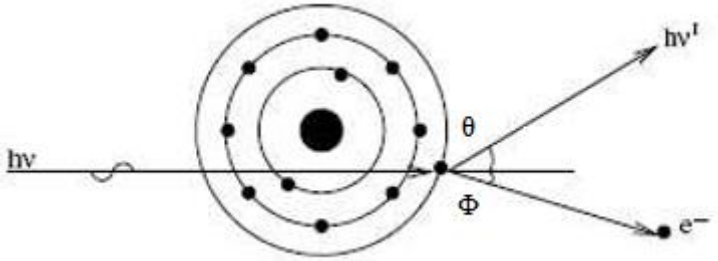

Fig. 2.8 Phenomenon of Compton Effect. [11]

In this interaction the electron receives some energy from the photon and it is emitted at an angle Φ. The photon with the reduced energy is scattered at an angle θ.

The energy hν' of the deviated photon depends on the deflection angle θ and on the hν energy of the incident photon according to the relation:

$$h\nu' = \frac{h\nu}{1+\frac{h\nu}{m_0c^2}(1-cos\theta)} \tag{2.6}$$

where m_0c^2 is the rest mass of the electron, equal to about 511 keV.

The energy transferred to the charged particles by means of the Compton scattering process is therefore given by the difference between the energy of the incident photon and that of the photon scattered at the angle θ:

$$E_k = h\nu - h\nu' \tag{2.7}$$

$$E_k = h\nu \left(1 - \frac{1}{1+\frac{h\nu}{m_0c^2}(1-cos\theta)}\right) \tag{2.8}$$

From this relation we can see that the maximum energy transfer to the electron occurs when θ = π. A simplified relation of the cross section of the Compton effect can be expressed by:

$$\sigma_c \propto \frac{Z}{E_\gamma}\left[\left(ln\frac{2E_\gamma}{m_0c^2}\right) + \frac{1}{2}\right] \tag{2.9}$$

Compton scattering depends mainly on the electron density of the material and it slowly decreases with energy. It predominates with a material having low atomic number, except at very low energies.

Production of Pairs

Pair production occurs at photon energies greater than 1.02 MeV and results in a creation of electron-positron pair due to the interaction of an incident photon with an atomic nucleus.

After losing its kinetic energy, the positron is annihilated, producing two photons traveling in opposite directions.

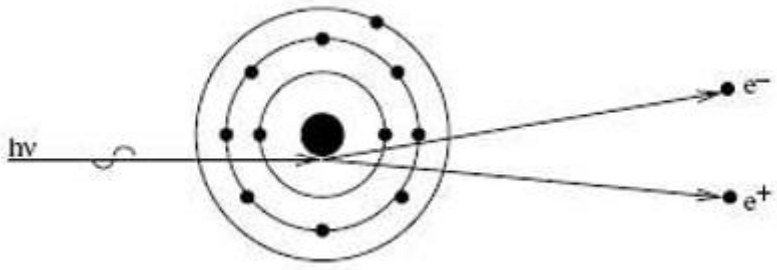

Fig. 2.9 Phenomenon of Pairs Production. [13]

The probability of pair production increase with higher energies and atomic number.

$$\sigma_{pp} \propto Z^2 \ln(h\nu) \tag{2.10}$$

The pair production process is an example of an event in which energy is converted into mass, as predicted by Einstein's equation $E = mc^2$. The reverse process, namely the conversion of mass in to energy, takes place when a positron combines with an electron to produce two photons, called annihilation radiation. [12]

Finally, in figure Fig.2.10 it is shown the trend of the cross sections according to the energy of the incident photon for the three mechanisms just described.

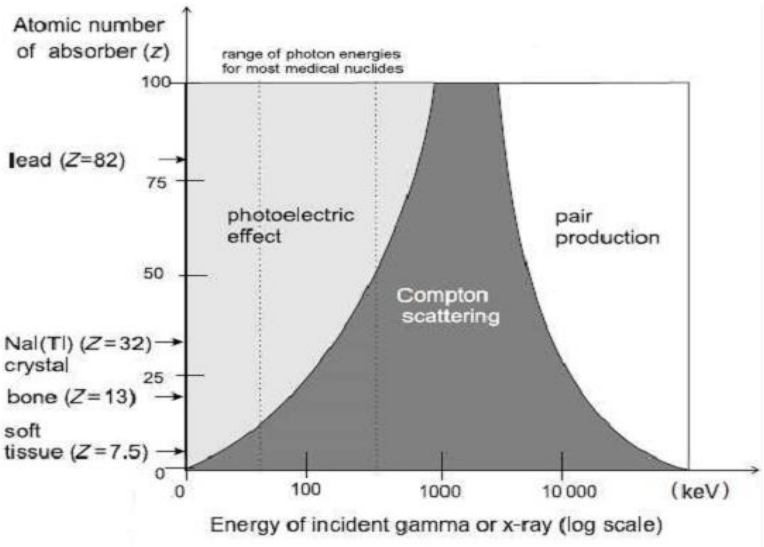

Fig. 2.10 Development of cross sections, in cases of Photoelectric Effect, Compton Scattering and Production of Pairs as a function of the incident photon energy. [14]

Recapitulating, the Photoelectric Effect is characteristic of low energy and high Z, so it is preferred in diagnostic in which low energy absorption is desired to avoid damage to the organism (radiography);

the Compton Scattering is typical of medium-high energies and it is preferred for therapies in which there is a need to good energy absorption (scintigraphy).

Finally, the Production of Pairs is typical of the high energies of the primary photon, and is used in therapies in which the phenomenon of annihilation is exploited to identify a certain area (positron emission tomography).

2.3

Hadrontherapy

Radiation therapy that uses hadronic particles allows an improvement of conventional radiotherapy techniques because this type of radiation interacts with the whole living matter in a different way: it releases little of its energy at the beginning of the path and most of it at a given depth.

It is thus possible to obtain better ballistic accuracy than that provided by conventional radiotherapy and then subsequently increase the energy released to the tumor, thus saving consistently the healthy tissues, the organs at risk that surround it. [15]

The term Hadrontherapy indicates the radiotherapy technique based on the use of *hadrons*, from the greek ἀδρός, *hadrós*, "stout, thick", that are composite particles made of quarks and are affected by strong nuclear interaction. [16]

In addition to protons, the most used hadrons are carbon ions; these deposit in each cell an amount of energy that is twenty times greater than that released by the proton and are therefore particularly suitable for destroying "radio-resistant" tumors, i.e. those that are not sensitive to X-rays and photons.

2.3.1. History

The need to measure ionizing radiation and to know its distribution within the human body has highlighted the development of radiotherapy, with the possibility of obtaining great benefits, from healing of tumor disease to minimizing side effects.

In 1946 the American physicist Robert R. Wilson proposed accelerated protons for localized cancer therapy, based on their favorable depth of dose distribution in the tissue.

The first clinical use of protons was in 1950 for pituitary hormone suppression in metastatic breast cancer.

Proton therapy has been developing slowly for many decades because mainly accelerators built for nuclear research were used.

Efficient proton therapy of ocular melanomas, deep and small tumors requiring 65 MeV protons (corresponding to 4 cm of penetration into soft tissues) developed following initial experiences. More than 15,000 patients have been treated in the world with excellent results. [16]

In Italy, in the INFN National Laboratory of the South, a proton therapy center of this type was created using a superconducting cyclotron dedicated to nuclear physics. Other European centers for ocular melanomas are found in Switzerland, France, Great Britain and Germany.

Heavy ion therapy, however, began in 1970 with Cornelius A. Tobias, who suggested that particles heavier than protons could provide additional benefits, such as reduced lateral dispersion.

In 1993 the first hospital to become operatively dedicated to the therapy was the Loma Linda University Medical Center in California, where protons were used. There are about 30 centers built for clinical hadrontherapeutic purposes. [17]

Most use protons (in the USA, Russia, Japan and Europe), while carbon ion therapy is still on the border between research and clinical practice. Today, the centers where patients are treated with carbon ion beams are: in Germany at Heidelberg and in Japan at the Heavy Ion Medical Accelerator Center (HIMAC) and at the Hyogo Ion Beam Medical Center (HIBMC).

On February 15th 2010 CNAO, National Center of Oncological Hadrontherapy, was inaugurated in Pavia, the first hospital center in Italy (and the fourth in the world, after the United States, Germany and Japan) expressly dedicated to the treatment of tumors by hadrontherapy.

2.3.2. Physics of Hadron Particles

The interaction events between any moving charged particle and the atomic nuclei or the electrons of the medium are:

- Ionization and Excitation
- Coulomb Multiple Scattering
- Nuclear Interactions

We describe in detail only the first two mechanism.

Ionization and Excitation

As already mentioned in Chapter 1, the mechanism mainly responsible for the energy deposition of a moving charged particle is the inelastic collision with the electrons of the medium.

The impacts with these particles are more frequent than those with the nuclei that determine the range of penetration of the beam, that is the maximum distance that the ions travel before stopping.

The events that can occur following an inelastic collision with atomic electrons are essentially two:

- *Ionization*: the electron is torn from the atomic bond, so the original atom becomes an ion and this can compromise a possible link with other atoms, destroying the molecule.

  The frequency of these events is what characterizes the RBE and in fact the LET is defined in proportion to their linear density (indeed the definition of LET is given in terms of energy cession, but the main cause of this transfer is precisely the events of ionization and excitation).

- *Excitation*: passage of an electron from its orbital to a more external atomic orbital, which occurs following a modest transfer of energy by the projectile. Then the electron returns to its original state, emitting a photon of frequency proportional to the energy difference of the two orbitals in question.

Bethe Equation

In 1930 Bethe formulated the equation that describes the release of energy in unit of distance. The relation found is:

$$-\frac{dE}{dx} = \frac{4\pi e^4 z^2}{m_0 v^2} NB \tag{2.11}$$

$$B = Z\left[ln\frac{2m_0v^2}{I} - ln\left(1-\frac{v^2}{c^2}\right) - \frac{v^2}{c^2}\right] \tag{2.12}$$

where:

- $-\frac{dE}{dx}$: *Linear Stopping Power* for charged particles in a given absorber.
  It is defined as the differential energy loss for that particle within the material divided by the corresponding differential path length. This value increases as the particle velocity is decreased.
- m_0: *electron rest mass.*
- e: *electronic charge.*
- N: *number density of the absorber atoms.*
- Z: *atomic number of the absorber atoms.*
- v: *velocity of the primary particle.*
- ze: *charge of the primary particle.*
- I: *average excitation and ionization potential of the absorber.*

For nonrelativistic charged particles (v<<c), only the first term in B is significant. Equation (2.11) is generally valid for different types of charged particles provided their velocity remains large compared with the velocity of the orbital electrons in the absorbing atoms. [10]

Since the term B varies slowly with the energy of the particles, the dependence of $\frac{dE}{dx}$ from the energy is $\propto \frac{1}{v^2}$ (in fact, the lower their velocity and the more they stay close to the electrons, resulting in a greater transfer of energy).

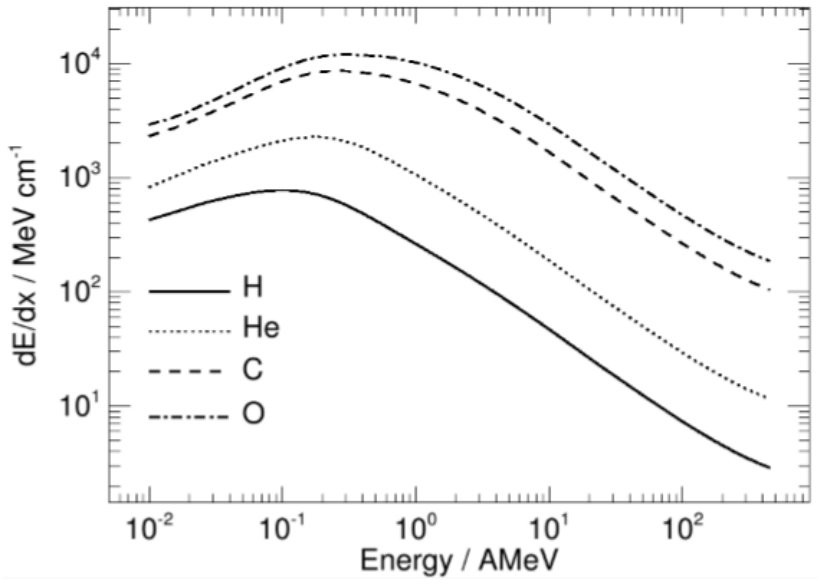

Fig.2.11 Loss of energy for different ions of interest in the therapeutic field as a function of the initial kinetic energy. [18]

In addition, particles with a higher charge will have greater stopping power. As can be seen, $\frac{dE}{dx}$ becomes constant at energies of several hundreds of MeV, while, at low energies, the formula diverges because it does not consider the possible exchange of charges between particles and atoms that would take place over long periods of time, i.e. at low velocities.

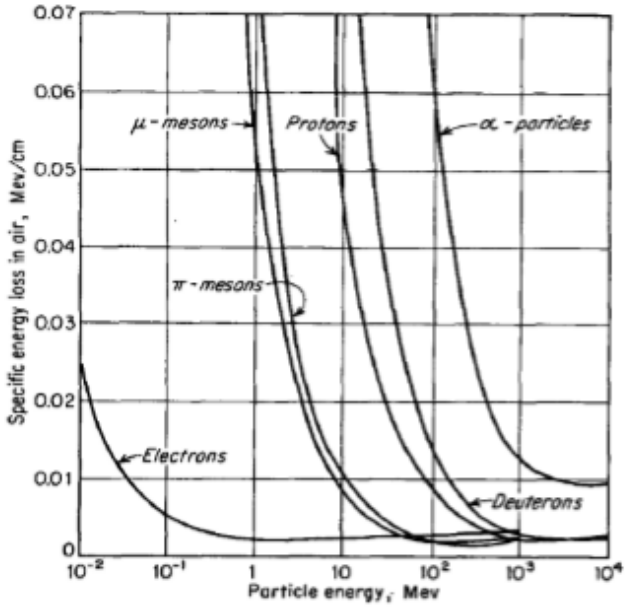

Fig. 2.12 Variation of the specific energy loss in air vs. energy of charged particles shown. [19]

Bragg Peak

Spread-Out Bragg Peak

Stopping power can also be plotted according to the distance traveled by the charged particle in the middle, obtaining the *Bragg curve*. The initial increase is expected due to the decrease in velocity, while the collapse occurs when the particles have collected so many electrons to cancel in charge.

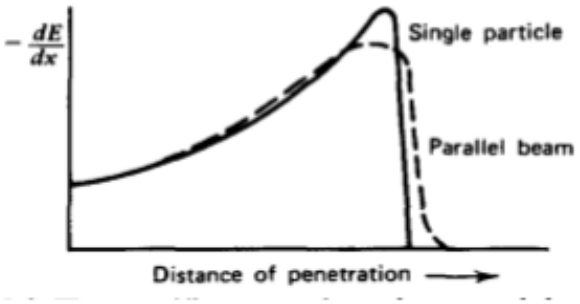

Fig. 2.13 The specific energy loss along an alpha track. [10]

The great clinical advantage of the Hadrontherapy compared to Conventional Radiotherapy lies in the particular trend of the dose profile released in the tissue as a function of depth. In fact, hadrons emit most of their energy at the end of the path, in correspondence with the "peak of Bragg", thus allowing to preferentially damage the diseased tissue. Its depth and its weight depend on the initial energy and the dispersion on the beam, respectively.

Using beams of hadrons lead to radiate in about a minute the deep tumors; the energy used to reach these areas at 25 cm below the skin, following the contour with millimeter precision, is about 50-200 MeV in the case of protons and about 400 in the case of carbon ion, managing to travel about 8 cm inside the organism.

Protons and ions penetrate the tissues without deviating much from the initial direction, and with their electric charge they take electrons from the molecules of the tissues, so depositing most of their energy in the last centimeters of path.

This circumstance allows to preserve the healthy tissues crossed in the best way, since, when all their energy is spent, the charged hadrons stop.

The release of the dose inside the target body occurs without producing Bremsstrahlung and therefore without irradiating tissues or organs deeper than their range (unlike electrons or gamma rays), making this radiotherapy particularly suitable for the treatment of tumors close to said organs "critical". [20]

However, since the Bragg peak is too narrow to cover a tumor often even a few centimeters, it is necessary to vary the energy of the particle beam, reducing it in small steps, so as to add many narrow peaks and achieve the desired effect.

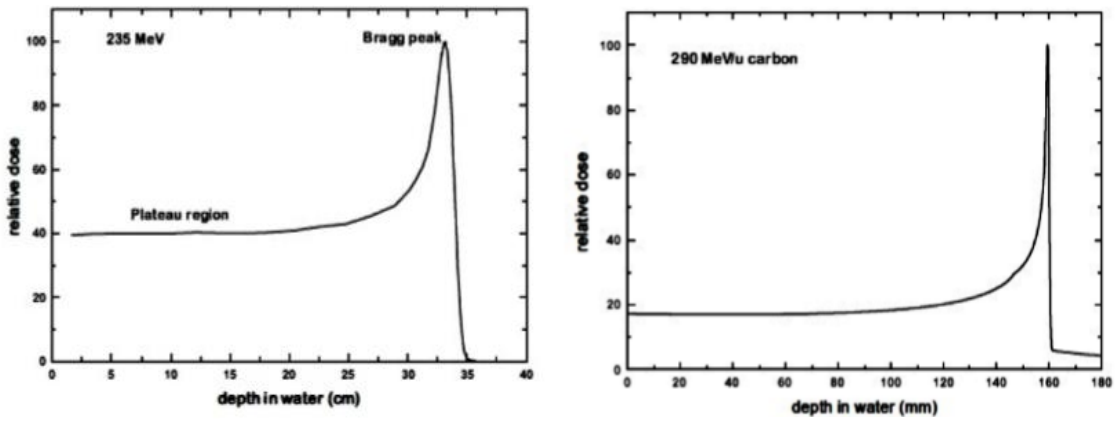

Fig. 2.14 Representation of two Bragg peaks: protons (left) and carbon ions (right). [21]

2.3.3 Systems to draw Spread-Out Bragg Peak

Among the measures that can improve the performance of radiotherapy treatments with hadrons, the choice of the beam transport system is without a doubt important.

It has the task of bringing the beam from the accelerator to the patient's body, with the lowest possible energy dispersions, the best possible collimation and an optimal delivery system of the dose (the terminal part, from which the ionizing radiation comes out before entering the tissues organic). This last part, in fact the beam delivery, is the most complex, since it must shape the beam to its optimal shape to respect the dose profile established in the treatment plan. [22]

Currently there are two beam delivering methods, *passive* scanning and *active* scanning with which it is possible to obtain the Spread-Out Bragg Peak (SOBP).

Passive System

The enlargement of Bragg peak and variation of the irradiation characteristics are obtained by inserting absorbent materials; these materials, causing phenomena of dispersion and loss of energy, are the causes and the modulation of their velocities.

The energy beam fixed by the accelerator is firstly widened laterally using diffusers, with an energy sufficient to cover the volume of the target, and the velocity is then modulated so as to obtain a SOBP as much as possible according to the longitudinal section of the cancer.

The type of passive irradiation has the advantage of not requiring accelerators capable of reaching the velocity during irradiation and this method is essential to reduce the energy of hadrons from the necessary.

The insertion of absorbing materials and collimators along the beam line, however, increases the effects of nuclear fragmentation. This, together with the fact that the deposition has passed over an area, do not give a high quality of radiation conformational radiation therapy. Another disadvantage in the technique is that it is a specific form of the tumor.

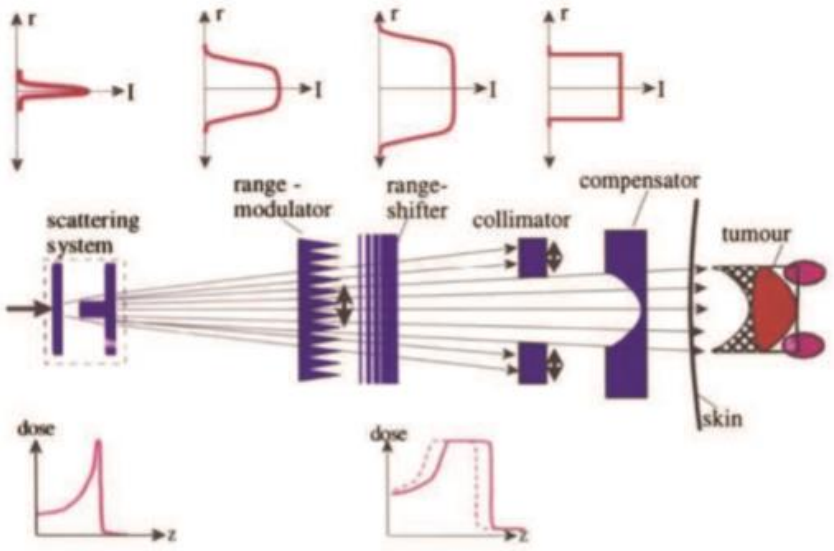

Fig.2.15 Schematization of passive scanning. To better understand the effects of the different modules for modifying the beam, transversal intensity profiles have been shown at the top, from which the enlargement and the cutting off are clear. At the bottom there are the forecast of the longitudinal dose deposit, first to peak of Bragg, then modulated to SOBP (dashed line) and moved rigidly to the desired range (continuous line of the second graph). The dotted area next to the tumor indicates those healthy tissues on which a not inconsiderable dose distribution due to the compensator effect is expected. The purple ellipses indicate organs at risk to avoid which it was decided to distribute the dose on healthy tissues before the tumor. Clearly this scanning method is far from ideal. [23]

So, the beam delivery method described above has clear limits in the distribution of the dose obtainable from a beam thus delivered. Based on interactions between ions and matter, whose description, as seen, is often approximate, it does not allow to predict with a good resolution how the dose will be deposited.

Active System

Active beam distribution systems in the plane normal to its axis are based on magnetic devices which deflect charged particles so as to conform the spatial distribution of the dose to the various sections of the target volume.

They consist in directly varying the energy of the incident beam using more powerful accelerators (synchrotrons).

The deflection of the beam takes place through a magnetic deviation system, described by the Lorentz Force:

$$\vec{F} = q\left(\vec{v} \times \vec{B}\right) \tag{2.12}$$

where q is the charge of the particle, $\vec{v}$ the velocity, × the vector product and $\vec{B}$ the external magnetic field applied to the moving load.

Having to deviate a beam of particles, not single ions, the problem of the energy straggling occurs again, seen between the uncertainties related to the range.

In fact, an uncertainty on the energy of the single hadrons of the beam implies an uncertainty on their velocity and, therefore, on their deviation by the magnetic field.

The fundamental role of the beam monitor used in active scanning comes into play: after deviating the beam it passes through this sensitive detector which registers its position with uncertainty of 0.1 mm, direction and intensity, thus eliminating the uncertainty about enlargement of the beam due to the deviation suffered (at least within the sensitivity of the beam monitor). The data collected by the beam monitor are immediately transferred to the computerized control system of the treatment plan (TPS, or Treatment Planning System).

It is therefore a first phase of monitoring on the initial conditions of the beam: direction, position and energy. Energy is known directly from the acceleration system. This beam delivery system does not deliver enlarged beams, individually modulated to obtain the SOBP.

It is instead of bundles highly collimated (from 3 to 10 mm FWHM) called *pencil beams* from which sum the SOBP is obtained. A fraction of the treatment is therefore constituted by the irradiation with many pencil beams, whose direction is rapidly changed by the electromagnets according to the instructions of the TPS.

It is not necessary to confuse the splitting of the bundle with the fractionation of the treatment: the last one concerns the scheduling of several sessions (fractions) that sometimes distance themselves from a few hours, sometimes days (depending on the amount of dose administered in the session).

The splitting of the beam into pencil beams rather than its mechanical modeling concerns the administration of the dose during a single session.

Within each fraction of the treatment, to maximize the efficacy of the therapy, we try to distribute the most homogeneously possible dose on the tumor volume. Therefore, we divide the tumor volume into different slices, we calculate the energies necessary to reach each of them and we irradiate them one by one through different pencil beams (whose number depends on the surface area of each slice).

In order to exploit this beam delivery system, the healthcare structure must be equipped with a synchrotron (see the Appendix), acting on which the TPS can quickly regulate the energies of the beams to irradiate all the slices in a single session. [25]

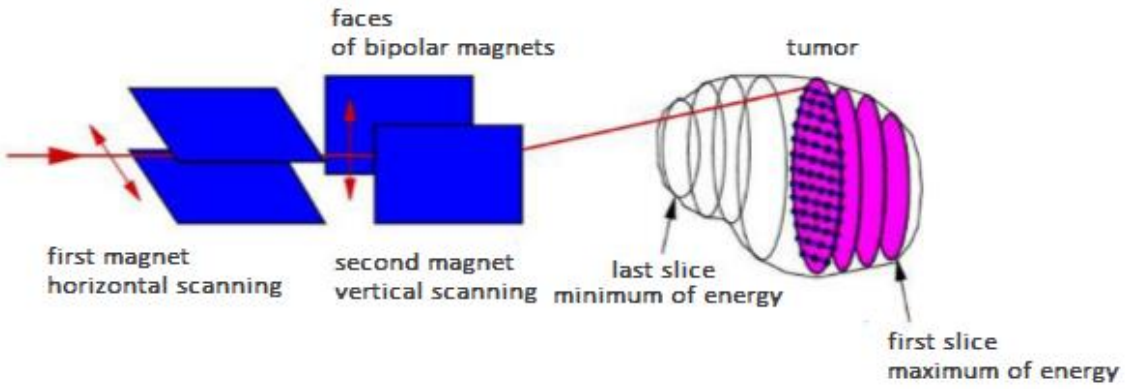

Fig. 2.16 Scheme of active irradiation: the tumor is divided into slices and each of these at target points. The area to be treated is virtually divided into cubic volumes, called spots, which are irradiated individually. The spots are normally grouped into slices, arranged transversely to the direction of arrival of the beams, and are scanned sequentially. Each spot is hit by the collimated beam provided by the accelerator, calibrating the energy so as to give rise to a Bragg peak located in its central point. [4]

So, the active irradiation method therefore has the advantage of not having any restrictions about the shape of the target and, at the theoretical level, any distribution of three-dimensional dose can be generated. It also minimizes the losses of the beam and the contamination of it by fragments due to the passive method.

The dose is deposited with the precision of the millimeter, thus preserving the critical organs placed near the tumor region. It is a method particularly suited to the treatment of head and neck tumors, in which case the patient is immobilized with appropriate masks.

The dimensions of a high energy proton beam used in hadron treatments are about 10 mm, and the width of their Bragg peak is about 20 mm; therefore, to deposit the

required dose on the entire volume of the tumor to be treated, certainly larger than those just considered, it is necessary to regulate the irradiation geometry accordingly.

This is the necessity for the development of Conformational Radiotherapy [18], a radiant treatment for external beams that conforms to the real extension and development of tumor mass.

Consider the dose profile as a function of the depth of a monoenergetic proton beam, which shows the Bragg peak at the end of the range. The overlapping of proton beams of different adequately weighted energies yields the formation of the SOBP (spread-out Bragg-peak) [24], which provides a uniform dose over the entire tumor region.

2.3.4 Problems of Fragmentation of Ions after the Interaction with Body and Lateral Dispersion

Since the interactions between the penetrating particles and target atoms occur randomly, the loss of energy is from consider itself a statistical process, subject to fluctuations around the average value, that is it reflects in a dispersion effect also of the values of the range, known as the range phenomenon *straggling*.

The distribution of energy loss is characterized by an almost Gaussian trend produced by the numerous multiple diffusion processes that affect, in greater extent, the entire ion beam, rather than the single particle, leading to an increase in the width of the Bragg peak.

As the ionic species varies, the effect of *range straggling* varies with the inverse of the square root of the mass number so that, with the same path, the more ions they have a narrower Bragg peak, a more rapid distal fall and a tail due to the fragments produced in reactions with target nuclei.

Furthermore, the *dispersion effect* it becomes more significant as the energy of the incident increases in order to, as the growing of penetration depth, the width of the Bragg peak increases, while its height tends to decrease due to the greater number of nuclear reactions occurring along the beam path.

In the tissues the dispersion pathway associated with a proton beam is about 1% while for Carbon ion is around 0.03%, as shown in Figure 2.Q, demonstrating the best qualities of the Carbon beams compared to protons.

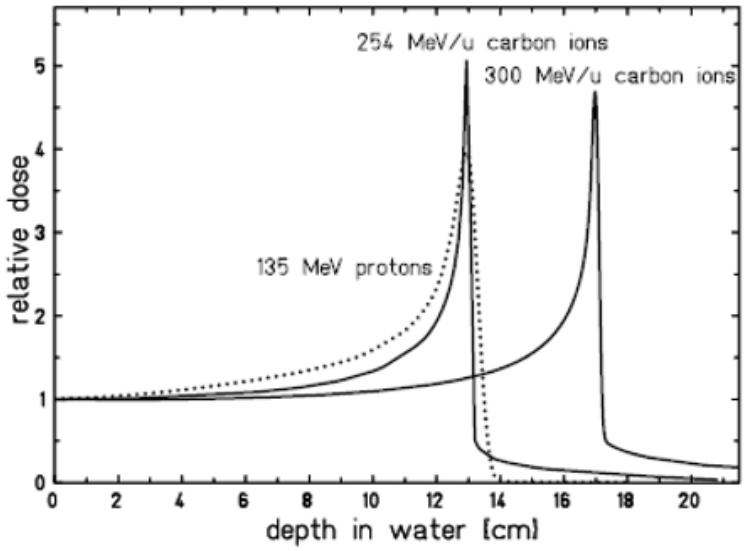

Fig. 2.17 Comparison of dose distributions with depth related to protons and carbon ions of different energy. It is observed the attenuation of the Bragg peak with the increase of the energy of the Carbon beam, the tail due to the fragmentation process and the better definition of the range in comparison with the protons. [25]

The *lateral scattering* phenomenon is the product of repeated elastic collisions due Coulomb interaction between projectiles and target nuclei, to which the contribution is added of nuclear reactions, especially in the distal region of the Bragg peak where the particles primary ones have stopped definitively and the residual dose is associable only to the contribution of the fragments.

The angular distribution of particles with respect to the incidence direction, after having gone through a certain thickness of matter, it can be interpreted as the result of multiple small-angle deflections, highly probable, and some rare scattering event at larger angles.

From the comparison with the experimental measures, it is possible to describe, with a good approximation, the lateral dispersion as a function of the angle α of deflection by a Gaussian distribution, with standard deviation σα given by following empirical formula (Molière, 1948):

$$\sigma_a = \frac{14.1\ MeV}{\beta pc} Z_p \sqrt{\frac{d}{L_{rad}}\left(1 + \frac{1}{9} log_{10} \frac{d}{L_{rad}}\right)} \qquad (2.13)$$

where p is the moment of the particles, L_{rad} is the length of radiation and d the thickness of the material crossed. From this formula we deduce that multiple diffusion

becomes more significant decrease in energy and that, with the same path within the medium, this effect it is more affecting the lighter ions.

From the point of view of clinical applications, the lateral dispersion of the beam assumes a fundamental role, especially in the case where the tumor volume is placed near critical organs. In these cases, the uncertainty on the range of the particles represents a big one limit.

In the figure below, it is shown a comparison in terms of lateral dispersion for beams of photons, protons and carbon ions from which emerges clearly that protons suffer more from the lateral scattering phenomenon than to photons for a penetration depth of more than 7 centimeters, while deflection suffered by the carbon beam is kept below the millimeter for a maximum distance of 20 centimeters.

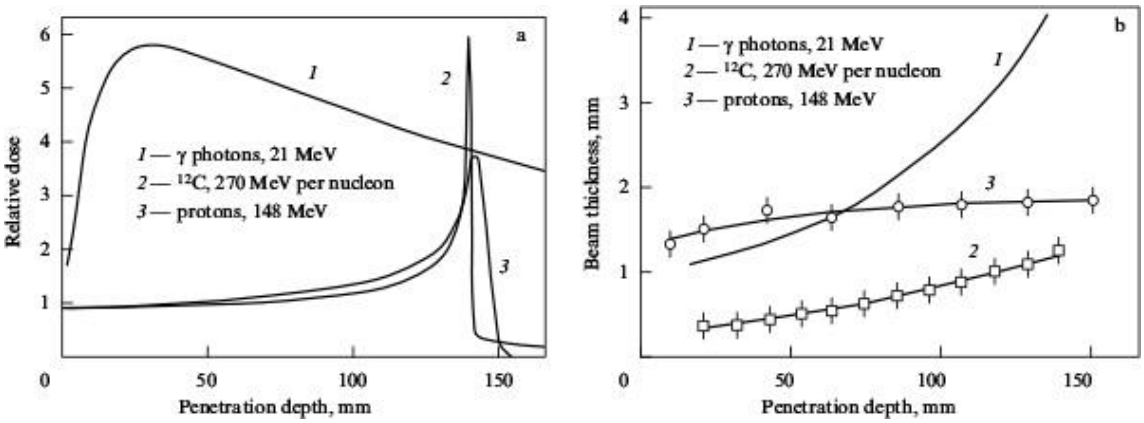

Fig. 2.18 Right: Comparison of the angular dispersion experienced by photons, protons and carbon ions as the water penetration distance varies. It is observed that the range of the carbon ion beam is equal to 14.5 cm. [26]

Differences between Heavy Ions and Light Ions

- Heavy ions are less affected by Coulomb's multiple diffusion and therefore by *lateral scattering*, so the beam remains much more uniform and the Bragg peak is more localized. This leads to an application of the most precise dose and conforms to the areas to be hit, making it easier to avoid healthy organs at risk.

- The phenomenon of *energy straggling*, which leads to a mitigation and enlargement of the Bragg peak, is once again more marked for light ions, so the use of heavy ions makes the application of the dose more selective, distributing a larger percentage in the peak area.

- Heavy ions are subjected to the phenomenon of *nuclear fragmentation*. The heavier they are, the more likely it is to produce fragments from the much lower mass and the much higher range. The fragments obtained from the primary beam in the distal zone of the tumor carry around further dose and, having the same velocity as the resulting ion, are able to travel far higher due to their lower weight.

  Beyond the peak the tail has a significant amplitude, due to the greater emission angle of the fragments with respect to the lateral scattering angle (due to multiple lateral scattering of the primary radiation).

  The tail effect over the Bragg peak requires a study of the beam geometry in order to avoid placing organs at risk immediately beyond the tumor zone, with respect to the direction of the beam.

  After all, always thanks to nuclear fragmentation, the task of reconstructing dose deposition (important for all ions, given the numerous theoretical and experimental uncertainties) is considerably simplified. In fact, fragmentation produces many secondary loads and prompt photons whose detection is fundamental for beam monitoring purposes.

  Light ions are not totally immune to nuclear fragmentation anyway: the protons can induce it in the target nuclei, avoiding the inconvenient tail effect and producing prompt loads and γ-rays (though in smaller numbers).

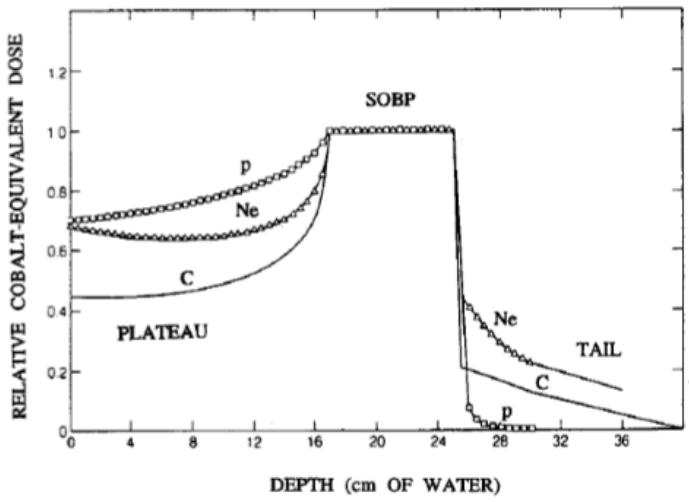

Fig. 2.19 Dose transmission curves with the depth that are obtained with a controlled variation of the energy of the proton beam, Carbon ions and Neon ions. [2]

- Carbon and Oxygen ions, again because of nuclear fragmentation, can achieve unstable configurations that decay β+. The mass of these is slightly lower than the initial mass (^{12}C -> ^{11}C, ^{16}O -> ^{15}O), but the charge remains unchanged and therefore in the collision the range of unstable configurations is slightly lower.

  The β+ emitters are an excellent confirmation of the beam range, as they constitute the principle of PET imaging techniques, on which the high medical experience now allows a good confidence in the reconstruction of the emitter's position.

  It would be incorrect to say that light ions do not allow to exploit PET techniques, but since they themselves cannot become nuclei that decay β+, the emitters resulting from the interaction of light ions with the propagation medium are nuclei of the medium itself. These, following a possible fragmentation, remain stationary, leading to a profile of β+ activity that is certainly less correlated to the position of the Bragg peak.

- Heavier nuclei have higher RBE and LET. Indeed, they are more efficient in producing irrecoverable biological damage from the cellular auto-repair mechanisms of DNA. This makes them particularly appropriate for the treatment of more radioresistant tumors.

- Light ions have higher OER, which indicates they are less efficient in damaging hypoxic tissues. The central areas of extensive or rapidly developing tumors become hypoxic due to the low blood flow rate, so even for these tumors the use of heavy ions is more advisable.

- Higher mass ions require more expensive, bulky, and therefore more difficult to install accelerators.

- With the same range, the energy required for heavy ions is much greater. This entails higher operating costs for the accelerators.

From this summary it seems that the points against the heavy ions are the effect of the tail fragmentation and the operating costs, but there is a big advantage: the greater biological efficacy of heavy ions means that even a small dose distributed on healthy tissues can induce many cellular necrosis processes.

Therefore, the problem is certainly not the effect of the dose tail, in which a small amount of dose is distributed by fragments with low biological efficacy, but the distribution of dose upstream of the Bragg peak.

This is in fact of intensity similar to that given by the protons, but of a much more dangerous quality.

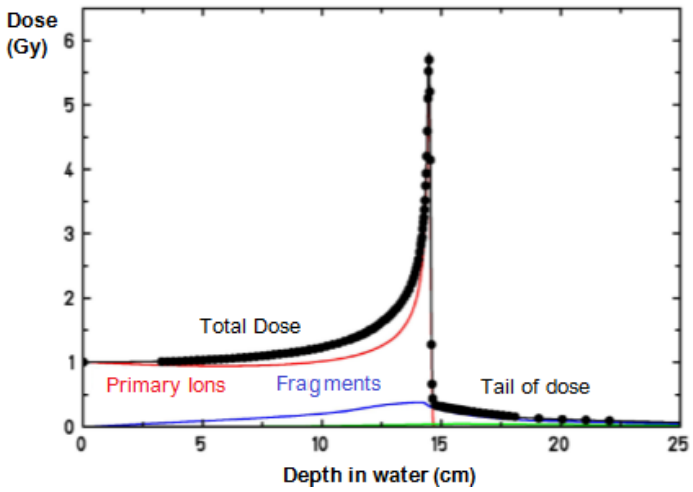

Fig.2.20 Dose deposited in water due to a carbon ion beam of 270 MeV/u. The contributions of the primary ions in red, the ones in the primary fragments in blue and those in the secondary fragments in green. The dose was normalized with respect to the input dose. [27]

The main distinction concerns heavy ions (Carbon and Oxygen nuclei) from light ions (Hydrogen and Helium nuclei, otherwise known as Protons and α-particles, respectively). [22]

Considering the phenomena described up to now, the choice of ion is an important issue in therapeutic treatments.

Currently the ions used are mainly Protons, a narrow minority of treatment centers use Carbon ions (mostly in Japan, excluding the CNAO of Pavia, the Heidelberg HIT and two hospitals in China) and yet no center is using ions of Helium and Oxygen whose potential for clinical purposes has already been analyzed. [28]

Chapter 3

Magnetic Hyperthermia

The first two chapters show that in cases of pancreatic cancer, which is an organ whose carcinogenic pathologies that are difficult to treat, due to the high rate of cell proliferation, a radiotherapy treatment which concentrates most of its energy in the tumor volume is preferred, minimizing damage to healthy tissues.

The combination between magnetic hyperthermia and radiation could be one of the most effective known radiosensitizers: clinical studies on different types of tumors demonstrate the potential of hyperthermia to could improve both local tumor control and survival after radiotherapy, without a significant increase in side-effects.

For a more fluent understanding of the topics of this chapter, it is important to talk about the principles behind the magnetic hyperthermia and its interactions with nanoparticles and the interactions on the cellular population under consideration. After explaining the operation and the advantages of this technique, we will focus on its potential use of radiotherapy techniques and improved treatments to treat tumours.

3.1

Hyperthermia for Cancer Treatment

The techniques of hyperthermia exploit an external heat source to increase tissue temperature and kill cancerous cells or at least prevent their further growth.

The achievement of high temperatures, as most studies revealed, causes direct injury to cancerous cells and sensitizes them to other treatment modalities, enhancing the radiation and chemotherapy action, without significant damages to normal tissues.

Hence, the procedures of hyperthermia using as adjuvant for cancer treatment employ a temperature range between 40–48 °C and the temperature is maintained at a treated site for one hour or more, guaranteeing an opportune sensitivity.

3.1.1 History

The use of heat to treat tumors is one of the oldest oncological therapies: an Egyptian papyrus of 5000 years ago described a method for treating breast cancer by means of cauterization, a medical practice or technique of burning a part of a body to remove or close off a pathologic part.

In the seventeenth century patients affected by infection fever have managed to fight diseases with the increase in body temperature and, moreover, the first case of using tanks of water circulating at 42 - 44 °C for treatment of inoperable tumors goes back to the end of the nineteenth century. [1]

In the second half of the nineteenth century the German scientist Carl D.W. Busch published an essay, in which he described the course of a patient's illness, which was subjected to the removal of a sarcoma on his face. After the operation she contracted an acute skin infection that led to high fever: the high temperature caused the tumor to regress.

This fundamental discovery led to numerous studies in which fever was induced in cancer patients, so it had been shown that high temperature damages cancer cells, without damaging healthy ones.

At the end of the nineteenth century the American surgeon William Bradley Coley managed to produce a toxin that caused erysipelas and consequently fever, exploiting the potential of the new discovery.

The study showed that the survival rate for some years (between one and seven) increased from 28 to 64%, depending on the body temperature reached. The higher the temperature, the longer the survival time increased, making this approach unpredictable: this factor revealed the weakness of the method.

Later studies called into question the therapeutic effects of heat in the case of cancer, and for several years the idea of using heat was set aside, partly because of the lack of scientific evidence and the absence of certain and consistent results.

In the second half of the twentieth century the interest in hyperthermia was awakened, also thanks to the first international congress on hyperthermic oncology held in Washington in 1975.

In those years hyperthermia was studied in relation to the treatment of bladder cancer, with studies clinical results and encouraging results. [2]

3.2.1 Hyperthermia to treat cancer

The hyperthermic treatment can damage tumor cells, especially for their membranes, cytoskeletons and nuclei functions, and the susceptibility to heat varies according to the phase of the cell cycle.

The heat above 41° C leads the cancer cells towards acidosis which reduces their vitality; on the other hand, healthy cells can dissipate excess heat through their well-ramified network of vessels, which in the case of high temperatures can dilate and therefore lead to thermal dissipation, as opposed to the abnormal vascularization of tumor areas.

However, the principal biological effects due to hyperthermia are:

- Cellular mortality with break point at 42.5-43 °C,
- Hypersensitivity during the late S phase of the cellular cycle,
- Thermotolerance (protein thermal shock),
- Radiosensitizing, time and temperature dependent.

Considering the extension of the treated region, hyperthermia can be classified into three types:

- whole body hyperthermia, achieved by using thermal chambers or blankets,
- partial hyperthermia, applied to treat locally advanced cancer by perfusion or microwaves,
- local hyperthermia, mainly for smaller volumes than organs (and the one investigated in this research project).

The blood vessels created in tumoural masses are devoid of muscular scaffolding; thus, a chaotic and irregular growth takes place with lack of elasticity; this leads to inability of vasodilatation, not allowing the dissipation of excess heat: this is one of the physiological foundations of the therapeutic efficacy of hyperthermia.

Specifically, depending on the area of the tumor mass:

- in the most internal part: cells are hypoxic precisely because they are farthest from the capillary network. These cells cannot be reached by chemotherapy drugs administered systemically (which tend instead to accumulate in well-vascularized healthy tissues), so they are more radioresistant.
  Thus, cells in internal part are thermos-sensitive, but not radio-sensitive (as explained in the paragraph 1.2.2).

- in the most external part: cells are well oxygenated, so more radio-sensitive.

This difference of sensitive between internal and external of the tumor mass is useful because, when the hypoxic tumor cells are hit by hyperthermia, they are more sensitive to the incident radiation, due to the increase in their level of oxygenation.

3.2

Magnetic Fluid Hyperthermia Therapy:

use of Nanoparticles

After an introduction of magnetic properties of nanoparticles and their uses in different biomedical branches we will deepen the arguments concerning the technique of magnetic hyperthermia for the purposes of our research.

3.2.1 Principles of Magnetic Nanoparticles

The term *nanoparticles* refers to materials with at least dimensions between approximately 1 and 100 nanometers (nm) and usually contain from several hundreds to 10^5 atoms. *Magnetic nanoparticles* are those nanoparticles that show some response to an applied magnetic field. [5]

Seeing as local hyperthermia exploits the heating of magnetic nanoparticles due to losses of hysteresis or the relaxation of Néel and Brown when they are subjected to a time-varying magnetic field of sufficient intensity and appropriate frequency (some hundreds of kHz), it is necessary to examine general properties of magnetism in order to better understand these physical quantities.

To study the response of magnetic materials to the application of a magnetic field it is necessary to define two fundamental quantities: the magnetic moment $\vec{\mu}$ and the magnetization $\vec{M}$.

The *Magnetic Moment* μ of an atom is expressed classically as the sum of two contributions: the motion of the electrons around the nucleus (orbital angular momentum, $\hbar\vec{L}$) and the rotation of the electrons around its own axis (spin angular momentum, $\hbar\vec{S}$).

In particular,

$$\vec{\mu} = \gamma\hbar\vec{J} \tag{3.2}$$

where **J** is the total angular momentum, expressed by $\vec{J} = \vec{L} + \vec{S}$.

The *Magnetization* $\vec{M}$ is defined as the total magnetic moment per unit of volume:

$$\vec{M} = \sum_i \frac{\boldsymbol{m}}{V} \tag{3.3}$$

in the hypothesis of a uniformly magnetized medium and given by the resultant between the spin moment and the orbital angular momentum of the electrons all inside the material.

The *Magnetic Induction* $\vec{B}$ consists of two contributions, one from the external magnetic field and one from the magnetization, thus:

$$\vec{B} = \mu_0\left(\vec{H} + \vec{M}\right) \tag{3.4}$$

where μ_0 is the magnetic permeability in the vacuum.

It is simpler to analyze the magnetic behavior of materials in response to exposure to an external field by introducing *Magnetic Susceptibility* χ:

$$\chi = \frac{\partial \vec{M}}{\partial \vec{H}} \tag{3.5}$$

Diamagnetic are materials with are χ negative e and generally of value $\chi \approx -10^{-5}$ emu/cm^3; these do not have a positive magnetic moment because the electronic shells are complete and they tend to shield the action of an applied field, aligning the magnetic moments in the opposite direction to that detected by the external field; Paramagnetic materials, on the other hand, have positive susceptibility, typically between 10-3 and 10-5 emu/cm^3, aligned in line with the direction of the external field.

So, magnetic materials are classified according to two parameters:

- the response of the material to the application of an external magnetic field;
- the value of the magnetic susceptibility of the material χ.

Most of the macroscopic magnetic properties of nanoparticles (that are ferromagnetic materials) are represented by the *Hysteresis cycle*. It is thus possible to define the saturation magnetization M_0, that is the maximum limit reachable through the application of an external field, the coercive field HC (the field necessary to completely demagnetize the material after application of the field and the magnetization), which represents the magnetization exhibited at zero field after reaching the saturation value.

Let us consider, in fact, a ferromagnet in the initial non-magnetized state: the application of a magnetic field $\vec{H}$causes the increase of the magnetic induction, until all the magnetic moments are aligned in the direction of $\vec{H}$, that is when the value M_0 is reached (which depends on the value of the magnetic moment and the number of atoms for unit of volume).

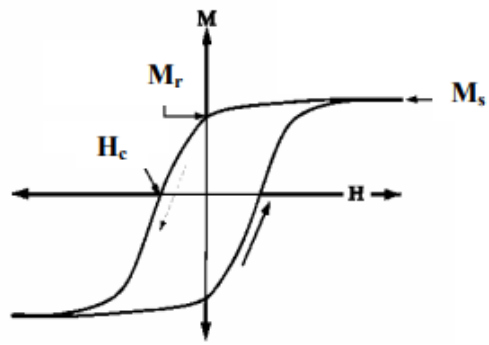

Fig. 3.1 Hysteresis curve of ferromagnetic materials. [6]

When the field is then brought to zero in the presence of a residual magnetization M_r, which can be zeroed by applying an opposite (coercive) field, HC, strongly dependent on the conditions of the material (treatment, deformations, etc.).

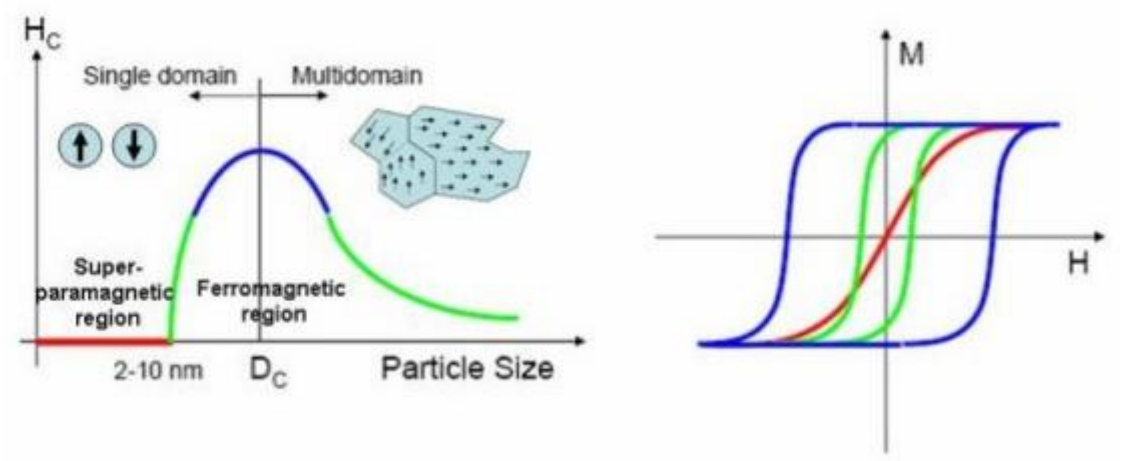

Fig.3.2 Illustration of the relationship between coercivity and size in small particles. [7]

Iron oxide nanoparticles have superparamagnetic proprieties (magnetism form typical of ferromagnetic or ferrimagnetic nano-structures) and their appropriate surface chemistry can be used for numerous in vivo applications in addition to hyperthermia, such as MRI contrast enhancement, tissue repair, immunoassay, detoxification of

biological fluids, drug delivery, and cell separation (we discuss them in paragraph 3.2.4).

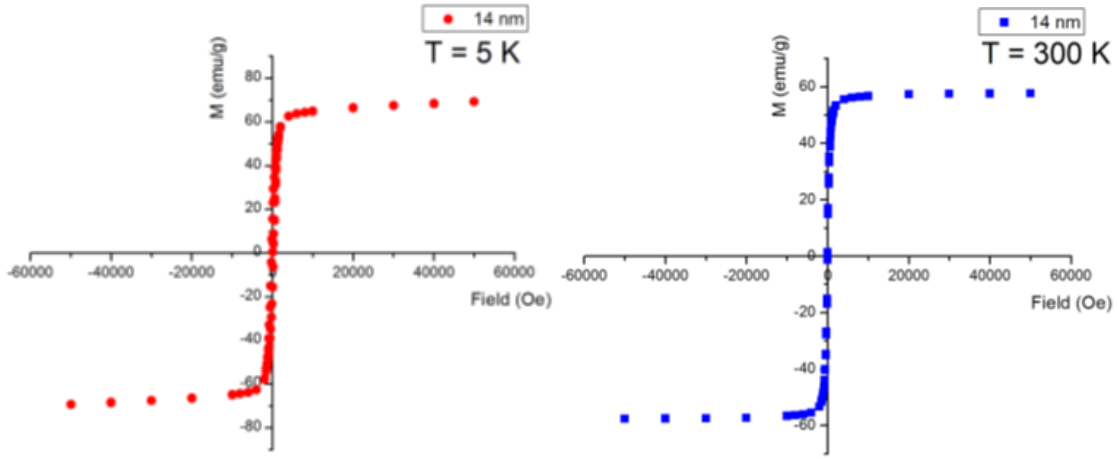

Fig.3.3 Hysteresis curves of MNPs measured at T = 300 and 5 K for HADROCOMBI experiment.

To be able to form a colloid suspension, the size of the nanoparticle should be much smaller than 1 μm. The usual diameter of the magnetic crystals ranges between 4 and 18 nm, either in isolated crystals or in agglomerated crystals forming larger particles. [8]

Because each crystal of ferromagnetic material present in the colloid is much smaller than the size of one domain, it is completely magnetized. It constitutes then a nanomagnet made of single domains fully magnetized.

It should be noted that, at present, the only ferro-fluid used for biomedical applications is based on suspensions of ferrimagnetic ferrite material. In fact, a suspension of small crystals of iron, as magnetite, for example, should be a better material than a ferrite because its magnetization is about 5 times higher than for Fe_3O_4.

However, pure iron nanoparticles are very unstable and very quickly oxidized into iron oxide in aqueous media. The development of ferromagnetic nanoparticles useful for biomedical applications will need, therefore, a coating protecting them from oxidation.

In addition to the value of its magnetization, the single monodomain is also characterized by another important property: its *anisotropy energy*.

As illustrated in Figure 3.4, the magnetic energy of a nanomagnet depends upon the direction of its magnetization vector (with respect to the crystallographic directions).

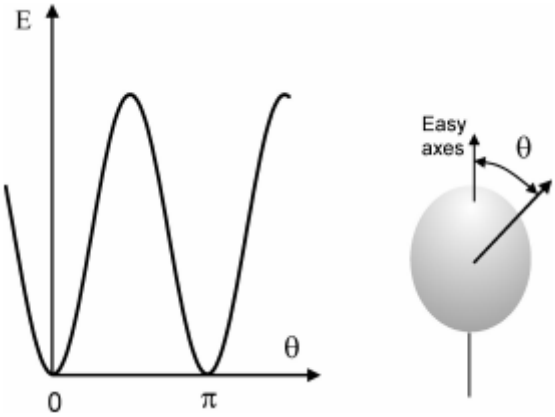

Fig. 3.4 Evolution of the magnetic energy with the tilt angle between the easy axis. [8]

The directions that minimize this magnetic energy are called anisotropy directions or easy axes. The magnetic energy increases with the tilt angle between the magnetization vector and the easy directions. [24]

The anisotropy energy represents the variation amplitude of this curve, and it is given by the product of the crystal volume times a constant, the anisotropy constant.

The anisotropy energy proportional to the crystal volume increases thus very rapidly as the crystal radius increases, as shown in the following equation:

$$E_a = K_a V \tag{3.6}$$

where K_a is the anisotropy constant and V the volume of the crystal.

The anisotropy energy determines also the *Néel Relaxation Time*, which constitutes another important parameter of the magnetic behavior of a single nanodomain particle.

The Néel relaxation defines then the fluctuations that arise from the jumps of the magnetic moment between different easy directions. The function that gives the evolution of the Néel relaxation time τN with the anisotropy energy E_a is the product of two factors.

One of these is an exponential function of the anisotropy; indeed, to flip from one easy direction to other one, the nanodomain magnetization has to jump over an anisotropy energy hump. This process is similar to a chemical reaction, which needs an energy equal to or larger than an activation energy to occur.

The kinetics of the phenomenon is given, therefore, by the Arrhenius law:

$$\tau_N = \tau_0(E_a)e^{\frac{E_a}{k_B T}} \tag{3.7}$$

where $E_a$is the total anisotropy energy, k_B is the Boltzmann constant, and T is the absolute temperature. $\tau_0(E_a)$ is the preexponential factor of the Néel relaxation time expression.

Regarding the materials used in magnetic hyperthermia therapy, nanoparticles can be distinguished in mono-domain and multi-domain depending on their size, in particular nanoparticles with a diameter greater than the critical one (the one for which maximum coercivity is present) are multidomain (as they present more Weiss domains within them), while those with a smaller diameter are called monodomain and present a unique Weiss domain.

These are called *Weiss domains* because at the beginning of the twentieth century, the French physicist Pierre-Ernest Weiss suggested the existence in the ferromagnetic materials of the so-called magnetic domains, regions in which about 10^{12}-10^{15} magnetic moments are aligned parallel and therefore the magnetization within the domains reaches the saturation level.

However, the alignment direction varies from domain to domain in a more or less random way and, therefore, the total magnetization of the system can also be null.

The domains are separated by the domain walls that are about 50-100 nm thick, where the orientation of the spins varies gradually; the magnetization process consequently consists in reorienting the domains in order to align them with respect to the field and in the increase of the dimensions of the domains aligned with the field to the disadvantage of the domains aligned in opposite way to the field. [8]

In multidomain MNPs, under the effect of an external magnetic field, the magnetic moments of the Weiss domains line up with the field. In the same way, even the moment magnetic field of a single domain superparamagnetic NP aligns with it. In the absence of an external magnetic field, the ferromagnetic NP will keep one nothing net magnetization while in superparamagnetic ones it will be nothing due to the rapid reversal of the magnetic moment.

As already mentioned, the mechanism responsible for the heat dissipation process is basically the inversion of the magnetization that can occur both by rotation of the

magnetization only (relaxation of Néel) and by the "mechanical" rotation of the whole nanoparticle (Brown relaxation).

The particles in a fluid can physically rotate to align their moments with the applied magnetic field; this causes a release of energy in the form of heat, due to the viscous friction between the rotating particle and the surrounding medium. Time and rotation capacity depend on the particle size, temperature, and viscosity of the fluid in which they are dispersed. [2]

The characteristic *Brown Rotation Time* is:

$$\tau_B = \frac{4\pi r_h^3 \eta}{k_B T} \tag{3.8}$$

where the radius r_h is the hydrodynamic radius of the particle, often greater than the radius of the magnetic volume, in that it includes the proper radius and any thickness of absorbed surfactant.

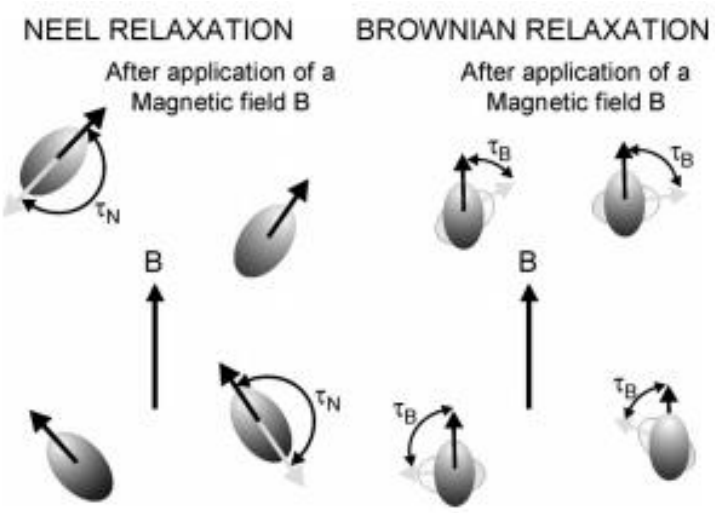

Fig.3.5 Mechanisms of the relaxation of Brown and Nèel. [8]

For suspended particles in colloidal ferrofluid the two relaxation mechanisms are both competitors; on the other hand, when the fluid is injected into a tumor, it is reasonable to suppose that the ability of the particles to move freely will be reduced because they will attach or eventually be incorporated into the cells. In this case Brown's relaxation losses cannot contribute to heating, which leads to a rapid decrease in efficiency of the nanoparticles in terms of released heat.

3.2.2 Magnetic Nanoparticles in Medical Care

During recent years, there has been much interest in novel materials in the area of nanotechnology. Magnetic nanoparticles belong to the group of nanotechnology-based materials with an impact in fields of analytical chemistry, biosensing, and nanomedicine.

The progresses made in nanotechnology have taken this method to a much higher degree of development; for example, the application of magnetic nanoparticles in medicine is moving towards targeting body regions otherwise difficult to reach, and chemical manipulation at the nanoscale has conferred the ability to conjugate biomolecules like antibodies for a more effective therapy or to accomplish specific targeting. In this way, MNPs may simultaneously combine several theranostic functionalities such as drug-carriers, contrast agents for magnetic resonance imaging (MRI), and/or magnetic heating agents. [9]

In the last years fifteen years scientists have developed applications for magnetic nanoparticles and microparticles aided in *diagnosis* and treatment *therapies* of diseases:

- Magnetic separation of biological entities contributed to the development of diagnostics,
- Magnetic nanocarriers contributed to drug delivery,
- Radio frequency-controlled magnetic nanoparticles provided a new approach for cancer treatment,
- Magnetic resonance imaging (MRI) applications in addition to cancer treatment.

The modification and functionalization of nanoparticles with various kinds of biomolecules was already exploited at that time. [10]

Nanomedicine introduced numerous novel materials for drug delivery and applications in molecular imaging where accurate detection is dependent on molecular signatures. Magnetic particles are also applicable in the microscopic manipulation of nano- and micro-sized objects. Applications of magnetic particles ranging from catalysis to drug delivery and remediation are only limited by their biocompatibility and immunogenicity, both of which can be controlled by proper layering and coating of particles. [11]

The simultaneous performance of diagnosis and therapy of cancer cells using magnetic nanoparticles is called *theranostic* approach.

Diagnostics of cancer

The greatest application of nanoparticles in this field is as contrast agent for MRI (Magnetic Resonance Imaging), non-invasive technique used for diagnostics, for pre-surgical evaluation and for monitoring the effects of a therapy.

The nanoparticles, locally modifying the relaxation time of the tissues and improving the sensitivity of the technique, allow to highlight pathologies and to create more contrasted images.

It is also possible to use nanoparticles for optical imaging, that is, by linking fluorophores, which emit a light signal if excited by a near infrared radiation (able to penetrate the anatomic tissues), making their localization possible. [2]

Therapy of cancer

Among the applications of nanoparticles in the therapeutic field, there is certainly the targeted and controlled release of drugs (Magnetic Drug Delivery).

Compared to the classic chemotherapeutic treatments this technique allows the administration of a lower dose of drug as well as the best control of the site of release, thus decreasing the side effects on healthy cells. The nanoparticles, once injected into the blood flow, reach, through magnetic field gradients, the place of interest where, stimulated by changes in pH, temperature, osmolality, etc., they release the drug anchored to the particle through a suitable polymeric coating. [12]

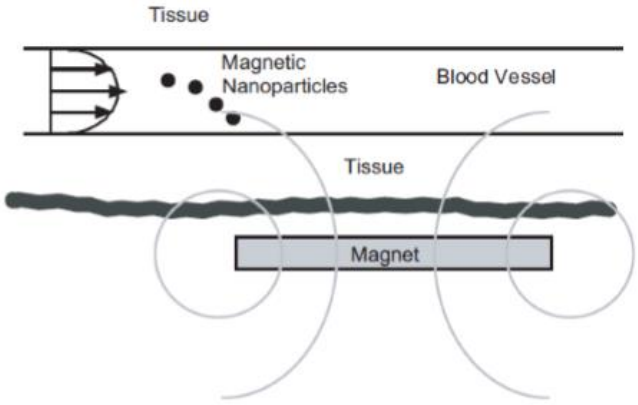

Fig. 3.6 Hypothetical system for magnetic drug delivery: the magnet is placed outside the body and the magnetic field gradient captures the carriers that circulate in the circulatory system. [3]

There is a synergistic effect of magnetic heating and administration of anticancer agents and a good move can be coating the MNPs of polymeric material, so as to have an anchorage with the medicines, which can be released over time (similar to Chemo). [13]

In fact, in principle, it is possible to anchor, on the same particle, specific antibodies for targeting, anticancer drugs, and fluorescent molecules. [14]

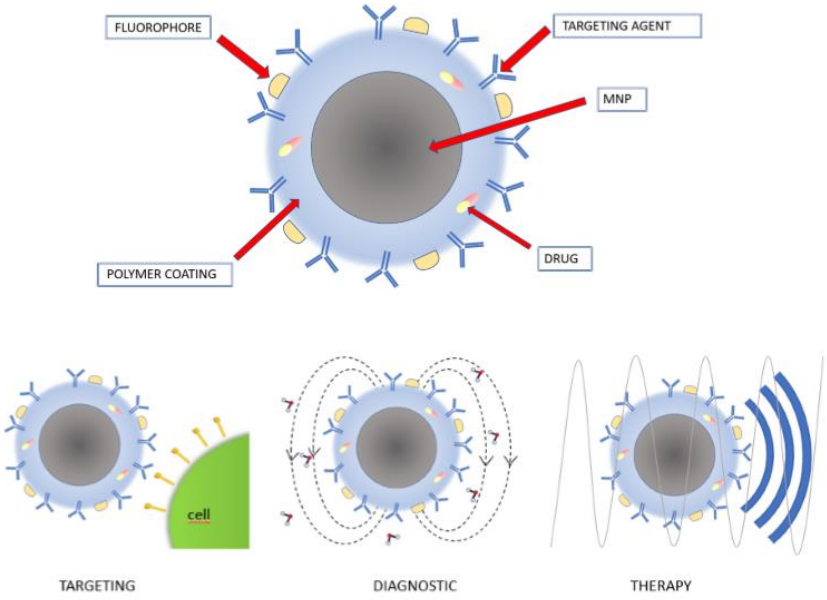

Fig. 3.7 Schematic representation of a multifunctional magnetic nanoparticle. [3]

3.2.3. Magnetic Nanoparticles in Hyperthermia Therapy

One of the procedures to lead cancer cells to necrosis or apoptosis consists in heating, but when used alone it does not destroy enough cells to cure the cancer: we combinate this effect with the action of magnetic nanoparticles that produce increase of temperature locally after their uptake in cellular population.

At the last twenty years of research it has proved experimentally the high efficiency of a superparamagnetic crystal suspension to absorb the energy of an oscillating magnetic field and convert it into heat. This property can be used in vivo to increase the temperature of tumor tissue and to destroy the pathological cells by hyperthermia.

This technique is also known as *Magnetic Fluid Hyperthermia* because MNPs are carried by a ferrofluid (a liquid that becomes strongly magnetized in the presence of a magnetic field) into the tumor and then exposing the patient to an alternating magnetic field of a certain intensity and appropriate frequency (hundreds of kHz and

about 10 kA/m). The increase of temperature is produced by the applying an alternating magnetic field (AMF) with the presence of the MNPs, iron oxide nanoparticles.

The frequency and intensity of the applied magnetic field have an upper limit dictated by the fact that there may be possible physiological responses at high frequencies including muscle stimulation, possible cardiac stimulation and arrhythmia.

Generally, the range of frequencies and safe intensities is considered to be between 0.05 - 1.2 MHz and 0-15 kAm^{-1}. [3]

While remaining within safe physical parameters, in the use of hyperthermic techniques, it is necessary to consider possible effects on board such as cerebral necrosis, edema, focal hemorrhages and infarcts. [15]

The penetration depth of alternating magnetic field is higher than any other activation mechanism (light or acoustic waves), allowing to reach deeper tissues; moreover, it is possible to administrate MNPs in a wide concentration range may stay at the tumor site for repeated therapy sessions.

Because the cell death process does not regress once the hyperthermic session is over, a temperature of about 42 ° C must be maintained for at least 30 minutes. [3]

The fact that the nanoparticles are so small allows that, following insert into the tumor, there is heating locally in the tumor tissue, so as not to damage healthy tissues; so, this procedure can give a good result especially for the difficult cases of radioresistant tumors, such as glioblastomas.

The fluid containing the MNPs is injected directly into the tumor or into the body, where it will be directed to the diseased area, using an organic coating that acts as a receptor for tumor antibodies. [16]

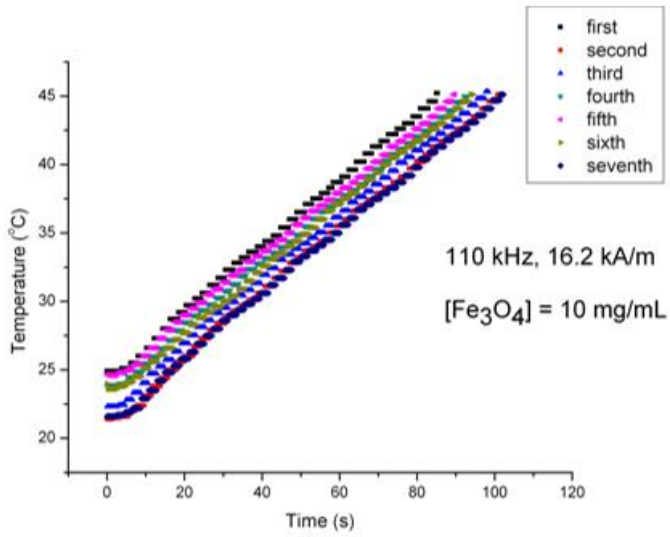

Fig.3.8 The increase of temperature (as a function of time) registered on a water dispersion of MNPs (concentration of Magnetite = 10mg/mL) at field H_{AC}=16.2 kA/m and frequency f =110 kHz.

The main parameter determining the heating of the tissue is the *Specific Absorption Rate* (SAR), defined as the rate at which electromagnetic energy is absorbed by a unit mass of a biological material. It is expressed in calories per kilogram and is proportional to the rate of the temperature increase $\left(\frac{\Delta T}{\Delta t}\right)$:

$$SAR = 4.1868 \frac{P}{m_e} = C_e \frac{\Delta T}{\Delta t} \tag{3.9}$$

where P is the electromagnetic wave power absorbed by the sample, m_e is the mass of the sample, and C_e is the specific heat capacity of the sample. Thus, the unit of measurement is $\frac{J}{skg} = \frac{W}{kg}$.

From this we deduce that MNPs at high values of SAR, with accurate temperature control, can be used to have efficient treatments of hyperthermia in vivo. For optimal treatment it is also appropriate to identify the corrections (and therefore to calibrate the parameters) between: temperature distribution, temperature dose, tumor volume.

Undoubtedly, even the quantity of nanoparticles inserted is fundamental for the dissipated energy rate and the maintenance of high temperatures for a sufficient time; in particular, it is considered that 5-10 mg of magnetic material in each cm^3 of tumor tissue may be appropriate for the therapy to achieve the desired effects. [3]

Once in place, there are 4 different mechanisms with which a magnetic material can generate heat in an alternate magnetic field [16]:

- Parasite current generation with magnitude > 1 μm,
- Hysteresis losses in magnetic particles > 1μm and magnetic multi-domain particles,
- Losses due to relaxation in superparamagnetic particles,
- Frictional losses in viscous suspensions.

The amount of heat generated inside the material depends on the type of magnetic particles inserted and on the characteristics of the applied magnetic field; particles placed around a tumor site will heat it differently depending on whether they are ferromagnetic or superparamagnetic and also, considered a specific sample, the heat released will depend on the value of the applied field, its frequency and the rate of cooling of the tissue by blood circulation. [15]

If the particles are ferromagnetic, the energy dissipated thermally is detectable in the area inside the hysteresis loop present in the magnetization curve and consequently, for a frequency H field f we will have a dissipating power PFM.

If the particles are superparamagnetic, the dissipated energy cannot be interpreted as the area inside a hysteresis cycle as it is non-existent; in this case there are two different treatments depending on whether the magnetic particles are inserted in a more or less viscous fluid and therefore free to rotate or which are fixed to the crystalline lattice and therefore static.

In the first case, the passage of energy from the magnetic field to the material takes place through a real rotation of the particles around the crystalline sites and we talk about the *relaxation of Brown*. Here the warming due to Brownian relaxation is linked to the viscosity of the fluid that impedes the rotation of the particle.

In the case in which the particles are statically anchored to the crystalline lattice, the heating occurs through the rotation of the magnetic moments inside them and is called *relaxation of Néel*; here the loss of energy in the sample is due to the crystalline anisotropy which would tend to maintain the magnetic moments aligned in a particular direction.

3.2.4 Uptake of Magnetic Nanoparticles in Cellular Population

The introduction of a higher concentration of MNPs inserted in the volume under examination will certainly increase intracellular uptake.

It is thought that MNPs are inserted into the cytoplasmic membrane of cells, or are internalized by pseudopodia or incorporated into phagosomes, or into vesicles in the perinuclear area, fused to form a large phage- soma.

To verify the uptake of the nanoparticles, the treated cells could be imaged, so as to understand the effect of the combination of therapies.

We therefore resort to the use of microscopes to understand the structure and functions of cells in relation to the entry of MNPs, such as:

- Scanning Electron Microscopy: the imaging of backscattered electrons allows probing the localization of high Z particles even in intracellular compartments. Disadvantage: confined field of view and long sample preparation.
- Confocal Laser Scanning Microscopy: good technique for in vivo cell imaging, with use of fluorescent proteins, quantum dots, fluorochromes, often combined with SEM for optimal results.
- Isotopic Tracing of the MNPs: through a) Use of ^{59}Fe with the exploitation of its γ emission, so as to have a monitoring (radiotracer). b) Variations in the natural abundance of stable isotopes.

The last two techniques compared to other methods of analysis, not only have high sensitivity, good accuracy and are saving time, but can distinguish endogenous and exogenous iron after exposure of animal models in vivo as well as test models toxicity in vitro.

In recent years experiments have been conducted to investigate the absorption of MNPs by tumor cells, and therefore to understand their biocompatibility. One of the techniques used is the ^{1}H Nuclear Magnetic Resonance, capable of verifying the absorption of NPs by biological systems.

In a case of cancerous nerve cells (glioblastomas) and incubation of two different types of MNPs for 24 hours, the results in Figure Fig.3.I shows that as the concentration of iron increases within the culture, there is a greater absorption from before in the extracellular area and then inside the cell. [17]

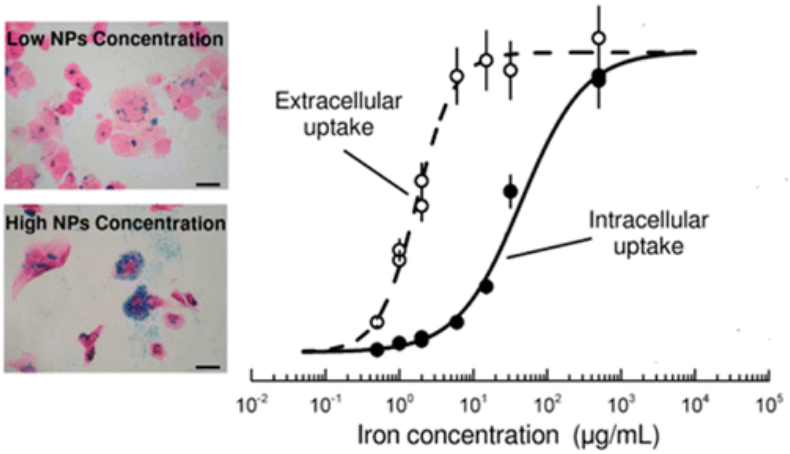

Fig. 3.9 Extracellular and intracellular uptake in function of Iron concentration in experiment of glioblastoma cells T98G. [17]

Using inductively coupled plasma optical emission spectrometry (ICP-OES) it was made the quantitative determination of the amount of NPs uptake. The result gives that the uptake in cellular population increases proportionally to the concentration of nanoparticles introduced, as illustrated in the following figure:

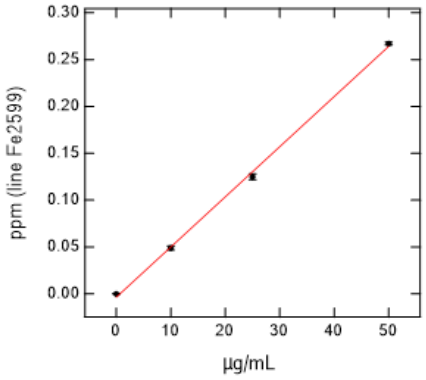

Fig. 3.10 BxPC3 cells uptake after 72 h of incubation using ICP-OES

3.2.5 Biological Response to the combined treatment of Magnetic Hyperthermia and Irradiation

In the temperature range of hyperthermia (41-43 ◦C), the main cellular effects that are relevant for cancer therapy are cell killing and alteration of cellular resistance to radiation exposure.

The advantages of combined hyperthermia-radiotherapy treatment depend in part on heat-induced damage, and, in part, on the microenvironment in which the tumor cell is located.

Experiments were conducted both in vitro and in vivo to understand how the combination hyperthermia-radiation can induce damage to the cell population. It has been shown that for in-vitro, heat-induced radiation damage occurs in all cell types, regardless of whether they are neoplastic or normal. The primarily heat interferes with the ability of cells to cope with radiation-induced damage on the DNA. Furthermore, the times between irradiation and heating must be very fast. In vivo, however, the matter is more complex, and the improvement of the damage caused by radiation in the presence of heating is due to two mechanisms:

- Direct radiosensitization (as in vitro)
- Indirect mechanism resulting from the heating that kills the population of radioresistant hypoxic cells. A vascular supply of the tumor is structurally and functionally abnormal when compared with that of the normal tissue from which it derives, and, as a result, it is not inclined to have oxygen and nutrients required by the growing mass of the tumor. [1]

The formation of new blood vessels (neo-vasculature) during tumor growth is generally insufficient; this determines at the cellular level a low presence of oxygen, low pH, lack of sugars and other nutrients. Thus, the malignant cell by itself is relatively resistant to ionizing radiation used in conventional radiotherapy, which require a well-oxygenated environment (being low-LET radiation).

By subjecting the tumor to the hyperthermic treatment, instead, it causes an increase in blood flow due to the organism's attempt to dispose of the released heat; an increase in the availability of oxygen within tumor cells makes the indirect action of X-rays more effective.

The precise mechanisms by which hyperthermia causes the death of tumor cells are complex and strongly depend on the heating profile [18].

Direct effect mechanisms include denaturation of proteins, inhibition of damage repair through inactivation of DNA damage repair pathways, which can lead to mitotic catastrophe and induction of senescence, apoptosis and necrosis [19].

The interaction between heating and radiation depends on various factors, like heating temperature and time, sequence and time interval between the two modulations (irradiation time, before or after heating). Based on these factors it is possible to evaluate the fraction of surviving cells, and therefore mortality of the population.

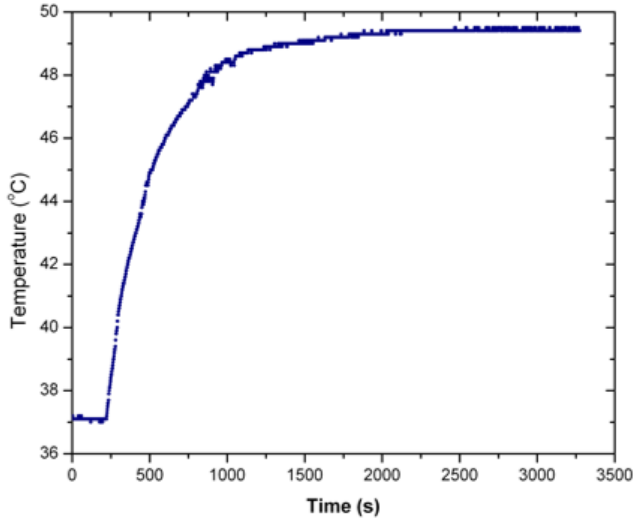

Fig.3.11 The increase of temperature (as a function of time) registered on cell pellet of BxPC3 (cells incubated for 48 h with 100 μg/ml concentration of MNPs) at field H_{AC}=16.2 kA/m and frequency f =110 kHz.

Considering experiments of population of BxPC3 xenografts in mice in vivo [13], the heat loss mechanisms during magnetization reversal lead to a local rise in temperature that can be controlled by modulating the field strength or frequency as well as the structural characteristics and mass of the MNPs. The thermal energy generated by MNPs depends on their SAR and the influence of degradation and intracellular aggregation in preserving SAR values.

Chapter 4

Experimental Procedure

This chapter describes the experimental procedure, postponing the treatise of the results to Chapter 5.

4.1

Introductory Phase: Characterization of Cellular Line of BxPC3

4.1.0 Defrosting & Pre-Plating of Cellular Population

For cell line BxPC3 characterization it has been determined its efficiency of plating and its cell generation time, useful informations for experimental testing.

For this purpose, we need a good number of cells, so let us start by defrosting a tube purchased by the Cell Bank Interlab Cell Line Collection (ICLC) and proceed to the first plating.

At the beginning, we take a sample tube from the container of Liquid Nitrogen (maintenance temperature of -196° C or -320.8° F) and heat it with hands conveniently covered with gloves. The defrosting is a critical phase for cells population because part of it could die. Now, into a hood, we use an automatic pipette to put defrosted cells into a test tube with culture medium RPMI, composed by 90% of water, vitamins, antibiotics as 50 mg/ml of Gentamicin, 2mM of L-glutamine and 10% of FCS (fetal calf serum) such that promote cellular growth. To remove tracks of dangerous substances we centrifuge the test tube with spin cycle to 1500 RPM for ten minutes; after that, we put the precipitate sample to another tube and further culture medium into a flask (the size of the flask is concerning to the number of cells that it is necessary to obtain).

This specimen is preserved in thermostat, set to 4-5% of CO_2, temperature of 37° C and 90% of humidity. We could observe under the microscope that many cells are already thickened, so we should wait for one day to see separated cells.

Fig. 4.1 Laminar flow hood where cellular experiments take place.

4.1.1 Determination of Generation Time and Evaluation of Growth Curve

To calculate the generation time, i.e. the time span used by cells to divide into two daughters, it is necessary to count the number of cells in the flask every almost 24 hours, considering that we started from a certain inoculum measured at zero time, so that we could create the growth curve.

To find the value of generation time and so cellular growth curves, we had executed one test at the beginning of time project: it was performed for a time interval of 0 – 141 hours; for the experiment we counted the number of cells at each time, and find generation time and the ratio between measured number and initial inoculum. Then, in Chapter Five, the curve obtained from these combination values is shown.

Time [h]	Inocula [cells/flask]
0	247800
21	247800
45	247800
70	247800
141	247800

Tab.4.1 Number of initial inocula of cells at each time.

The procedure for this experiment is the following: after 24 h from defrosting and pre-plating we start to acquire data until almost 140-190 hours, and begin to take the flasks from the thermostat and rinsing out waste with sterile PBS, we add the enzyme Trypsin-EDTA to the container (usually 1 ml for T25 flask) and we place in the thermostat again for about five minutes.

The enzyme Trypsin-EDTA aims to detach the cells from the special wall of the flask on which they would remain if they were not well clothed and free to reproduce. To inactivate the trypsin action, it is advisable to add at least twice the culture medium into the flask, and then remove one part to go to the cell counter.

To know the number of cells present in a certain amount of the solution, it is necessary to use a special instrument, called Coulter Counter, capable of assessing the amount of cells per millilitre according to the time.

In fact, a part of these cells, trypsinized, is put into 0.5 ml in 19.5 ml of isotonic and counted; for each count, two measurements are made to obtain the number of cells as the average value of the counts.

Fig. 4.2 Counter Coulter.

The function that permits this value has been entered in the Origin program corresponds to the following equation:

$$N(t) = N_0\, 2^{t/Tg} \tag{4.1}$$

where $N(t)$ is the number of cells that are growing exponentially in function of time, N_0 the number of initial cells and Tg is the generation time, which corresponds to the duration of an entire cellular cycle (after a time equal to Tg the number of initial cells has doubled).

This process will be repeated every 24 hours for the next 5-7 days. The cellular populations could grow up exponentially day-by-day, but after further days mortality starts to overcome generation, so growth curve decreases.

Once the bottom of the flask is completely covered by cells, the "saturated" growth curve and culture is confluent, so at this stage the cells are no longer exponentially growing. In fact, we could see at the microscope generation of colonies from big part of plated cells.

4.1.2 Evaluation of Efficiency of Plating (E.P.) and Survival (Surv)

Following the same road of the last paragraph, to determine the E.P. it is necessary to calculate the ratio between n, the number of cells present in the flask at time t, and n_0, the number of surviving cells of the initial inocula. To do this, we use the data and the mode described in 4.1.1, so the equation is:

$$E.P. = \frac{n}{n_0} \tag{4.2}$$

Macroscopically and with the aid of an optical microscope, it is possible to count colonies were counted surviving cell colonies. It should be remembered that clonogenic survival of one cell is defined as its capability of originating a colony consisting of at least fifty individuals.

Now, we could find the value of Survival, defined as the ratio between the efficiency of plating in a certain condition and the value of initial inocula. In fact:

$$Surv = \frac{E.P.(n)}{E.P.(0)} \tag{4.3}$$

Obviously, the value of Survival at dose zero (or control) is equal to the unit.

4.1.3 Evaluation of Cellular Growth by counting of colonies

Another method for assessing the growth trend of the population is the same process described before, but with flask fixation and staining, so that colonies can be counted at more or less 24 hours for about a week.

The count of colonies is a process possible thanks the optical microscope or with naked eye, discriminating from single cells.

In our test, we started from a 2000 cells inocula by considering the efficiency of plating about 10% (with first type of culture medium), so that we have a final number of cells about 200,000.

We set up five inocula of about 2000 cells one and put them in thermostat at time t = zero; after 24, 48, 120, 144 and 168 hours we extracted a flask, we fixed it and coloured, so we can count the colonies formed.

During the fixation process, culture medium is removed from the flasks and rinsed with the buffered saline (PBS) and we add a concentration of ethanol to 70%. So that the surface of the flask is completely covered and left to act for almost ten minutes, then the ethanol is removed: the cells are now dehydrated and ready to be coloured.

For staining process, GIEMSA STAIN (Sigma) Dye is diluted to 10% with distilled water to obtain a solution that is inoculated into the capsules in such a way that the surface is completely covered and allowed to act for a laying time 15 minutes. Then the solution with the dye is removed and the capsules are rinsed.

Fig. 4.3 Fixation of cell population.

Fig 4.4 Colonies visible to naked eye and ready to clonogenic assay.

However, we used this clonogenic essay method to achieve a population growth curve as well as to evaluate cytotoxicity introduced by various factors such as nanoparticle uptake, hyperthermia and irradiation (we will see these points in detail in the next paragraphs).

Following these operations, specimens were observed: we can count the colonies formed by surviving cells for each flask.

It should be remembered that the term "surviving cell colonies" refers to those cells that originated from colonies of more than fifty individuals. The size of the colonies depends on different factors, such as the time interval between irradiation and fixation (which can range from 10 to 13 days in dependence of the cellular line), the cell line characteristics and the dose with which they are have been irradiated.

The colonies were visible to the naked eye and for the count; it is possible to use an electronic microscope.

4.1.4 Survival Curve of the only Cell Line BxPC3 with Photonic Radiation

Cell cultures were irradiated with X-ray beams at the National Institute of Cells Tumors in Milan, where the LINAC accelerator mentioned in the Appendix is installed.

The goal of this experiment was to determine cell survival by exposure of different doses of 6 MV X-rays (0, 0.5, 1, 2, 3, 5, 7 Gy) by irradiating a clonogenic assay. We know that X-ray radiation has a low RBE value, so we had chosen higher doses than the ones employed with hadronic radiation (see the next paragraph).

The following experimental procedure was set up: shortly before the irradiation, the flasks were completely filled with culture medium and transported to the Centre. The flasks were placed horizontally within a water puppet positioned on the bed under the tube from which the beam emerges, so that the wall to which the cells adhered were located at a depth of 5 cm.

The radiation field in which the flasks were irradiated was uniform and 20 cm x 20 cm in area. This protocol was followed even for the control sample, which was not irradiated.

After the irradiation, we use trypsin to remove cells from the bottom of flasks and re-plate in culture medium, count and plate at appropriate inoculums in T25 flasks (five for each dose) and placed in a thermostat at 37 ° C, 4.5% of CO2 and 90% of humidity.

The inoculum was established basing on the expected survival (estimated by considering the radiation dose). After two weeks of treatment, we proceeded to fix with 70% ethyl alcohol and color with a solution of 10% Giemsa histologic dye to visualize cellular colonies with a number of cells superior to fifty.

Dose [Gy]	Inocula [cells/flask]
0	1407
0,5	2193,28
1	2525,44
2	3018,24
3	5073,76
5	9820,8
7	19835,2

Tab.4.2 Inocula of cells depending on the concentration of irradiation doses.

The efficiency of plating as a function of dose, EP(D), was obtained from the ratio between the number of surviving cells N(D) and the number N_0 of cells inoculated, and the uncertainty on EP(D) is about 10% resulting from the hypothetical error considering the biological process and human error of counting in initial inocula and after the measurements, and the treatment post-irradiation.

4.2

Evaluation of Cytotoxicity due to Nanoparticles

The introduction of nanoparticles brings damage and mortality to the cell population. Experimentally we proceed with the growth of many cells, the interaction with different concentration of nanoparticles, and then we evaluate what is the cytotoxicity affected by this culture, considering the various concentrations.

4.2.1 Properties of Nanoparticles

Another important step for the project was to assess the cytotoxicity caused by the introduction of nanoparticles in cell culture.

As previously mentioned, they have the role of creating localized hyperthermia when heated with an alternating magnetic field, in order to make the cells more exposed to radiation.

During the experimental phase, we used three types of nanoparticles:

- NPs of Magnetite (Fe_3O_4) in liquid (red)
- NPs of Magnetite (Fe_3O_4) in gel at 0.5% (green)
- NPs of Magnetite (Fe_3O_4) in gel at 2% (blue)

The Specific Absorption Rate (SAR) represents the rate of absorption of electromagnetic energy per unit of mass of biological material. It quantifies the heat generated by the magnetic particles and is measured in W/g. It is a useful parameter for comparing the efficacy of different magnetic particles.

From the experimental data the SAR of the nanoparticles is obtained through the formula:

$$SAR = \frac{\Delta T}{\Delta t}\Big|_{t=0} \frac{C_f}{m_{MNP}} \tag{4.3}$$

where C_f is the specific heat of ferrofluid, m_{MNP} is the mass fraction of nanoparticles in the sample, obtained by dividing the total mass of the nanoparticle cores into the fluid

(m_{MNP} = $\rho_f m_{MNP} V_f$) for ρ_f V_f, with ρ_f and V_f density and volume of ferrofluid respectively.

Figure 4.5 shows the SAR value in three different solutions.

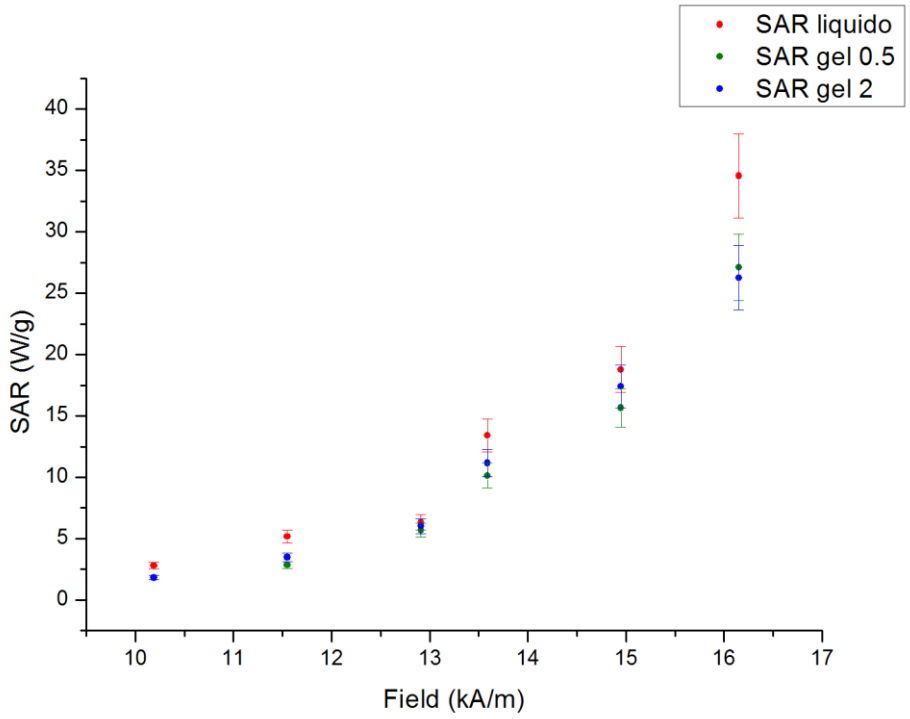

Fig.4.5 SAR Values in function of applied field on samples of 3mg/ml in liquid, gel at 0.5% and gel at 2%.

The group of INFN of Florence prepares NPs and we received them in three different batches, then the group of Hyperthermia of Milan testes them for hyperthermia at 109.8 kHz and 16.15 kA/m, values of magnetic field that will be used for cellular treatment (see paragraph 4.3).

The group valued the SAR of the three samples at 10 mg/ml, and they found for the first two batches the value of almost 120 W/g, and a value almost of eight times lower (15 W/g) at third batch.

This deep difference could be due to a problem of leak of Fe during coating substitution with DMSA. Therefore, we used the first two different lots of the same type of nanoparticles and we will call them "NP1" and "NP2" to distinguish them in the various tests and because the results from different usage are surprisingly different.

The diameter is d = 14nm and the coating is DMSA (Dimercaptosuccinic Acid). Measurements were made at 109.8 kHz (coil with 17 windings and Capacitor A200).

4.2.2 Evaluation of Efficiency of Plating & Survival of Population of BxPC3 with uptake of Nanoparticles

To evaluate the toxicity of nanoparticles in cellular cultures, we had performed several tests. Specifically, for each concentration of nanoparticles introduced, we realized the clonogenic assay, that is, we examined the colonies of survived cells approximately two weeks after the introduction.

Sample preparation procedure for each test was the following: BxPC3 pancreatic cells come sown in T25 flasks, and two days later, is removed to T25 flasks the culture medium previously administered and the soil is put containing nanoparticles at a specific concentration.

The T25 flasks thus treated are placed in an incubator at 37 °C and after predetermined time (24h/48h incorporation of nanoparticles, samples cells are trypsinized, and the cells are suspended again in fresh ground, counted and centrifuged to 1500 RPM for 10 minutes).

Evaluation of Cytotoxicity of a cellular population BxPC3 due to Nanoparticles of Magnetite at the following concentrations: 0, 10, 25, 50 µg/ml

We have grown the cells in Teflon containers with Mylar substrate and treated by different concentrations of NP1 (10, 25, 50 / ml) for a 24 hour incubation period.

Flasks were evaluated in laboratory for cytotoxicity due to nanoparticles only with always the same procedure used to make the clonogenic assay.

[C] NPs [µg/ml]	Inocula [cells/flask]
0	2088,52
10	1930,88
25	4983,2
50	10024,16

Tab.4.3 Inocula of cells depending on the concentration of nanoparticles to be inserted.

After about two weeks, the specimens were removed from the incubator and proceeded with fixation and staining to determine the concentration efficiency of the plating efficiency and thus build the survival curve.

The fixation and staining procedure is the same used to characterize the cellular line.

At a later time, we decided to delete concentration at 10 μg/ml because it gave a very similar result of 25 μg/ml and retry the precedent experiment.

Some of the containers obtained in this case were taken to the laboratory where hyperthermia tests were performed; others were evaluated in the radiobiology laboratory for cytotoxicity due to nanoparticles only with always the same procedure used to make the clonogenic assay.

[C] NPs [μg/ml]	Inocula [cells/flask]
0	1851,6
25	5205,9
50	10814

Tab.4.4 Inocula of cells depending on the concentration of nanoparticles to be inserted.

After about two weeks, the specimens were removed from the incubator and proceeded with fixation and staining to determine the concentration efficiency of the plating efficiency and thus build the survival curve, using the same procedure already mentioned for the characterizing of cellular line.

Evaluation of Cytotoxicity due to Nanoparticles at a concentration of 100 μg/ml in a BxPC3 cell population, with a lifetime of: i) 24 h; ii) 48 h

Based on the absorption time of nanoparticles in the cellular population we can define cytotoxicity.

First, BxPC3 pancreatic cells come sown in T25 flasks, with inoculum of 10^6 cell/flask with concentration of 100 μg/ml and leave in thermostat for 24 or 48 hours. The flasks thus treated are placed in incubator at 37 °C and after the specific time are trypsinized, and the cells are suspended in new medium, ready to start clonogenic assay.

[C] NPs [µg/ml]	Inocula [cells/flask]
0 (room)	1569,04
0	1521,92
50	10006,4
100	9979,2

[C] NPs [µg/ml]	Inocula [cells/flask]
0 (room)	1548,8
0	1557,6
50	10056
100	10069,2

Tab.4.5 Inocula of cells depending on the concentration of nanoparticles, with uptake of 24h (left) and 48h (right).

4.3.a

Test of Magnetic Hyperthermia on Cellular Pellet with uptake of Nanoparticles

The purpose of Hyperthermia tests on cell populations in which a certain concentration of nanoparticles has been to understand what is the optimum concentration of nanoparticles in relation to a rise in temperature up to 42 °C, so that they have a good mortality of tumoural population.

Various tests have been carried out with different concentrations and time of uptake, but let us now limit ourselves to describing the experimental apparatus, postponing the results to the next chapter.

For the goal of the project, the group of Hyperthermia of INFN - Milan implemented a measure setup with Magnetherm, using a circulation system of thermostatic water at 39°C; this is to bring the sample to 37°C before switching on the magnetic field for the measure of temperature.

We verified that to succeed the scope of the procedure and so arrive at 42°C it is necessary to prepare a cellular sample in pellet shape suspended in a maximum volume of 0.2 ml with medium culture in mini-Eppendorf of 0.2 ml, recovered by Teflon and put in a support in polystyrene (almost 1 or 1.5 million of cells for container).

These short sizes of tubes allow executing at the same time treatments of hyperthermia at two samples “twins”, one sterile for biological analysis (cellular survival with clonogenic assay) and the other to contaminate with optical fiber for real time control of temperature. The entire setup is shown in figure Fig.4.6.

In particular, to perform the hyperthermia measurements on the nanoparticles the experimental apparatus is as follows:

- MagneTherm System (function generator, oscilloscope, power supply DC);

- Fiber Optic Thermometer FOTEMP 1-4;

- Laudor Thermalization System.

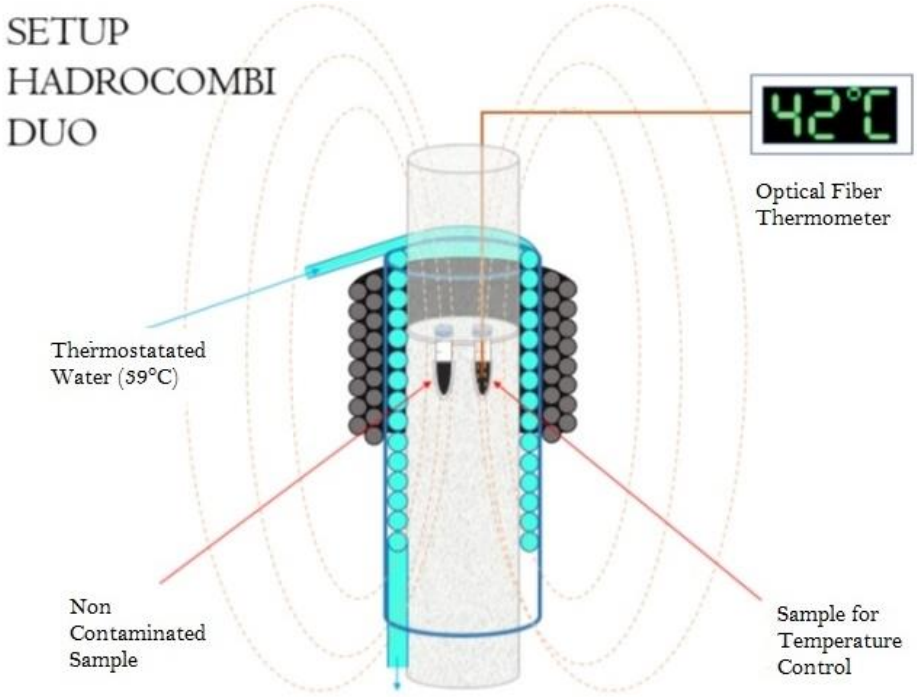

Fig. 4.6 Setup for Magnetic Hyperthermia experiments.

The sample (contained in a polypropylene Eppendorf tube) is placed in the center of the copper coil, inside a of cable polystyrene cylindrical holder.

Before starting the measurements, the sample is sounded and agitated for some minutes to reduce the degree of agglomeration of nanoparticles, and it is expected that the temperature will be stable, thanks to the help of the system of thermalization.

In this apparatus, two coils are available: one consisting of 9 windings, the other of 17 windings. The capacitors are instead five (A200, A88, B22, B11, B6.2), which can be coupled with the coils in order to obtain the field strength and the desired frequency.

The sample temperature is measured by optical fiber. The FOTEMP it has a measuring range from -200 C to 300 C, with standard deviation of 0.2 C. The outer fiber optic sheath consists of Teflon, and the tip of the sensor is attached to a GaAs crystal.

A light source, through the optical fiber, excites the semiconductor, which is in direct contact with the environment where to measure the temperature. The GaAs sensor reflects the received light, 3 with a phase shift proportional to the temperature of the

crystal. A miniature spectrometer and a mathematical algorithm ensure measurements of Fast and accurate temperatures.

Returning to the experimental procedure, at first we had implemented different tests with NP1 using the “pellet” mode and for each of them we start to work in radiobiological laboratory a month before the hyperthermia measure (defrosting, propagations, planting, treatments of injection, etc.), in order to acquire high quantities of cells. In fact, to observe the effective increment of temperature during the hyperthermia we need many millions of cells, so we could proceed to realize a consistent cellular pellet.

For each experiment, we prepared two pellets with a certain concentration of NP1 and put in cryogenic ampoules, one to be used in the experiment of hyperthermia, carried out with almost few millions of cells, and the other one to remain in laboratory at ambient temperature for the entire period of the process in order to realize the clonogenic assay (see next paragraph). The possibility to insert two samples simultaneously inside the coil allows to have a sample for temperature control during hyperthermal treatment.

This procedure is necessary because the measurements on the cells must be performed while maintaining sterile the sample that will then be subjected to biological studies, therefore it is not possible to measure directly the temperature of the last one.

The pellet of hyperthermia covered with Teflon was brought to “Hyperthermia group”, after stabilizing (thanks to the thermalization system) at 37 °C the sample temperature, hyperthermia tests are performed at frequency of 110 kHz and field of 16.2 kA / m.

BxPC3 pancreatic cells come sown in fourteen T25 flasks, with inoculum of 10^6 cell/flask. Two days later, after removing medium culture, we treat flasks with nanoparticles concentration of 50 and 100 μg/ml (8 flasks with 100 μg/ml and 2 flasks with 50 μg/ml).

The T25 flasks thus treated are placed in incubator at 37 °C and after 24 and 48 hours samples cells are trypsinized, and the cells are suspended in new medium, counted and centrifuged at 1500 RPM for 10 minutes.

After that, the cell pellet is re-suspended with the shortest possible amount of medium (necessary to ensure cell survival) and placed in an Eppendorf covered with Teflon. At this point, after stabilizing (thanks to the thermalization system) at 37 ° C the sample

temperature, hyperthermia tests are performed at frequency of 110 kHz and field of 16.2 kA / m.

The choice of a smaller Eppendorf (V = 0.2 ml) than the ones used usually for nanoparticles only (V = 1.5 ml) tests is due to the need of minimizing the loss of heat by dispersion. In fact, several tests (see figure below) were performed by using Eppendorf of volume (V = 1.5 ml), but without reaching the required temperature.

Magnetic Hyperthermia Test on cellular pellet BxPC3 with concentration of nanoparticles of 50 µg/ml

We had prepared two pellet with concentration of 50 µg/ml and put them in cryogenic ampoules, one to be used in the experiment of hyperthermia, carried out with almost three millions of cells, and the other one to be stored in laboratory at ambient temperature for the entire period of the process.

After the estimating time of hyperthermia process (one hour), the ampoule in laboratory was replanted and put in thermostat with the following inocula, in order to obtain a clonogenic assay (see the next paragraph).

[C] NPs [µg/ml]	Inocula [cells/flask]
50	10814
50*	~10^6

Tab.4.6 Inocula of cells depending on the concentration of nanoparticles to be inserted, for the experiment of magnetic hyperthermia.

Magnetic Hyperthermia Test on cellular pellet BxPC3 with concentration of nanoparticles of 100 µg/ml and uptake of 24h or 48h.

We had prepared two pellets with concentration of 100 µg/ml with different uptake and put in cryogenic ampoules, one to use in the experiment of hyperthermia and the other one to remain in laboratory at ambient temperature for the entire period of the process.

After the estimating time of hyperthermia process (one hour), the ampoule in laboratory was replanted and put in thermostat, in order to prepare a clonogenic assay. At a first time, we used tube of 1 ml, but in order to reduce heat dispersion we decided to change and use tubes of 0.2 ml.

4.3.b

Cytotoxicity due to Nanoparticles and Hyperthermia

At this stage of the project, it was thought to evaluate the cytotoxicity of the cell population by the injection of nanoparticles, combined with the action of hyperthermia.

For assessing the mortality induced by this combination we proceeded as described above, that is by propagating a cell population, inserting a certain concentration of nanoparticles, creating hyperthermia and performing the clonogenic assay.

Moreover, the "Hyperthermia group" received a different batch of nanoparticles, which we called NP2, whose results were unsatisfactory.

Evaluation of Cytotoxicity of a cellular population BxPC3 due to Nanoparticles of Magnetite of two different batches, at two different concentration

Starting from the usual propagation procedure of the cell population, we inserted two concentrations of two different batches of nanoparticles with uptake of 48 hours.

In particular, we prepared three tubes: one to be stored in laboratory, one in the hyperthermia machine in order to measure the temperature and the last one in the machine in order to obtain clonogenic assay.

This test was carried out for evaluating the optimal situation in which temperature rise. To evaluate the cytotoxicity, the following attempts have been made, each one with uptake of 48 hours: 100 μg/ml of NP2; 50 μg/ml of NP2; 100 μg/ml of NP1 and 50 μg/ml NP1.

4.4

Treatment of Cellular Population with Hadronic Radiation:

Experiment at CNAO

This paragraph describes the experimental procedure which is the core of the project: determining which cytotoxicity is inflicted on the cellular population under investigation in the case of both the combination of nanoparticles, hyperthermia and irradiation with hadronic radiation, more specifically carbon ions. Three types of tests were performed, with the same population allowed to grow in the same methodologies described so far:

- Irradiation Only,
- Irradiation + Nanoparticles,
- Irradiation + Nanoparticles + Hyperthermia.

4.4.1 Survival Curve of the Cell Line BxPC3 with Hadronic Radiation

Cell cultures were irradiated with Carbon Ions at the CNAO (Centro Nazionale di Adroterapia Oncologica) in Pavia, where a 25 m diameter synchrotron can accelerate both protons and carbon ions.

The hadronic radiation is produced by two ion-sources, pre-accelerated by a linear accelerator, and injected into the synchrotron ring where they are accelerated further and extracted up to 250 MeV for protons and 480 MeV / u for Carbon Ions.

The goal of this experiment was to determine cell survival by exposure of different dose values of hadronic radiation of 6 MeV (0, 0.5, 0.75, 1, 1.5, 2 Gy) using a clonogenic assay.

In particular, the treatment was carried out by exposing the cells contained in the T25 flasks to a SOBP (Spread-Out Bragg Peak) of carbon ions at a depth of 15 cm, which corresponds to an average LET of 45 keV / μm.

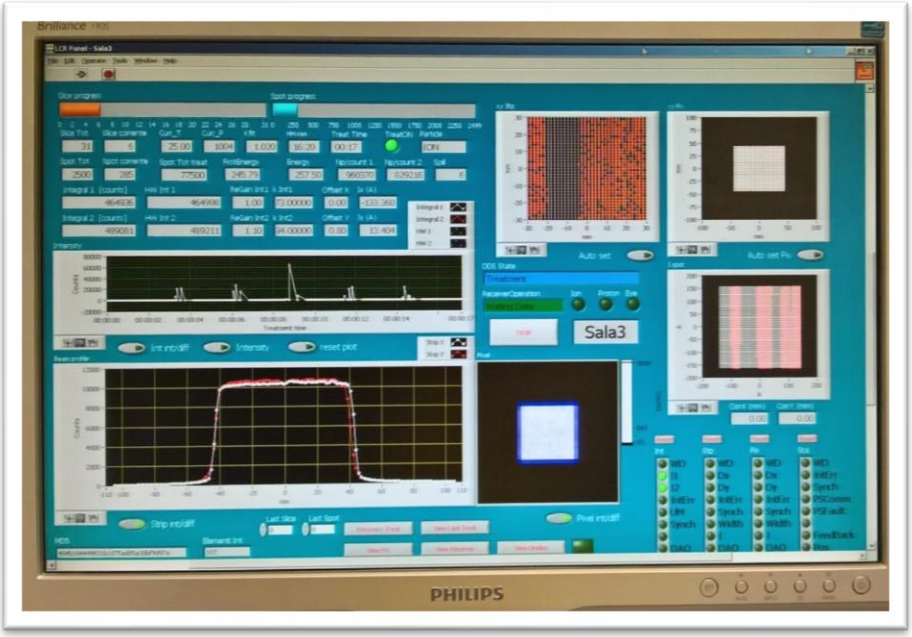

Fig.4.7 Display of treatment irradiation with Ions C. SOBP trend is shown lower left.

The following experimental procedure was set up: shortly before the irradiation, the flasks were completely filled with culture medium and transported to the room of irradiation. This protocol was followed even for the control sample, which was not irradiated.

After the irradiation, we use trypsin to remove cells from the bottom of flasks and re-plate in culture medium, count and plate at appropriate inocula in T25 flasks (five for each dose) and placed in a thermostat at 37 ° C, 4.5% of CO2 and 90% of humidity. The inoculum was established based on the expected survival (estimated considering the radiation dose).

Dose [Gy]	Inocula [cells/flask]
0	1386,7
0,5	1969,5
0,75	2572,7
1	3298,5
1,5	6420
2	14040

Tab.4.7 Inocula of cells depending on the concentration of irradiation doses.

After two weeks of treatment, we proceed to fix with 70% ethyl alcohol and colour with a solution of 10% Giemsa histologic dye to visualize cellular colonies so that only those with a number of cells superior to fifty.

4.4.2 Survival Curve of the Cell Line BxPC3 with Hadronic Radiation and NPs

Also in this case flasks of cellular culture were prepared for each dose of radiation, with the addition of a nanoparticle concentration of 50 μg / ml and a 48 hour uptake time. Otherwise, the procedure is the same mentioned for the only irradiation.

Dose [Gy]	Inocula [cells/flask]
0	1464,75
0 (NPs)	1927
0,5	3144
0,75	6051,2
1	9944
1,5	21480
2	40304

Tab.4.8 Inocula depending on the concentration of uptake of NPs and irradiation doses.

4.4.3 Survival Curve of the Cell Line BxPC3 with Hadronic Radiation, NPs and Hyperthermia

After the usual uptake of nanoparticles and the irradiation with carbon ions at the indicated doses we proceeded to the technique of hyperthermia, which involves the use of the device already discussed in section 4.2. The expected temperature increase is for thirty minutes and up to a value of 42 °C.

Dose [Gy]	Inocula [cells/flask]
0	1408,75
0 (NPs+HT)	2005,6
0,5	3916
0,75	7970
1	16944
1,5	31491
2	52364

Tab.4.9 Inocula of cells depending on the concentration of uptake of nanoparticles, irradiation doses and treatment of hyperthermia.

Details about experimental results and the apparatus necessary to develop the tests are shown in the next chapter and in the appendix, respectively.

Fig.4.8 Apparatus of Hyperthermia

Chapter 5

Experimental Results

The aim of this experimental work was to understand what the concentration of nanoparticles was that gives a good uptake in the cell population and manages to heat it up to 42 ° C, giving a lowering of the population's plate efficiency and mortality; the action of nanoparticles must be such as to be combined with the decrease in survival given by irradiation.

From the results we found that the optimal nanoparticle concentration to be inserted in the cell population is 50 μm/ml, after a 48 hour uptake time.

Results were obtained step by step, so as to have an idea of what the population growth curve was and therefore understand how to perform the clonogenic assay, the optimal concentration of a certain type of nanoparticles, the experimental setup up of hyperthermia and the survival curves of the population bombarded with hadron radiation.

5.1

Characterization of Cell Line BxPC3

5.1.1 Generation Time and Efficiency Plating: Cell Growth

Growth curve of BxPC3 cells (procedure described in Chapter 4) is shown in the following graph:

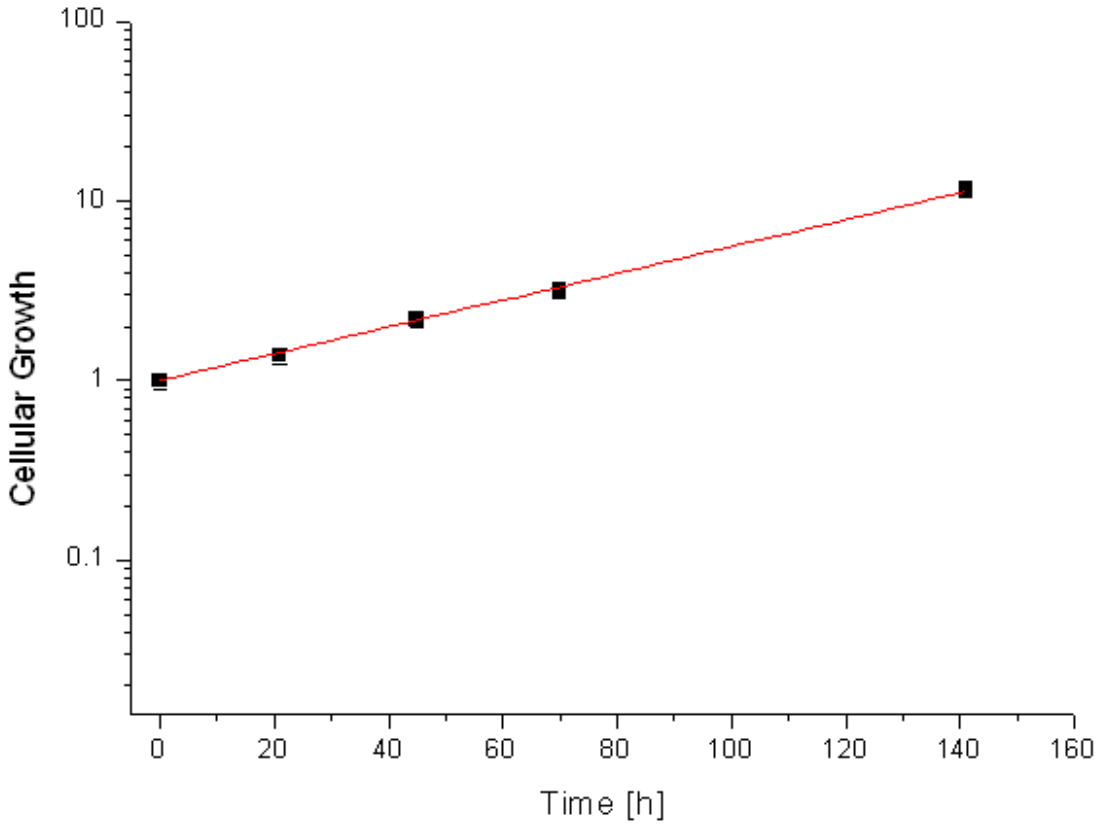

Graph.5.1 Growth Curve of BxPC3 cells as a function of time after plating.

The fitting curve is obtained using *Origin 8.6*, a software that allows fitting parameters based on the $\chi 2$ minimization method.

So, in this case, we find the value of time generation that is about 40 hours: this means that each cell divides in two daughters into less than two days, important information for obtaining the incubation time after irradiation to carry out the clonogenic assay.

Moreover, the y-axis represents each ratio between the number of cells counted at each time and the initial inoculum.

5.1.2 Cellular Growth by counting of colonies

Graph.5.2 shows the Average number of cells / colony as a function of time after plating.

As can be seen at about seven days a colony is composed on average of ten cells; the result is on line with what expected for this cell line.

From this valuation it was also possible to find the average number of cells in a colony, and show the trend as a function of time:

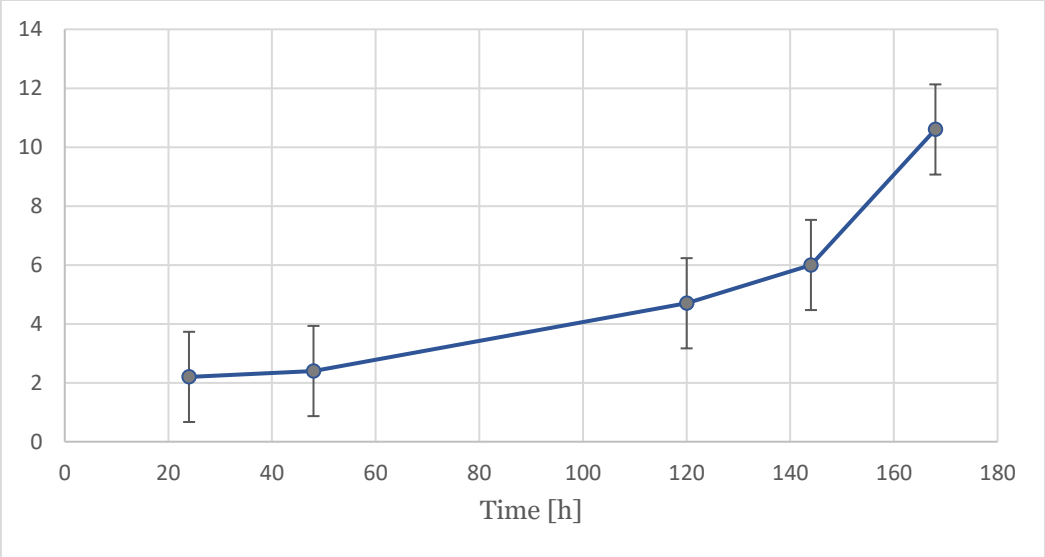

Graph.5.2 Average number of cells / colony as a function of time after plating.

5.1.3 Cytotoxicity due to Photon Radiation

Graph.5.3 shows BxPC3 cells survival curve after photon irradiation in the dose interval between 0 - 7 Gy. The experiment was performed at Fondazione IRCCS (Istituto Nazionale dei Tumori) of Milan.

The curve shows the typical shoulder at the lower doses as expected for photon irradiation.

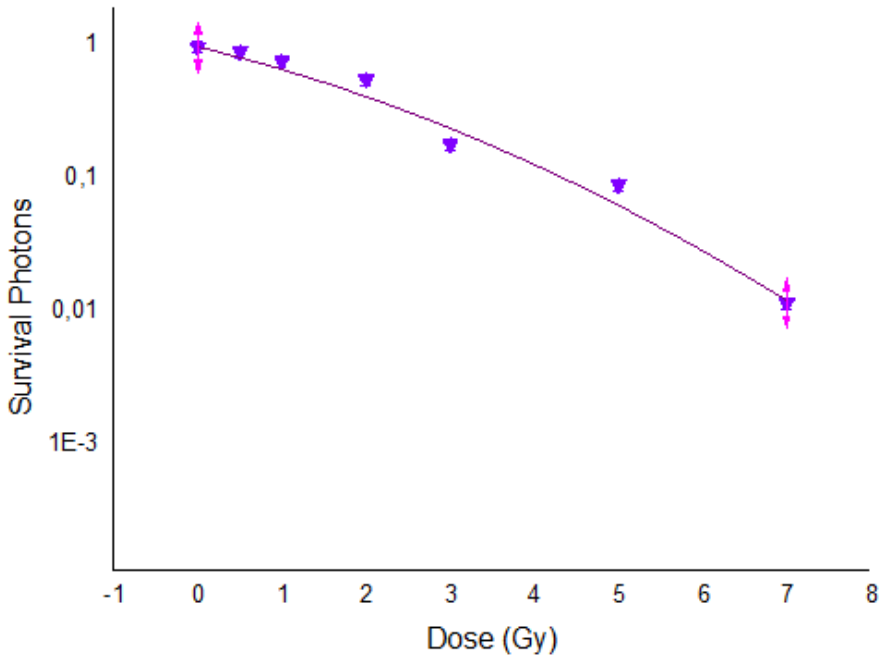

Graph.5.3 Survival Curve for photonic radiation determined in the experiment done at Fondazione IRCCS (Istituto Nazionale dei Tumori) of Milan.

Dose	*Surv*	*Err(10%)*
0	1	0,1
0.5	0,922	0,0922
1	0,784	0,0784
2	0,568	0,0568
3	0,1864	0,01864
5	0,0928	0,00928
7	0,01202	0,001202

Model	*Linear Quadratic*
Equation	$y = e^{(-\alpha x - \beta x^2)}$
Reduced Chi-Sqr	5,6958
Adj. R-Square	0,93738
α (Gy-1)	0,35097 ±0,08923
β(Gy-2)	0,03916 ±0,01477

5.2

Cytotoxicity due to Nanoparticles

5.2.1 Efficiency of Plating & Survival of Population of BxPC3 with uptake of Nanoparticles

One of the most important aspects of the project is the optimization of the concentration of nanoparticles to be inserted in the population in vitro, so as to ensure a good uptake but not an excessive mortality given only by such introduction. This means that, since the project aims to evaluate a combined action of magnetic hyperthermia and irradiation, the cytotoxicity of the nanoparticles does not have to go too far to affect the cell population, rather, the hope is that they go directly into the on the way cells to allow local release of heat more efficiently, the purpose of hyperthermia.

In this regard, a test was performed with the inclusion of concentrations of 0 (control), 10, 25, 50 and 100 µg / ml in the population appropriately grown, and the results gave a decrease in the efficiency of plating related to the increase of the concentration of nanoparticles.

The following tables and graphs show E.P. and Survival of BxPC3 cells, as a function of nanoparticles concentration with time uptake of 24 hours.

NPs µg/ml	*Inocula*	*Average Colony Counts*	*E.P.*	*Surv*	*Err(10%)*
0	2088,52	538,8	0,258	1	0,1
10	1930,88	392,6	0,2033	0,788	0,0788
25	4983,2	546,2	0,10961	0,425	0,0425
50	10024,16	766	0,0764	0,296	0,0296

Test 1

Then, another experiment has been performed, in order to review these values and to do a combination experiment with magnetic hyperthermia (see the next paragraph).

		Test 2			
NPs µg/ml	*Inocula*	*Average Colony Counts*	*E.P.*	*Surv*	*Err(10%)*
0	1851,6	346,2	0,18697	1	0,1
25	5205,9	381,6	0,0733	0,392	0,0392
50	10814	615,4	0,0569	0,304	0,0304

Tab.5.1 Results of E.P. and Survival in cases of different nanoparticles concentration.

As can be seen cell survival decreases with the increasing of nanoparticles concentration. At the concentration of 10 µg/ml cell survival is 78.8%, whereas it drops to average percentages of about 40% and 30% respectively for 25 and 50 µg/ml.

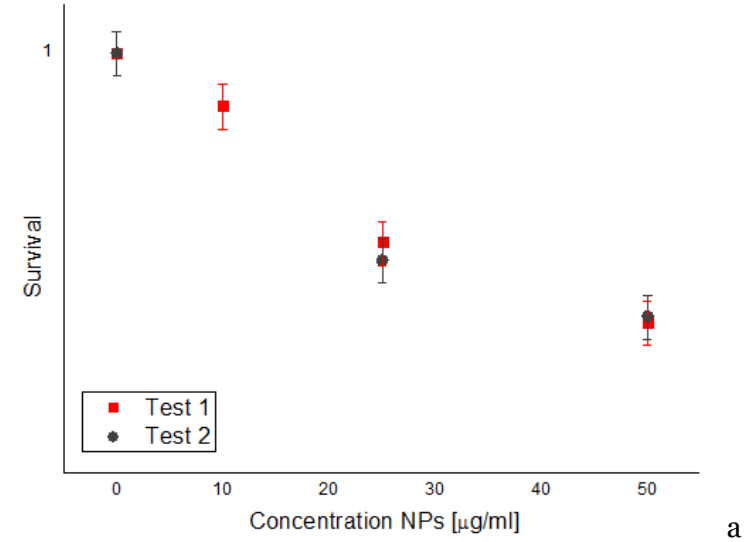

a

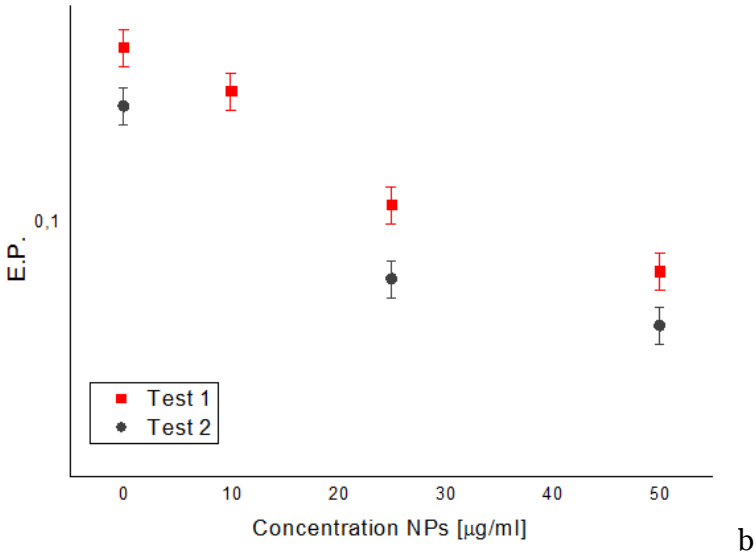

b

Graph.5.4 Comparison of cell survival (a) and E.P. (b) in two tests as a function of nanoparticles concentration.

5.2.2 Efficiency of Plating & Survival of BxPC3 cells as a function of Nanoparticles Time Uptake

This experiment was performed to determine the optimal time of uptake. For both the concentrations 50 and 100 µg/ml similar values of survival were obtained for 24 and 48 hours.

NPs µg/ml	*Inocula*	*Average Colony Counts*	*E.P.*	*Surv*	*Err(10%)*
0 (room)	1569,04	323,6	0,2688		
0	1521,92	421,6	0,2126	1	0,1
50	10006,4	889,4	0,0889	0,418	0,0418
100	9979,2	797,6	0,0799	0,376	0,0376

Tab.5.2 Results of E.P. and Survival for uptake time of 24 hours.

NPs µg/ml	*Inocula*	*Average Colony Counts*	*E.P.*	*Surv*	*Err(10%)*
0 (room)	1548,8	416,6	0,26898		
0	1557,6	332,8	0,2137	1	0,1
50	10056	860,8	0,0856	0,4	0,04
100	10069,2	824,4	0,0819	0,38	0,038

Tab.5.3 Results of E.P. and Survival for uptake time of 48 hours.

As it can be observed in the table, the plate efficiencies obtained for the sample with uptake of the nanoparticles for 24 hours are almost the same as those obtained in the sample with a 48hour uptake; moreover, the concentration of 50µg/ml seems to cause the same cytotoxicity of the concentration 100µg/ml.

Therefore, to avoid nanoparticles wasting, a concentration of 50 µg/ml has been chosen.

The figure 5.1 shows the cell pellet (about 106) in 0.2 ml Eppendorf tube.

Fig.5.1 Eppendorf tube of 0.2 ml with cell pellet and uptake of nanoparticles.

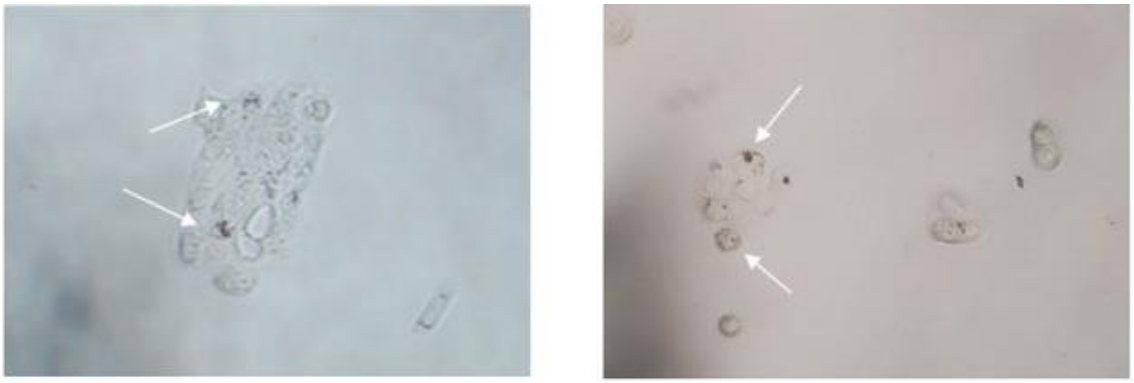

Fig.5.2 Bright field images of fixed BxPC3 cells after 24 h of incubation with 10 μg/ml (left) and 25 μg/ml (right). The white arrows denote some cellular localizations of accumulated iron oxide nanoparticles.

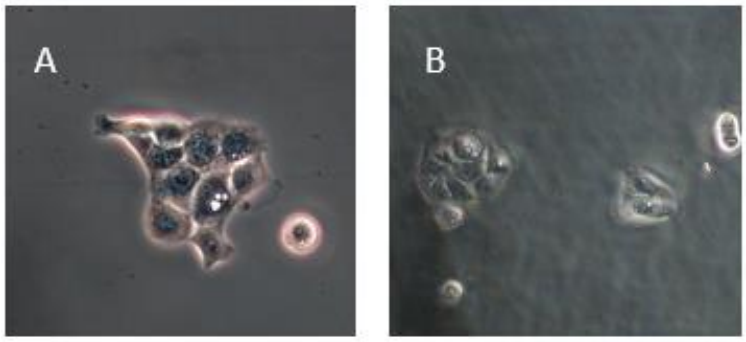

Fig.5.3 20x phase contrast optical images of fixed BxPC3 cells

after 24 h of incubation with: A) 10 μg/ml and B) 25 μg/ml.

5.3

Hyperthermic Effect due to Nanoparticles

Once the effect of the uptake of the nanoparticles in the cell population has been verified, it is necessary to perform hyperthermia tests to verify if the nanoparticles can heat properly the sample and if this introduction brings a higher mortality, and therefore inhibits the proliferation, of the carcinogenic population.

Specifically, a part of the population used for the mortality studies introduced by the nanoparticles was used to perform the hyperthermia test, for which the sample is brought to a temperature of 42 °C.

The test of hyperthermic treatment has been repeated for several nanoparticles batches in temperature range 37-42°C and it was found that the temperature did not reach the typical levels of hyperthermia, but this elevation has found a plateau already at 39 °C. We think that the failure of this test is due to a different type of nanoparticles and the timing of uptake of 24h. it has been found that the time

The experimental setup for cell measurements has two sample holders, so that a sample can be kept, sterile used for survival studies and have a sample for temperature control. The choice of a smaller Eppendorf (V=0.2 ml) than the ones used usually for nanoparticles only (V=1.5 ml) is due to the need to minimize the loss of heat by dispersion. In fact, several tests were carried out using Eppendorf of volume (V=1.5 ml) L, but the temperature never reached 42 °C.

In fact, for the evaluation of the cytotoxicity due to the presence of nanoparticles in the culture, several tests were performed with different treatment modes. However, an optical fibre was used in order to measure temperature increase due to the alternating magnetic field on the cellular pellet with concentration of nanoparticles of 50 μg/ml.

Back from these failed results, a new test was carried out, with a concentration of nanoparticles of 100 μg/ml and an uptake time of 48 h and using two different batches: the pellet is visibly darker than the previous time (symptom of a greater presence of nanoparticles).

In addition, we find that using the NP1 we obtain a plateau at 42 ° C, a great success.

5.4

Cytotoxicity due to Hadronic Radiation:

Results of Experiment at CNAO

Nanoparticles had been administered (50 μg/ml of nanoparticles in the culture medium for 48h) to the cells, which were irradiated with 5 different doses (0.5, 0.75, 1, 1.5, 2 Gy) of carbon ions at the Center National Oncological Hadrontherapy in Pavia (CNAO). As explain in the Chapter 4, after almost two weeks it was possible to carry out the clonogenic assay to the samples obtain from this experiment, in order to determinate the percentage of survival.

The results will show a growth in mortality from irradiation alone to the combination of nanoparticles, hyperthermia and carbon ions.

Moreover, it was possible to make a comparison with the result obtained with bombardment of photons, and therefore a comparison of the RBE: the carbon ion beams have a RBE radiobiological effect much greater than the photons.

Also, MFH + HT combined treatment causes more effects than single treatment; in fact there is a decrease in cell survival.

We can therefore conclude that although single hyperthermal treatment is not effective as an anticancer treatment, applied in combination with hadrontherapeutic treatment it seems to increase its efficacy.

Recalling the greater capacity of carbon ion treatment compared to conventional radiotherapy in preserving healthy tissues, the hadrontherapy treatment combined with magnetic hyperthermia seems to be a very promising antitumor therapy, which could be applied daily once the clinical protocol is established.

5.4.1 Survival Curve of the Cell Line BxPC3 with Hadronic Radiation

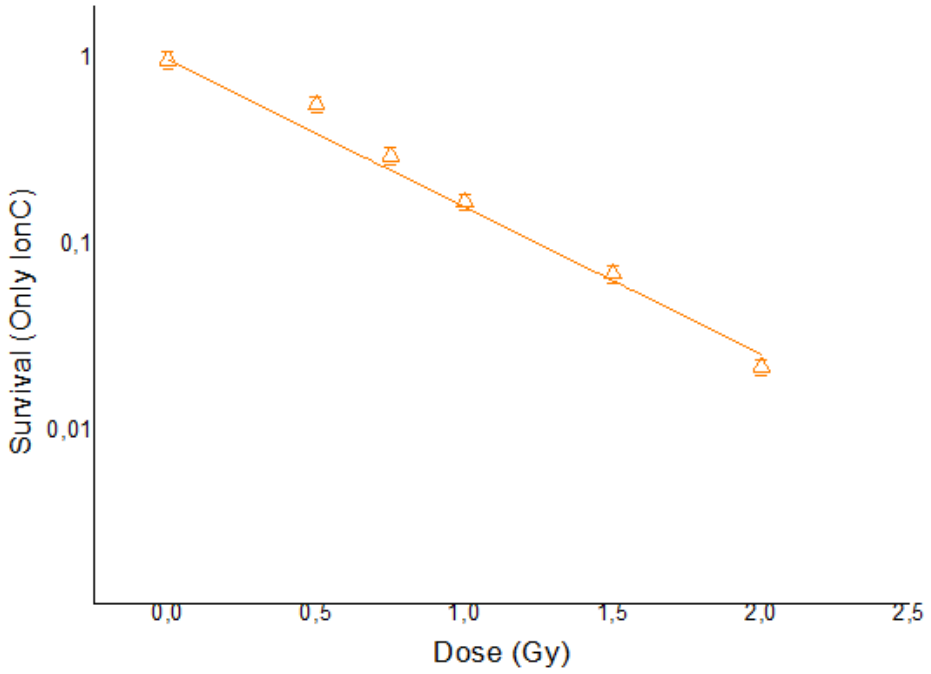

Graph.5.5 Survival Curves for Ions C alone, determined in the experiment done at CNAO (Centro Nazionale Adroterapia Oncologica) of Pavia.

Dose	*Surv*	*Err(10%)*
0	1	0,1
0,5	0,573047	0,0573047
0,75	0,3042411	0,03042411
1	0,1728369	0,01728369
1,5	0,0704715	0,00704715
2	0,0223505	0,00223505

Model	*Exponential Fit*
Equation	$y = e^{(-\alpha x)}$
Reduced Chi-Sqr	3,08184
Adj. R-Square	0,9592
α	1,82446 ±0,03415

Tab.5.4 On the left: Results of cellular survival in function of dose in the case of Ions C alone. On the right: Values of the exponential fit of survival curve and its parameters.

In the table on the left we see how the survival percentage varies (i.e. the ratio between the efficiency of plating at dose D and the efficiency of plating of the zero-dose control); specifically, already at a dose of 0.5 Gray we see a result with a decrease of about half of cell survival. On the right there are the values of the exponential fit of survival values as a function of the dose, thus the curve interpolation parameters.

5.4.2 Survival Curve of the Cell Line BxPC3 with Hadronic Radiation and NPs

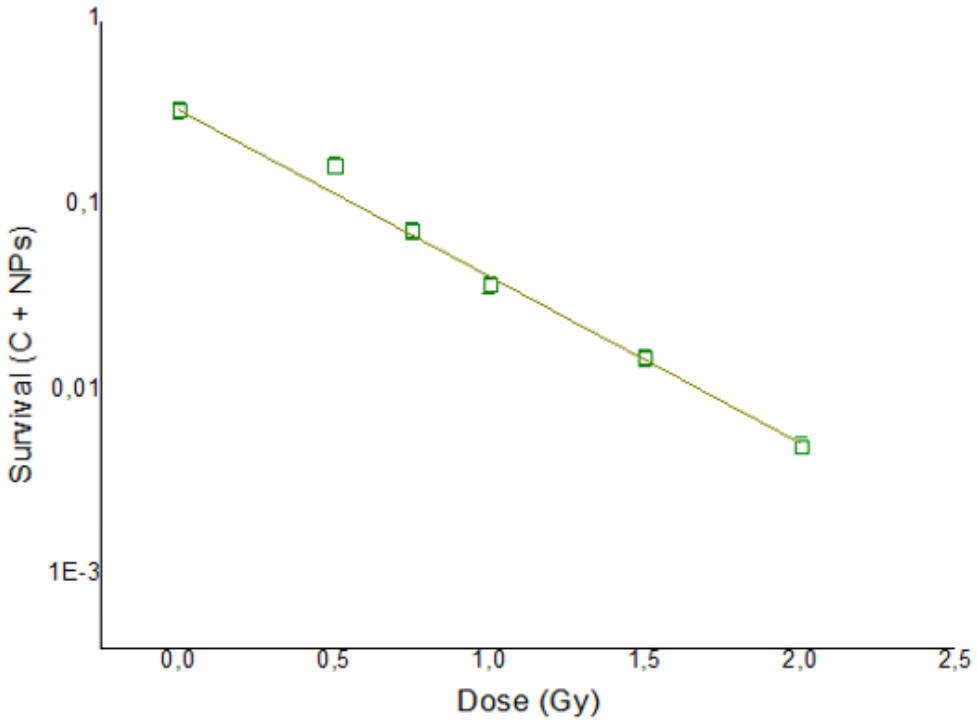

Graph.5.6 Survival Curves for Ions C and NP, determined in the experiment done at CNAO (Centro Nazionale Adroterapia Oncologica) of Pavia.

Dose	*Surv*	*Err(10%)*
0	1	0,1
0 (NP)	0,3261223	0,03261223
0,5	0,1639723	0,01639723
0,75	0,0734061	0,00734061
1	0,0374521	0,00374521
1,5	0,0147303	0,00147303
2	0,0053531	0,00053531

Model	*Exponential Fit*
Equation	$y = ke^{(-\alpha x)}$
Reduced Chi-Sqr	2,07789
Adj. R-Square	0,97261
α	2,07279 ±0,035
k	0.326

Tab.5.5 On the left: Results of cellular survival in the case of Ions C and NPs, in function of dose. On the right: Values of the exponential fit of survival curve and its parameters.

It is evident that compared to the case of the only hadronic radiation there is a lower survival rate, therefore the presence of the nanoparticles, or their absorption only by the cells, leads to a decrease in the efficiency of plating and thus a lower survival.

5.4.3 Survival Curve of the Cell Line BxPC3with Hadronic Radiation, NPs and Hyperthermia

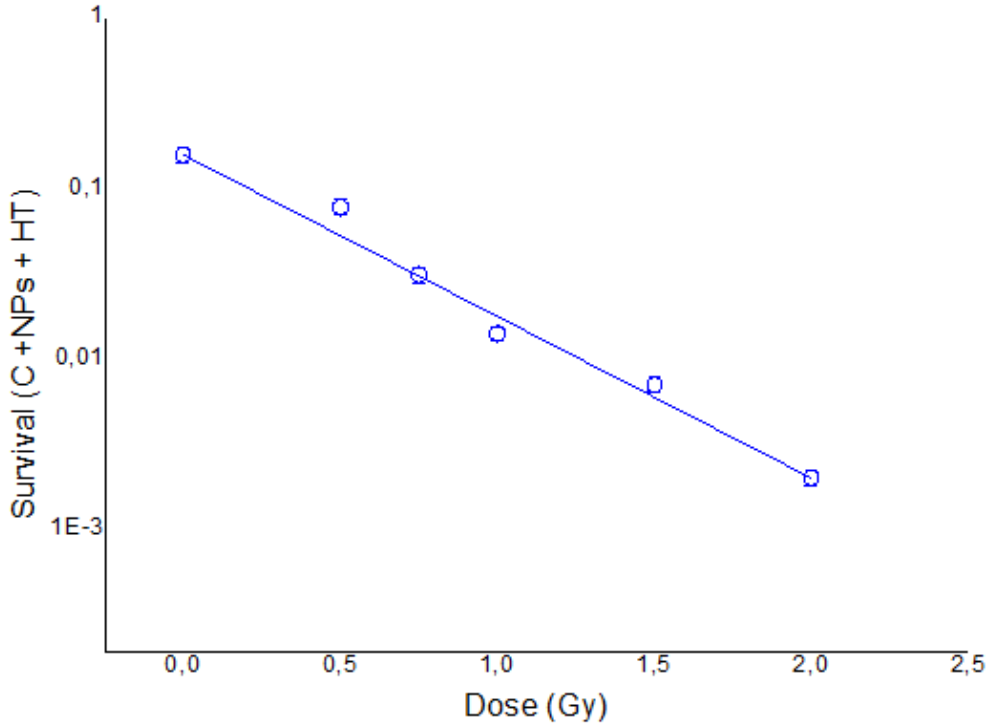

Graph.5.7 Survival Curves for Ions C, NPs and Hyperthermia, determined in the experiment done at CNAO (Centro Nazionale Adroterapia Oncologica) of Pavia.

Dose	*SOP*	*Err(10%)*
0	1	0,1
0(NP+HT)	0,1555147	0,01555147
0,5	0,0766609	0,00766609
0,75	0,0308183	0,00308183
1	0,0138058	0,00138058
1,5	0,0065892	0,00065892
2	0,0024818	0,00024818

Model	*Exponential Fit*
Equation	$y = ke^{(-\alpha x)}$
Reduced Chi-Sqr	3,85655
Adj. R-Square	0,95031
α	2,18049 ±0,03607
k	0.156

Tab.5.6 On the left: Results of cellular survival in the case of Ions C, NPs and Hyperthermia, in function of dose. On the right: Values of the exponential fit of survival curve and its parameters.

The result of the combination of uptake of nanoparticles, irradiation and heat-raising treatment is surprising: the cell population has a radical decrease in cell survival already at very low doses, and is held at lower values but still very close to increasing

doses. At the maximum dose we have an almost total mortality of the population in question.

Uniting the three trends in a single graph we clearly see that the effect that leads to a lower cell survival is given by the combination of the three agents:

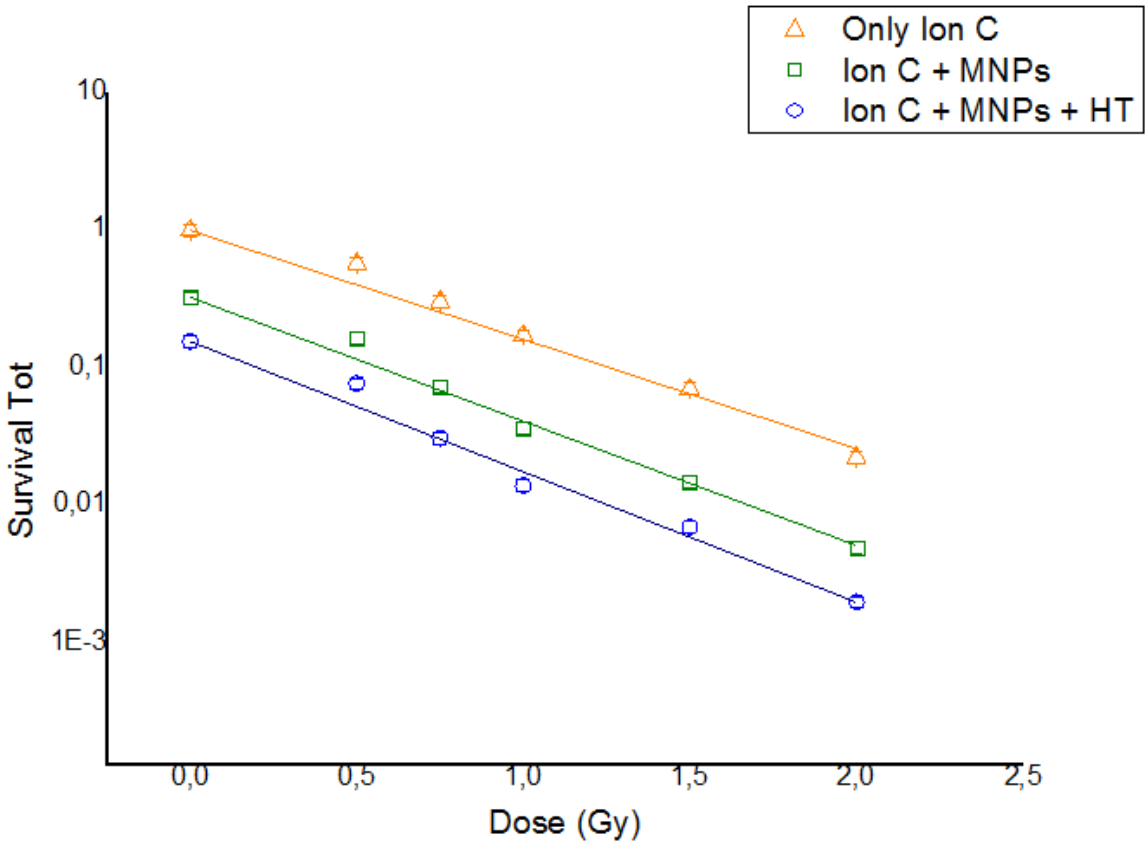

Graph.5.8 Survival Curves for Ions C alone, Ions C and NP, and Ions C, NPs and Hyperthermia, determined in the experiment done at CNAO (Centro Nazionale Adroterapia Oncologica) of Pavia.

It is already evident from the survival curve of the only hadronic radiation a decreasing exponential trend without shoulders at low doses, which confirms the higher biological damage caused by high LET radiations. Moreover, the combination of uptake of nanoparticles, carbon ions irradiation and consequent magnetic hyperthermia increase the mortality (and so decrease the survival) of the population of cells.

The following graph Graph.5.9 was made by normalizing the Survival values found for a) Ions C + NPs and b) Ions C + NPs + Hyperthermia. In fact, each value at a certain dose is divided for the value at the corresponding control, i.e. dose zero with already the uptake of nanoparticles (a), or with the uptake and treatment of hyperthermia (b).

In the tables there are the new results, with an error of 15%, given by considering the sum of the precedent error of 10%.

Dose	*Surv*	*Err(15%)*
0 (NP)	1	0,15
0,5	0,502793	0,075419
0,75	0,225087	0,033763
1	0,11484	0,017226
1,5	0,045167	0,006775
2	0,016414	0,002462

Model	*Exponential Fit*
Equation	$y = e^{(-\alpha x)}$
Reduced Chi-Sqr	0,87949
Adj. R-Square	0,97335
α	2,0566 ±0,5297

Tab.5.7 Results of Survival normalized at the control in the case of Ion C and NPs.

Dose	*Surv*	*Err(15%)*
0(NP+HT)	1	0,15
0,5	0,492949	0,073942
0,75	0,198167	0,029725
1	0,088776	0,013316
1,5	0,042368	0,006355
2	0,015959	0,002394

Model	*Exponential Fit*
Equation	$y = e^{(-\alpha x)}$
Reduced Chi-Sqr	1,93942
Adj. R-Square	0,93934
α	2,14522 ±0,05563

Tab.5.8 Results of Survival normalized at the control in the case of Ion C, NPs and HT.

Moreover, it is possible to calculate the Dose Enhancement Factor (DEF) which represents the ratio between the alpha parameter found in the case of combination of more effects and the alpha parameter referred to the irradiation alone.

$\boldsymbol{DEF}$	$\frac{\alpha_{IonC+MNPs}}{\alpha_{IonC}}$
$\boldsymbol{\alpha_{IonC}}$	1,82446
$\boldsymbol{\alpha_{IonC+MNPs}}$	2,0566
$\boldsymbol{\alpha_{IonC+MNPs+MFH}}$	2,1452

Finding this value, we could estimate if the addition of a more agents (NPs, hyperthermia) makes the cellular population more radiosensitive. In fact, DEF expresses the percentage of variation of the slope of the trends, and in the case in examination we find that the values are:

1,13 $\pm$ 0,04 (error), in the case of Ions C and NPs

1,18 $\pm$ 0,04 (error), in the case of Ions C, and Hyperthermia.

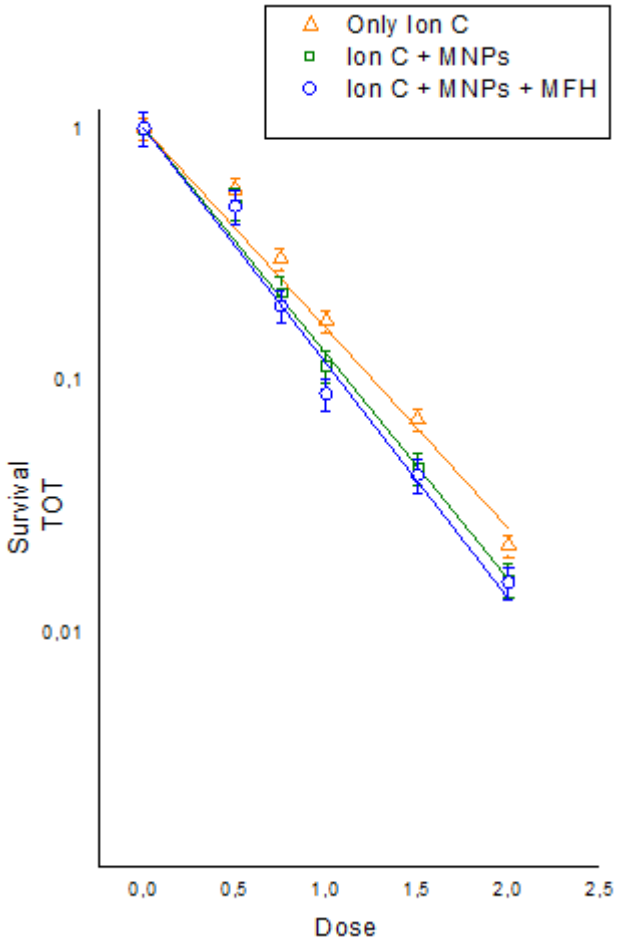

Graph.5.9 Survival curves of Ions C alone (orange), Ions C and NPs (green) and Ions C, NPs and Hyperthermia (blue), given by the normalization at control of each case.

From the graph it is already possible to deduce, and confirmed by result above, that the slope of the curves is increasing by adding radiosensitizing factors, but there is no particular difference between the irradiation with previous uptake of NPs and the similar case with the addition of the hyperthermic treatment. This result could suggest that even the presence of nanoparticles will bring an increase in the mortality of the population, but there is no significant difference (considering the conditions of this experiment) with the addition of heat treatment.

Unfortunately, for problems concerning the reproducibility of nanoparticles with always similar proprieties and expected results, at the moment it was not possible to perform other relevant experiments in such a way as to make a comparison with the results below.

In fact, the groups are waiting to the experiment (at the same found conditions) in order to make a statistic and then a protocol of treatment. It could be appropriate to carry out an experiment with the same condition of hyperthermia and NPs already tried, but irradiating the cellular population with photons.

Conclusions

This thesis work is based on a set of experimental data on survival curves of cancerous pancreatic BxPC3 cells, after irradiation with Carbon Ions and combined or not with magnetic hyperthermia and nanoparticles. The effect of nanoparticles uptake is the reduction of the plating efficiency up to 30%. In fact, the insertion of nanoparticles (concentration of 50 μg/ml and a time of uptake of 48 h), the action of carbon-ion radiation (Dose range 0-2 Gy) and a rise in temperature typical of hyperthermia treatments (37 °C to 42 °C), give cytotoxicity and a survival dropping. From the survival curves we found the exponential decreasing trend, typical of high LET radiation (that is, in fact, Ions Carbon beam), whose slope increase with the addition of radiosensitizing. Moreover, it is more significant the increase of percentage slope between Ions Carbon alone and its combination with NPs (13%), than between this last one with the combination of Ion Carbons, NPs and Hyperthermia (5%), and this suggests the effect of radiosensitive of nanoparticles, leaving many question to our toxicity in hypothetical vivo treatment. Future studies with photons and the same protocol could give some other potential in other cases of tumor and in radiotherapy with low-LET radiations.

Bibliography

Chapter 1

[1] Dipartimento di Scienze della Salute (DISSAL), Università di Genova
[2] Radiation Therapy for Pancreatic Cancer, Ahmad Amoush and Maryam Aletan (2016)
[4] Johns H. E. and J. R. Cunningham, 1983, *The Physics of Radiobiology*, 4th edn. C.C. Thomas, Springfield, IL.
[5] Epidemiology of pancreatic cancer. Milena Ilic et al. (2016)
[6] https://www.vitamindwiki.com/Pancreatic+Cancer+massively+deregulates+the+local+Vitamin+D+receptors+and+CPY24A1+%E2%80%93+July+2014
[7] https://seer.cancer.gov/statfacts/html/pancreas.html
[8] Analysis of Toxicity in a Group of Patients Treated for Pancreatic Cancer with Combined Modality 3D Radiation Therapy (2013)
[9] https://empoweryourknowledgeandhappytrivia.wordpress.com/2015/02/20/who-discovered-x-rays/
[10] https://en.wikipedia.org/wiki/Cyclotron#/media/File:Berkeley_60-inch_cyclotron.jpg
[11] D.Caramella, F.Paolicchi, L.Faggioni, La dose al paziente in diagnostica per immagini, Springer Science & Business Media, 2012.
[12] Stereotactic Radiotherapy for Pancreatic Cancer? Christopher H. Crane, MD1 and Christopher G. Willett, MD2
[14] Radiotherapy combined with hyperthermia for primary malignant melanomas of the esophagus. M. C. C. M. Hulshof et al.
[15] Manual therapies for cervicogenic headache: a systematic review. Aleksander Chaibi et al. (2012) 13:351–359
[16] M. Krämer and M. Scholz. Treatment planning for heavy-ion radiotherapy: calculation and optimization of biologically effective dose. Phys. Med. Biol. 45, 3319-3330 (2000)
[17] M. Krämer et al. Technology in Cancer Research & Treatment Vol. 2, N. 5, 427 (2003)

[18] Jay S. Loeffler and Marco Durante. Charged particle therapy–optimization, challenges and future directions. Nature Reviews Clinical Oncology, 2013.
[19] M. Krämer and M. Scholz. Treatment planning for heavy-ion radiotherapy: calculation and optimization of biologically effective dose. Phys. Med. Biol. 45, 3319-3330 (2000)
[20] https://pt.slideshare.net/abishadh/4-rs-of-radiobiology-15355292/2

Chapter 2

[1] https://fondazionecnao.it/it/tumori-al-pancreas
[2] U. Amaldi, M. Silari The Blue Book: The TERA Project and the Centre of Oncological Hadrontherapy, Vol. I-II, INFN-LNF, Frascati, Italy (1995)
[3] *John Kimball (8 April 2012). "DNA repair". Retrieved 2012-06-24.*
[4] Elkind & Sutton - 1960
[5] https://phyusdb.files.wordpress.com/2013/03/practical_radiotherapy_planning.pdf
[6] http://large.stanford.edu/courses/2012/ph241/ali1/docs/003019-pdf.pdf
[7] R. Orecchia and al. “Particle Beam Therapy (Hadrontherapy): Basis for Interest and Clinical Experience” PII: S0959-8049(97)10044-2
[8] 2 UOC Oncologia Radioterapica, IRCCS AOU San Martino IST - Istituto Nazionale per la Ricerca sul Cancro, Genova.
[9] http://www.recentiprogressi.it/allegati/01940_2015_07/fulltext/06_Rassegna%201%20-%20Corvo.pdf
[10] G. Knoll, Radiation Detection and Measurement, third edition, Wily and Sons Inc.
[11] W.K. Weyrather Medical Applications of Accelerated Ions Lecture Notes in Physics 651, 469-490 (2004)
[12] http://shodhganga.inflibnet.ac.in/bitstream/10603/26739/6/06_chapter1.pdf
[13] Review of Radiation Oncology Physics: A Handbook for Teachers and Students - 1.4.4 Slide 3 (150/194) (IAEA)
[14] http://oftankonyv.reak.bme.hu/tiki-index.php?page=Physical+processes+important+for+radiation+detection

[16] Gli acceleratori nella terapia dei tumori, Ugo Amaldi, Analysis, N2-3/2008, Pag.108-118
[17] http://www.technologicalminds.it/ingegneria-biomedica/adroterapia-lotta-contro-i-tumori.html
[18] T. Schwab Ph. D. Thesis, GSI Report 91-10 (1991)
[19] A. Beiser, Revs. Mod. Phys. 24, 273 (1952)
[20] U. Amaldi, R. Bonomi, S. Braccini et al.; Accelerators for Hadrontherapy: From Lawrence Cyclotrons to Linacs; Nuclear Instruments and Methods in Physics Research (2010), 563-577
[21] IAEA, "Absorbed Dose Determination in External Beam Radiotherapy", Technical Report Series 398 (2000).
[22] Marco Arrighetti:"Monitoraggio on line dei trattamenti adroterapici con fasci di carbonio mediante la rilevazione di particelle secondarie"
[23] Dieter Schardt, Thilo Elsässer, and Daniela Schulz-Ertner. Heavy-ion tumor therapy: Physical and radiobiological benefits. Reviews on Modern Physics, 2010.
[24] U. Amaldi "Cancer therapy with particle accelerators" Nuclear Physics A654 375-399 (1999).
[25] W.K. Weyrather
[26] Laser ion acceleration for hadron therapy, S V Bulanov[1,2,3], J J Wilkens[4], T Zh Esirkepov[2,3], G Korn[5], G Kraft[6], S D Kraft[7], M Molls[4] and V S Khoroshkov[8]
[27] Uspekhi Fizicheskikh Nauk and P N Lebedev Physics Institute of the Russian Academy of Sciences
[28] F. Collini. Misura dell'emissione dei gamma prompt prodotti da fasci di elio e ossigeno in adroterapia. Master's thesis, Università degli studi di Pavia, 2014
[29] http://edcan.org.au/assets/edcan/files/EdCaN-Specialty-Module-Four-Cancer-Treatment-Principles_1.pdf
[30] https://www.scribd.com/doc/79739991/Radioterapia

Chapter 3

[1] "Hyperthermia: A Potent Enhancer of RT" (2007)
[2] Francesca Brero Thesis Work "Effetto combinato di adroterapia e ipertermia magnetica su cellule tumorali pancreatiche". (2017)
[3] Q.A. Pankhurst; J. Connolly; S.K. Jones; J. Dobson, Applications of magnetic nanoparticles in biomedicine, Journal of Physics D: Applied Physics (2003).

[4] Magnetic nanomaterials for hyperthermiabased therapy and controlled drug delivery, Challa S.S.R. Kumar; Faruq Mohammad, Advanced Drug Delivery Reviews (2011)
[5] Magnetic Nanoparticles: Surface Effects and Properties Related to Biomedicine Applications Bashar Issa et al. Int. J. Mol. Sci. 2013, 14, 21266-21305
[6] Buonsanti Thesis Work "Eterostrutture nanocristalline a base di ossido di titanio e ossido di ferro"
[7] Massimo Terrin Thesis Work: "Nanoparticelle di ossido di ferro per ipertermia magnetica da decomposizione controllata di ferro acetilacetonato"
[8] Magnetic Iron Oxide Nanoparticles: Synthesis, Stabilization, Vectorization, Physicochemical Characterizations, and Biological Applications Sophie Laurent et al.
[9] Fundamentals and advances in magnetic hyperthermia E.A.Perigo, G.Hemery
[10] Katz E., Willner I. Integrated nanoparticle-biomolecule hybrid systems: Synthesis, properties, and applications. Angew. Chem. Int. Ed. 2004;43:6042–6108. doi: 10.1002/anie.200400651.
[11] Saha S., Loo S.C.J. Application-driven multi-layered particles—The role of polymers in the architectural design of particles. Polymer. 2015;71:A1–A11. doi: 10.1016/j.polymer.2015.06.033.
[12] Alexiou C, Arnold W, Klein R J, Parak F G, Hulin P, Bergemann C, Erhardt W, Wagenpfeil S and Lubbe A S, Locoregional cancer treatment with magnetic drug targeting, Cancer Res. 60 6641-8, 2000
[13] "High Therapeutic Efficiency of Magnetic Hyperthermia in Xenograft Models achieved with Moderate Dosages in the Tumor Area" (2014)
[14] A. Lascialfari, C. Sangregorio, Magnetic Nanoparticles in Biomedicine: Recent Advances, Chemistry Today, 29(2), pp.20-23, 2011.
[15] Ajay Kumar Gupta; Mona Gupta, Synthesis and surface engineering of iron oxide nanoparticles for biomedical applications, Biomaterials (2005).
[16] "Preparazione e Caratterizzazione di NanoParticelle di Ossido di Fe per Ipertermia Magnetica da Coprecipitazione di sali di Ferro" (Lorenzo Meneghetti Thesis Work, 2013)
[17] NMR as evaluation strategy for cellular uptake of Nanoparticles. (2014) Orlando, Lascialfari, et al. American Chemical Society
[18] J.R. Lepock, H.E. Frey, K.P. Ritchie, Hyperthermia, Radiation And Chemotherapy: The Role Of Heat In Multidisciplinary Cancer Care, Semin Oncol, 2014.

[19] J.R. Lepock, H.E. Frey, K.P. Ritchie, Protein Denaturation in Intact Hepatocytes and Isolated Cellular Organelles During Heat Shock, The Journal of Cell Biology, Volume 122, Number 6, 1267-1276, 1993.